The Dissertation Committee for Juan Felipe Pedraza Avella
certifies that this is the approved version of the following dissertation:

Dynamics of asymptotically AdS spaces and holography

Committee:

Willy Fischler, Supervisor

Jacques Distler

Can Kilic

Andrew Neitzke

Sonia Paban

Dynamics of asymptotically AdS spaces and holography

by

Juan Felipe Pedraza Avella, B.S., M.S.

DISSERTATION

Presented to the Faculty of the Graduate School of

The University of Texas at Austin

in Partial Fulfillment

of the Requirements

for the Degree of

DOCTOR OF PHILOSOPHY

THE UNIVERSITY OF TEXAS AT AUSTIN

August 2015

Dedicated to my family.

Acknowledgments

Many people contributed to the research presented in this thesis. I would like to start by thanking my supervisor, prof. Willy Fischler, for his excellent support and guidance over the past five years. I am also grateful to my collaborators: Cesar Agón, Tom Banks, Elena Cáceres, Mariano Chernicoff, Brandon DiNunno, Mohammad Edalati, Bartomeu Fiol, Antonio García, Alberto Güijosa, Matthias Ihl, Niko Jokela, Arnab Kundu, Sandipan Kundu, Patricio Letelier,[1] Fabio Lora, Phuc Nguyen, Paolo Ospina, Javier Ramos, Walter Tangarife and Di-Lun Yang. For all the time we spent discussing physics, which lead to many successful ideas [1, 2, 3, 4, 5, 6, 7, 8, 9, 10, 11, 12, 13, 14, 15, 16, 17, 18, 19, 20, 21, 22, 23, 24]. Finally, I would like to thank my fellow students and the professors of the UT Theory Group, for sharing their vast knowledge in individual discussions, seminars and journal club meetings.

This material is based upon work supported by the National Science Foundation under Grant PHY-1316033 and by the Texas Cosmology Center, which is supported by the College of Natural Sciences, the Department of Astronomy at the University of Texas at Austin and the McDonald Observatory.

[1] R.I.P.

Dynamics of asymptotically AdS spaces and holography

Juan Felipe Pedraza Avella, Ph.D.
The University of Texas at Austin, 2015

Supervisor: Willy Fischler

This thesis presents a series of studies on the evolution and out-of-equilibrium dynamics of strongly coupled quantum field theories by means of the AdS/CFT correspondence. We use a handful of analytic and semi-analytic techniques to investigate the response of the system due to different types of perturbations, some of them leading to thermalization, cooling down or coherent oscillations of the quantum fields. We characterize the processes by studying the evolution of non-local observables such as two-point functions, Wilson loops and entanglement entropy. Our results may be relevant to heavy-ion collision and condensed matter physics experiments.

Table of Contents

List of Tables

List of Figures

Chapter 1

Introduction

1.1 Preface

The AdS/CFT correspondence [25, 26, 27] describes an equivalence between a classical gravitational dynamics and a large N gauge theory. This remarkable correspondence has proved to be very useful in addressing aspects of strongly coupled dynamics in various models, ranging from understanding aspects of strongly coupled Quantum chromodynamics (QCD) to condensed matter-inspired systems. See [28, 29] for recent reviews on some of these attempts.

Most of such endeavours usually discuss equilibrium properties of a class of strongly coupled $SU(N)$ gauge theories at large N. However, since this is a correspondence between the path integrals of the corresponding Quantum Field Theory (QFT) and the classical Gravity description, it is natural to assume that it extends to time-dependent dynamical situations as well. In fact, dynamical processes in a prototypical field theory model are extremely interesting to explore and learn about, since we do not have a good understanding of the governing rules and laws for systems completely out-of-equilibrium, specially at strong coupling. In this regime, AdS/CFT correspondence is po-

tentially a very useful tool.

Such time-dependent issues fall under two broad categories: the study of quantum quenches, where a system is prepared in an energy eigenstate of a given Hamiltonian. The Hamiltonian is then perturbed by a time-dependent external parameter. Recent developments in cold atoms experiments have initiated a very active research where this perturbation occurs abruptly, see *e.g.* [30] for a condensed-mater approach and [31, 32, 33] for a review of the holographic attempts. The other broad issue is to understand the physics of thermalization of strongly coupled system. See *e.g.* [34, 35, 36] for earlier works on this. More recently, there has been a renewed interest to understand the physics of thermalization at strong coupling to shed light on the physics of the quark-gluon plasma (QGP) at the Relativistic Heavy Ion Collider (RHIC) and the Large Hadron Collider (LHC). Most of these works rely heavily on numerical efforts that study gravitational collisions and black hole formation in an asymptotically anti de-Sitter (AdS) space, see *e.g.* [37, 38, 39, 40, 41, 42, 43].

The main motivation of this thesis is to develop new computational tools to study such time-dependent scenarios without restoring to the heavy numerical machinery. In the process, we use a handful of analytic and semi-analytic techniques to investigate the response of system due to different types of perturbations, some of them leading to thermalization, cooling down or coherent oscillations of the quantum fields. The main goal is to gain new insights into the broad subject of out-of-equilibrium quantum field theory and to learn, at least qualitatively, useful lessons which are presumably not heavily

dependent on the details of the model.

The remaining part of this Chapter is merely introductory and can be safely skipped by the cognoscenti. In section 1.2 we introduce the reader to the main concepts of the AdS/CFT correspondence: its original derivation and the main entries of the holographic dictionary. In section 1.3, we close with the general outline and a brief discussion of the results.

1.2 The AdS/CFT correspondence

1.2.1 Maldacena's derivation

Let us consider a stack of N coincident D3-branes in type IIB string theory, living on a flat 10-dimensional spacetime. The system have open strings ending on the D-branes as well as closed strings propagating in the bulk. Maldacena's idea was to consider the low-energy limit of this system, where the branes decouple from gravity. If we take $E \ll l_s$ we can neglect the massive degrees of freedom of the theory and we can write down an effective action. Schematically,

$$S = S_{\text{sugra}} + S_{\text{branes}} + S_{\text{interactions}} \,. \tag{1.1}$$

The first term in (1.1) corresponds to the massless modes of the closed string sector, which is nothing but type IIB supergravity. The second term represents the excitations of the D3-branes (*i.e.* the open string sector), and the last term accounts for the interactions between open and closed strings. Let us focus on the second term in (1.1). Open strings can in principle be attached to any of the D3-branes so the worldvolume theory exhibits a $U(N)$ gauge

symmetry. However, the factor $U(1)$ describing the position of the center of mass of the branes decouples from the internal degrees of freedom. This factor can be neglected when studying the dynamics of the system, leaving only a $SU(N) = U(N)/U(1)$ symmetry. Also, the system of D3-branes preserves half of the 32 supersymmetries of the type IIB theory. Since the worldvolume theory lives in 3+1 dimensions, then, it must be maximally supersymmetric. This theory is known as $\mathcal{N} = 4$ super-Yang-Mills (SYM). Its field content consists of one vector A_μ, six scalars ϕ^I $(I = 1...6)$, and four Weyl fermions χ^i_α, $\chi^{\bar{i}}_{\dot{\alpha}}$ $(i, \bar{i} = 1, 2, 3, 4)$. The Lagrangian density of the SYM theory contains two free parameters g_{YM} and θ_{YM}, and is given by

$$\begin{aligned}\mathcal{L}_{\text{SYM}} = \text{Tr}\Bigg[& -\frac{1}{2g^2_{YM}} F_{\mu\nu}F^{\mu\nu} + \frac{\theta_{YM}}{8\pi^2} F_{\mu\nu}\tilde{F}^{\mu\nu} - i\bar{\lambda}^a \bar{\sigma}^\mu D_\mu \lambda_a - D_\mu \Phi^i D^\mu \Phi^i \\ & + g_{YM} C^{ab}_i \lambda_a [\Phi^i, \lambda_b] + g_{YM} \bar{C}_{iab} \bar{\lambda}^a [\Phi^i, \bar{\lambda}^b] + \frac{g^2_{YM}}{2} [\Phi^i, \Phi^j]^2 \Bigg].\end{aligned} \tag{1.2}$$

It can be shown that in the strict low energy limit $E \to 0$ (or equivalently $l_s \to 0$ keeping E fixed) the interaction term in (1.1) is negligible and, thus, the system naturally decouples in two sectors [25]: free supergravity in 9+1 dimensions and $\mathcal{N} = 4$ SYM in 3+1 dimensions.

On the other hand, if N is sufficiently large, the branes can deform substantially the spacetime and we can have an alternative description of the system: in this limit, the D3-branes act as a source of an extremal black brane geometry [44]. The backreacted metric takes the following form:

$$ds^2 = \left(1 + \frac{L^4}{r^4}\right)^{-1/2} \eta_{\mu\nu} dx^\mu dx^\nu + \left(1 + \frac{L^4}{r^4}\right)^{1/2} \left[dr^2 + r^2 d\Omega_5^2\right] . \tag{1.3}$$

In addition, the solution is supplemented by a constant dilaton ϕ, which is related to the coupling constant of the type IIB theory through $g_s = e^{\phi}$, a constant axion χ and N units of Ramond-Ramond F_5 flux. In (1.3), L is the only length scale and is given by

$$L^4 = 4\pi g_s N l_s^2 \,. \tag{1.4}$$

We can consider taking the following limits: if $r \gg L$ the geometry reduces to the Minkowski metric in 9+1 dimensions. Hence, we say that solution is asymptotically flat. In the near horizon limit, $r \ll L$, the geometry looks singular at first glance since $L^4/r^4 \to \infty$. Finally, in the intermediate region, $r \sim L$, the geometry takes the form of a "throat" with radius of curvature L. Notice that the g_{tt} component of the metric is not constant. This implies that the energy E_r of an object measured by an observer located at certain r differs from the energy E of the same object measured by an observer at infinity,

$$E = \left(1 + \frac{L^4}{r^4}\right)^{-\frac{1}{4}} E_r \,. \tag{1.5}$$

Thus, objects located close to the horizon experience a gravitational redshift.

Let us now study the low energy limit of this system. We can do so by taking $l_s \to 0$ while keeping both g_s and N fixed. In the asymptotic region we get rid of the massive modes and we obtain free supergravity in flat space. On the other hand, in the near horizon region we can have modes with arbitrarily large energies as a consequence of the gravitational redshift. The intermediate region acts as a gravitational barrier, so modes in the asymptotic region cannot

interact with modes in the near horizon region. Again, we obtain that the system decouples in two sectors: free supergravity in 9+1 dimensional flat space and type IIB string theory in the near horizon geometry. If we redefine the radial coordinate according to

$$z = \frac{L^2}{r}\,, \tag{1.6}$$

and then take the limit of large z we obtain the geometry of the near horizon region,

$$ds^2 = \frac{L^2}{z^2}\left(\eta_{\mu\nu}dx^\mu dx^\nu + dz^2\right) + L^2\,, d\Omega_5^2, \tag{1.7}$$

which is the direct product of a 5-dimensional AdS space $(L^2/z^2)(\eta_{\mu\nu}dx^\mu dx^\nu + dz^2)$ and a 5-sphere $L^2 d\Omega_5^2$. In other words, the geometry near the stack of D3-branes ($r \to 0$ or $z \to \infty$) can be written as the product $\mathrm{AdS}_5 \times \mathrm{S}^5$, where both factors have the same radius of curvature L.

We have presented two ways of describing the same physical systems: a stack of N D3-branes. In both cases we obtained as the low energy description type IIB supergravity on Minkowski space and a second theory: SYM and type IIB string theory on $\mathrm{AdS}_5 \times \mathrm{S}^5$, respectively, the latter one in the $N \to \infty$ limit. Since the SYM theory exists for any N it is natural to conjecture that [25]:

$\mathcal{N} = 4$ SYM theory with gauge group $SU(N)$ = Type IIB string theory on $\mathrm{AdS}_5 \times \mathrm{S}^5$ with N units of Ramond-Ramond five-form flux.

Here, the = sign indicates a full duality: the two sides are just different languages to describe the same physical system. The above statement

is known as the AdS/CFT correspondence, because AdS describes the non-compact part of the spacetime in the string theory side, and gauge theory is a conformal field theory (CFT). As such, there are many other examples of this duality that arise from string– (or M–) theory constructions, giving rise to different CFTs. For example, besides the usual D3-brane system, other dualities that are studied involve the near-horizon geometries and low-energy world-volume theories of multiple D1/D5, M2 and M5 branes, respectively [45]. Its worth pointing out that the AdS boundary conditions can also be relaxed, in which case the dual gauge theory is not necessarily conformal. For this reason, the term "AdS/CFT" is often replaced by "gauge/gravity" or "gauge/string" correspondence, which have wider connotation.

In the following sections we will explain the meaning of this duality in more detail and we will introduce different computational tools that we need for the remaining part of this thesis.

1.2.2 Main entries of the dictionary

1.2.2.1 Symmetries

To start convincing ourselves of the equivalence between the two descriptions we can compare the symmetries of the two sides of the correspondence. The isometry group of the AdS metric is $O(2,4)$, which coincides with the conformal group in $3+1$ dimensions. More precisely, the bulk diffeomorphisms induce conformal transformations on the boundary theory. We can identify various subgroups as follows: the subgroup $O(1,3) \subset O(2,4)$ acts as

the Lorentz symmetry on the boundary. The transformation $z \to \lambda z$, $x^i \to \lambda x^i$ induces the scale transformation on the boundary. Now, besides the conformal group on the super Yang-Mills side we have the R-symmetry group $SU(4)_R$. On the gravity side it acts as $SU(4) \to SO(6)$ inducing rotations on the S^5 factor. We also have the electric-magnetic duality or strong-weak duality. To see this, we define complex parameter

$$\tau = \frac{\theta_{YM}}{2\pi} + \frac{4\pi i}{g_{YM}^2}\,, \tag{1.8}$$

which combines the coupling constant g_{YM} and the theta angle θ_{YM}. Taking into account the translations $\tau \to \tau + 1$ and the inversions $\tau \to -1/\tau$ we obtain the $SL(2,\mathbb{Z})$ group, which acts according to

$$\tau \to \frac{a\tau + b}{c\tau + d} \qquad\qquad ad - bc = 1\,, \quad a, b, c, d \in \mathbb{Z}\,. \tag{1.9}$$

In the gravity side of the correspondence, this duality corresponds to the $SL(2,\mathbb{Z}) \subset SL(2,\mathbb{R})$, which acts on the dilaton-axion system. This duality becomes manifest after we identify $g_{YM}^2 = 4\pi g_s \equiv 4\pi e^{\phi}$ and $\theta_{YM} = 2\pi\chi$, where ϕ is the dilaton and χ is the Ramond-Ramond scalar, or axion.

Taking into account (1.4) and the relation between the string coupling constant and the coupling constant of the SYM theory, we can write

$$L^4 = g_{YM}^2 N l_s^4 = \lambda l_s^4, \tag{1.10}$$

where $\lambda \equiv g_{YM}^2 N$ is the so-called 't Hooft coupling, which effectively measures the strength of the interactions of the SYM theory in the large N limit. In

order to neglect the stringy modes we can work in the limit $L \gg l_s$, which in the language of the gauge theory translates into the condition $\lambda \gg 1$. We observe that in the limit where type IIB string theory reduces type IIB supergravity, the gauge theory is strongly coupled. This is one of the most powerful observations of the AdS/CFT correspondence. It implies that we can study the nonperturbative aspects of a quantum field theory in terms classical supergravity.

1.2.2.2 Fields and correlators

In order to translate between one side of the duality to the other, we should keep in mind that gauge theory is conformal: it does not have asymptotic states or an S matrix, so the natural objects to consider are correlation functions of gauge invariant operators. Indeed, in the AdS/CFT dictionary we find a one-to-one map between bulk fields $\phi(x, z)$ and operators in the gauge theory side $\mathcal{O}$. For instance, if we deform the $\mathcal{N} = 4$ SYM theory by means of a marginal operator (essentially the Lagrangian of the theory $\mathcal{O} \sim \mathrm{Tr}\, F^2$) the net effect is to change the value of the coupling constant. But changing the value of the coupling constant in the gauge theory is equivalent to changing the value of the coupling constant in the gravity side, $g^2_{YM} = 4\pi g_s$, which is equivalent to expectation value of the dilaton field. This expectation value is fixed by the boundary conditions of the dilaton at $z = 0$ and, hence, changing the coupling constant of the gauge theory is equivalent to changing the boundary value of the dilaton. Schematically, we learn that $\phi(x, z)|_{z=0}$ acts as

a source that couples to the corresponding operator $\mathcal{O}$.

In order to make this map more precise, let us review the field content on the gravity side. Type IIB supergravity in $d = 10$ dimensions has the following bosonic fields:

Field	Sector
ϕ (dilaton)	NSNS
$g_{\mu\nu}$ (metric)	NSNS
$B_{\mu\nu}$ (Kalb-Ramond field)	NSNS
χ (axion)	RR
$A_{\mu\nu}$ (2-form)	RR
$A_{\mu\nu\sigma\rho}$ (self-dual 4-form)	RR

Small fluctuations of these fields follow an equation of motion of the form $\Delta\,\phi = 0$, where Δ is the covariant Laplacian in the bulk. If we decompose the Laplacian as $\Delta = \Delta_{\mathrm{AdS}_5} + \Delta_{\mathrm{S}^5}$, the fields viewed as living on AdS_5 acquire the mass equal to the eigenvalue of Δ_{S^5}. For example, scalar fields decompose as $\phi(z, y) = \sum_{k=2}^{\infty} \phi_k(z) Y_k(y)$, where z represent the coordinates along AdS_5 and y are the coordinates along S^5, and the mode ϕ_k acquires the mass $m^2 = k(k-4)/L^2$, where L is the radius of S^5.

The bosonic field content in the compactified theory is the following (only the lowest modes are listed):

Field	$SO(6)$ representation
$h_{\mu\nu}$ graviton	$\mathbf{1}$
$A_{\mu\nu}$ 2-forms	$\mathbf{6}$
A_μ 1-forms	$\mathbf{15}$
ϕ scalars	$\mathbf{20} \oplus \mathbf{10} \oplus \mathbf{10}^* \oplus \mathbf{1} = 42$

Solutions to the Klein-Gordon equation $(\Delta_{AdS_5} + m^2)\,\phi = 0$ have the following asymptotics at the boundary: $\phi(z, x^\mu) \sim z^{4-\Delta}$ and $\phi(z, x^\mu) \sim z^{\Delta}$, where $\Delta = 2 + \sqrt{m^2 + 4}$. In particular, the partition function of supergravity (or string theory) depends on the behavior at the boundary. According to [26, 27], we can identify

$$\mathcal{Z}_{\text{string}}[\phi_0] = \left\langle e^{-\int d^4x \phi_0(x)\mathcal{O}(x)} \right\rangle_{\text{CFT}} , \tag{1.11}$$

where the term in the left hand side is the string partition function with boundary condition[1] $\phi \to z^{4-\Delta}\phi_0$ as $z \to 0$ and the term in the right is the generating functional of correlation functions of the gauge theory. Notice that ϕ_0 has weight $4 - \Delta$ under the scaling transformations:

$$\begin{aligned}
\phi_0(\lambda x) &= \lim_{z\to 0} z^{\Delta-4}\phi(z, \lambda x) \\
&= \lambda^{\Delta-4} \lim_{z\to 0} (\lambda^{-1}z)^{\Delta-4}\phi(z, \lambda x) \\
&= \lambda^{\Delta-4} \lim_{v\to 0} v^{\Delta-4}\phi(\lambda v, \lambda x) \\
&= \lambda^{\Delta-4} \lim_{v\to 0} v^{\Delta-4}\phi(v, x) \\
&= \lambda^{\Delta-4}\phi_0(x).
\end{aligned}$$

Therefore, for the right-hand side of (1.11) to be well-defined, $\mathcal{O}$ has to have conformal weight Δ, $\mathcal{O}(\lambda x) = \lambda^{-\Delta}\mathcal{O}(x)$.

From the formula (1.11) we can match right away several operators. First, consider the variation of the metric, on the right-hand side it couples

[1] Here we assume that $m \geq 0$ so the term $z^{4-\Delta}$ dominates near the boundary. Otherwise the leading asymptotic behavior is given by z^{Δ}.

to the stress-energy tensor $T_{\mu\nu}$. Second, variations of the dilaton and axion fields correspond to varying the coupling constants, *i.e.* adding the operators $\mathrm{Tr}\, F_{\mu\nu}F^{\mu\nu} + \cdots$ and $\mathrm{Tr}\, F_{\mu\nu}\tilde{F}^{\mu\nu} + \cdots$, respectively, and so on (the dots here represent contributions from scalars and fermions).

AdS field	CFT operator
$h_{\mu\nu}$	$T_{\mu\nu}$
ϕ	$\mathrm{Tr}\, F_{\mu\nu}F^{\mu\nu} + \cdots$
χ	$\mathrm{Tr}\, F_{\mu\nu}\tilde{F}^{\mu\nu} + \cdots$

We will work exclusively in the large N, large λ limit of the duality, in which case type IIB string theory reduces to type IIB supergravity and the left hand side of (1.11) can be treated in the saddle point approximation. In this regime, the above relation becomes

$$S_{\text{on-shell}}[\phi_0] = -\Gamma_{\text{CFT}}[\phi_0], \tag{1.12}$$

where $S_{\text{on-shell}}[\phi_0]$ is the supergravity action evaluated on-shell and $\Gamma_{\text{CFT}}[\phi_0]$ is the generating functional of connected correlation functions in the SYM theory. The correlation functions of $\mathcal{O}$ can be computed by differentiating with respect to the source,

$$\begin{aligned}
\langle \mathcal{O}(x) \rangle &= \frac{\delta S_{\text{on-shell}}}{\delta \phi_0(x)}\Big|_{\phi_0=0}, \\
\langle \mathcal{O}(x_1)\mathcal{O}(x_2) \rangle &= -\frac{\delta^2 S_{\text{on-shell}}}{\delta \phi_0(x_1)\delta\phi_0(x_2)}\Big|_{\phi_0=0}, \\
\langle \mathcal{O}(x_1)\cdots\mathcal{O}(x_n) \rangle &= (-1)^{n+1}\frac{\delta^3 S_{\text{on-shell}}}{\delta \phi_0(x_1)\cdots\delta\phi_0(x_n)}\Big|_{\phi_0=0},
\end{aligned} \tag{1.13}$$

etc.

Finally, in order to make use of the formulas (1.13) one has to consistently regularize and renormalize the two sides of the equalities. The relevant divergences on the SYM side come from UV, so one introduces a momentum cutoff $p \leq \Lambda$. Similarly, on the gravity side divergences come from the infinite volume of AdS, so one introduces an IR cutoff $z_0 \geq \epsilon$. From purely dimensional analysis one expects $\epsilon \sim 1/\Lambda$. In the minimal subtractions scheme, one proceeds by adding covariant counterterms to the action in order to subtract the positive powers of Λ (ϵ^{-1}) and logarithms. Such approach is called holographic renormalization [46, 47].

1.2.3 States and geometries

1.2.3.1 Black holes

Introducing a finite temperature into the system means adding energy without modifying other quantum numbers such as the brane charges. The string theory setup we have discussed above can be easily modified in order to introduce these effects. First, recall that we obtained the original correspondence by taking a decoupling limit of extremal D3-branes, which saturate the BPS bound $M = N/(2\pi)^3 g_s l_s^4$. Then, adding temperature means adding energy but no charge to the system, so it is natural to take a decoupling limit for non-extremal D3-branes with $M > N/(2\pi)^3 g_s l_s^4$. The net effect of this is solely to replace the bulk metric to (AdS-Schwarzschild)$_5 \times$S^5. The line element for this background is given by

$$ds^2 = \frac{L^2}{z^2}\left(-h dt^2 + d\vec{x}^2 + \frac{dz^2}{h}\right) + L^2\, d\Omega_5^2\,, \tag{1.14}$$

where

$$h = 1 - \frac{z^4}{z_{\rm H}^4}\,. \tag{1.15}$$

The asymptotic behavior reveals that the UV physics is not affected by the presence of temperature, as we would expect. However, the IR physics is dramatically modified. As we can see, the metric above has a regular event horizon at $z = z_{\rm H}$ with Hawking temperature T. The simplest way to calculate it is to demand that the Euclidean continuation of the metric (1.14),

$$ds^2 = \frac{L^2}{z^2}\left(h dt_E^2 + d\vec{x}^2 + \frac{dz^2}{h}\right) + L^2\, d\Omega_5^2\,, \tag{1.16}$$

obtained as usual by the replacement $t \to it_E$, be regular. Since the Euclidean time direction shrinks to zero size at $z = z_{\rm H}$, we must require t_E to be periodically identified with appropriate period β, *i.e.* $t_E \sim t_E + \beta$. A simple calculation shows that

$$\beta = \pi z_{\rm H}\,. \tag{1.17}$$

The period β of the Euclidean time circle is then interpreted as the inverse temperature, $\beta = 1/T$. The reason for this is that, at finite temperature T, one is interested in calculating the partition function $\mathrm{Tr}\, e^{-\beta H}$, where H is the Hamiltonian of the theory. In a path integral formulation, the trace may be implemented by periodically identifying the Euclidean time with period $1/T$.

Surprisingly, not only the temperature but also all the thermodynamical properties of the black hole turn out to be the same as those of the dual gauge theory. The first quantity of interest we can compute is the entropy density of $\mathcal{N} = 4$ SYM theory [48]. We do not know how to compute this in

the gauge theory, but in the large N, large λ limit we can use the supergravity description. In this description the entropy is just the Bekenstein-Hawking entropy [49, 50], $S_{\rm BH} = A/4G$, proportional to the area of the horizon. According to (1.14) the horizon lies at $z = z_h$ and $t = \text{const.}$, and has 'area'

$$A = \int d^3x d^5\Omega \sqrt{g}\,. \tag{1.18}$$

The determinant of the metric factorises into the determinant of the metric on S^5 times $L^3/z_{\rm H}^3$, where the latter factor is just the determinant of the three-metric on a $z = z_{\rm H}, t = \text{const.}$ slice in (1.14). Integrating we obtain $A = aV_3$, where

$$a = \frac{L^3}{z_{\rm H}^3} \times \pi^3 L^5\,, \tag{1.19}$$

$V_3 = \int d^3x$ is the (infinite) volume in the 123-directions and π^3 is the volume of a unit five-sphere. Taking into account all the above terms, we can now express the entropy density per unit volume in the 123-directions in terms of gauge theory parameters as

$$s_{\rm BH} = \frac{S_{\rm BH}}{V_3} = \frac{a}{4G} = \frac{\pi^2}{2} N^2 T^3\,. \tag{1.20}$$

The N and the T dependence of this result could have been anticipated. The former follows from the fact that the number of degrees of freedom in an $SU(N)$ gauge theory grows as N^2, whereas the latter follows from dimensional analysis, since the temperature is the only scale in the $\mathcal{N} = 4$ theory. What is truly remarkable about the result above is that it shows that the entropy density attains a finite value in the limit of infinite coupling, $\lambda \to \infty$. Moreover,

this result is 3/4 of the Stefan-Boltzmann value for a free gas of quarks and gluons. This factor is not a mistake of the AdS/CFT calculation, rather it is a prediction for a finite temperature strongly coupled SYM theory. It appears that

$$s_{\rm SYM} = \mathcal{F}(\lambda) s_{\rm free}\,, \tag{1.21}$$

where $\mathcal{F}(\lambda)$ is a function which smoothly interpolates between a weak coupling limit of 1 and a strong coupling limit of 3/4. Indeed, Feynman graph calculations valid for small λ give [51, 52]

$$\mathcal{F}(\lambda) = 1 - \frac{3}{2\pi^2}\lambda + \dots\,. \tag{1.22}$$

The constant term is from a one loop computation and the leading correction is from two loops. On the other hand, a string theoretic calculation gives that for strong coupling [53]

$$\mathcal{F}(\lambda) = \frac{3}{4} + \frac{45}{32}\frac{\zeta(3)}{\lambda^{3/2}} + \dots\,, \tag{1.23}$$

consistent with a monotonic function $\mathcal{F}(\lambda)$. This last expression follows from considering the leading α' corrections to the supergravity action. Thus, the 1/4 deficit compared to the free field value is a strong coupling effect predicted by the AdS/CFT correspondence.

We can also study many other thermodynamical properties of the SYM theory, but in order to do so we need to compute the expectation value of the stress-energy tensor $\langle T_{\mu\nu}(x)\rangle$ at finite temperature. The operator $T_{\mu\nu}$ is dual to the bulk metric, so we need to analyze the asymptotic behavior of $g_{\mu\nu}$ and then

follow the recipe for computing correlation functions studied in the previous section. This process can be performed with quite generality, assuming a specific for of the bulk metric. In particular, if we assume that the metric is written in the Fefferman-Graham form [54]

$$ds^2 = \frac{L^2}{z^2}\left(g_{\mu\nu}(z,x)dx^\mu dx^\nu + dz^2\right) , \tag{1.24}$$

the dual CFT metric $ds^2_{\rm CFT} = g_{\mu\nu}(x)dx^\mu dx^\nu$ can be directly read off as $g_{\mu\nu}(x) = g_{\mu\nu}(0,x)$. The full function $g_{\mu\nu}(z,x)$ is uniquely determined (via the Einstein equations in the bulk) from this boundary value together with data dual to the expectation value of the CFT stress-energy tensor $\langle T_{\mu\nu}(x)\rangle$. More specifically, in terms of the near-boundary expansion

$$g_{\mu\nu}(z,x) = g_{\mu\nu}(x) + z^2 g^{(2)}_{\mu\nu}(x) + z^4 g^{(4)}_{\mu\nu}(x) + z^4\log(z^2)h^{(4)}_{\mu\nu}(x) + \dots , \tag{1.25}$$

the standard GKPW recipe for correlation functions [26, 27] leads after appropriate holographic renormalization to [46, 47]

$$\langle T_{\mu\nu}(x)\rangle = \frac{N^2}{2\pi^2}\left(g^{(4)}_{\mu\nu}(x) + X^{(4)}_{\mu\nu}(x)\right) , \tag{1.26}$$

where the quantity

$$X^{(4)}_{\mu\nu} = -\frac{1}{8}g_{\mu\nu}\left[\left(g^{(2)\alpha}_{\alpha}\right)^2 - g^{(2)\beta}_{\alpha}g^{(2)\alpha}_{\beta}\right] - \frac{1}{2}g^{(2)\alpha}_{\mu}g^{(2)}_{\alpha\nu} + \frac{1}{4}g^{(2)}_{\mu\nu}g^{(2)\alpha}_{\alpha} \tag{1.27}$$

is related to the conformal anomaly and turns out to cancel the logarithmic divergence. In (1.27) it is understood that the indices of the tensors $g^{(n)}_{\mu\nu}(x)$ are raised with the inverse boundary metric $g^{\mu\nu}(x)$.

A few comments are in order. Note that the pure AdS spacetime can be seen as the "ground state" of the gauge theory. Any other field that we turn on (including the metric) will result in an excited state and/or a deformation of the theory. Indeed, given the form of the AdS metric, it is easy to see that $g^{(2)}_{\mu\nu} = g^{(4)}_{\mu\nu} = h^{(4)}_{\mu\nu} = 0$ and so it follows that $\langle T_{\mu\nu}(x)\rangle = 0$, which is the correct value for the Poincaré invariant ground state of SYM. For the AdS-Schwarzschild metric (1.14) we first have to rewrite it in the Fefferman-Graham form through the trivial bulk diffeomorphism

$$z = \frac{z'}{\sqrt{1 + \frac{z'^4}{4z_{\rm H}^4}}}\,. \tag{1.28}$$

The resulting metric can be written as

$$ds^2 = \frac{L^2}{z'^2}\left[-\frac{\left(1 - \frac{z'^4}{4z_{\rm H}^4}\right)^2}{\left(1 + \frac{z'^4}{4z_{\rm H}^4}\right)}dt^2 + \left(1 + \frac{z'^4}{4z_{\rm H}^4}\right)d\vec{x}^2 + dz'^2\right]\,, \tag{1.29}$$

from which we can read off the metric of the gauge theory, $g_{\mu\nu} = \eta_{\mu\nu}$, and the first terms in the near-boundary expansion $g^{(2)}_{\mu\nu} = 0$, $g^{(4)}_{\mu\nu} = z_{\rm H}^{-4}/4\ \mathrm{diag}(3,1,1,1)$ and $h^{(4)}_{\mu\nu} = 0$. In this case, the stress-energy tensor reads

$$\langle T_{\mu\nu}(x)\rangle = \frac{\pi^2 N^2 T^4}{8}\begin{pmatrix} 3 & 0 & 0 & 0 \\ 0 & 1 & 0 & 0 \\ 0 & 0 & 1 & 0 \\ 0 & 0 & 0 & 1 \end{pmatrix}. \tag{1.30}$$

This is precisely the expected value for a conformal fluid at equilibrium with energy density $\varepsilon = (3\pi^2/8)N^2T^4$. Here the factor T^4 reflects the usual Stefan-Boltzmann law while N^2 reflects the number of degrees of freedom in the plasma. Note also that the energy density and the pressure are related as

$\varepsilon = 3p$ making the stress tensor traceless, as expected for a conformal field theory. Furthermore, the thermodynamic relations

$$d\varepsilon = Tds, \quad dp = sdT \quad \text{and} \quad \varepsilon + p = Ts \tag{1.31}$$

hold for both, the thermodynamics of the black hole and the thermodynamics of the gauge theory.

1.2.3.2 Time-dependent backgrounds

We have argued that the effect of turning on non-trivial values of fields in the bulk, including the metric, corresponds to having an excited state and/or a deformation of the dual gauge theory. Then, it is natural to assume that general time-dependent backgrounds are dual to out-of-equilibrium states in the boundary CFT. We can imagine, for instance, a process that interpolates between the vacuum of the theory (*i.e.* empty AdS) and a thermal ensemble (a Schwarzschild-AdS black hole), in a complete dynamical setting. This means that the time-dependent configurations we are looking for should capture the physics of gravitational collapse in the bulk, or equivalently, black hole formation. In the following we will review the simplest of such models and comment on its properties and physical limitations.

In order to find a background that captures the relevant physics, we have to couple the action that gives rise to AdS with an external source

$$S = S_0 + \alpha\, S_{\text{ext}} \ , \tag{1.32}$$

where α is a constant and

$$S_0 = \frac{1}{16\pi G_N^5}\int d^5x\sqrt{-g}\,(R-2\Lambda)\;, \qquad \Lambda \equiv -\frac{6}{L^2}\,. \tag{1.33}$$

We have taken the point of view of a 5-dimensional effective description, so we do not have to worry about the compact part of the geometry. Moreover, for the physics we want to study in the present context we do not need to specify the form of $S_{\rm ext}$. On general grounds, however, it might correspond to deforming the theory by a relevant, irrelevant or marginal operator $\mathcal{O}$. The equations of motion that follow from the above action take the following form

$$R_{\mu\nu} - \frac{1}{2}\,(R-2\Lambda)\,g_{\mu\nu} = 8\pi\alpha G_N^5\,T^{\rm ext}_{\mu\nu}\,, \tag{1.34}$$

and lead to the well-known AdS-Vaidya solution:

$$ds^2 = \frac{L^2}{z^2}\left(-f(v,z)dv^2 - 2dvdz + d\vec{x}^2\right)\;, \qquad f(z,v) = 1 - m(v)z^4\,, \tag{1.35}$$

with

$$8\pi\alpha G_N^5\,T^{\rm ext}_{\mu\nu} = \frac{3z^3}{2L^6}\frac{dm}{dv}\delta_{\mu v}\delta_{\nu v}\,. \tag{1.36}$$

The metric (1.35) is written in terms of Eddington-Finkelstein coordinates (so that v labels ingoing null trajectories) and represents a 5-dimensional infalling shell of null dust.[2] The function $m(v)$ can be in principle arbitrary and captures the information of the black hole formation. Quite generally, $m(v)$ is chosen to interpolate between zero as $v \to -\infty$ (corresponding to pure

[2]For $m(v) = const.$, the metric (1.35) reduces to the usual AdS-Schwarzschild black hole.

AdS) and a constant value as $v \to \infty$ (corresponding to AdS-Schwarzschild). A particular example of such a function is

$$m(v) = \frac{M}{2}\left(1 + \tanh\frac{v}{v_0}\right) , \tag{1.37}$$

where v_0 is a parameter that fixes the thickness of the shell. At this point one might think of considering solutions where $m(v)$ is not necessarily a monotonically increasing function of v. However, this would lead to several issues, as we will discuss below.

One constraint that any reasonable energy-momentum tensor should obey is the Null Energy Condition (NEC), which is given by the following inequality: $T^{\text{ext}}_{\mu\nu} n^\mu n^\nu \geq 0$, where n^μ is a lightlike vector, *i.e.* $n^\mu n_\mu = 0$. For the metric (1.35) there are two solutions to the null normal equation $n^\mu n_\mu = 0$. Without any loss of generality we can write them as

$$n^\mu_{(1)} = (0, 1, 0, 0, 0) \ , \quad n^\mu_{(2)} = \left(1, -\frac{1}{2}f, 0, 0, 0\right) \ , \tag{1.38}$$

The null vector $n^\mu_{(1)}$ imposes a trivial constraint, but the null vector $n^\mu_{(2)}$ imposes that

$$z^3 \frac{dm}{dv} \geq 0 \, . \tag{1.39}$$

Since $z \geq 0$, the inequality in (1.39) imposes that mass function is always increasing, $m'(v) \geq 0$. This condition seems to be correlated with other simple observations which we will discuss momentarily.

Before proceeding further, let us introduce the apparent horizon for the background (1.35), following the notations in [55]. The apparent horizon is

given by the null hypersurface which has vanishing expansion of the outgoing null geodesics. For (1.35) the tangent vectors to the ingoing and the outgoing null geodesics are

$$\ell_- = -\partial_z \ , \quad \ell_+ = -\frac{z^2}{L^2}\partial_v + \frac{z^2}{2L^2} f \partial_z \tag{1.40}$$

such that we satisfy

$$\ell_- \cdot \ell_- = 0 = \ell_+ \cdot \ell_+ \ , \quad \ell_- \cdot \ell_+ = -1 \ . \tag{1.41}$$

The codimension 2 spacelike hypersurface, which is orthogonal to the above null geodesics, has an area: $\Sigma = (L/z)^3$. The expansion parameters associated with this hypersurface are

$$\theta_\pm = \mathcal{L}_\pm \log \Sigma = \ell^\mu_\pm \partial_\mu \left(\log \Sigma\right) \ , \tag{1.42}$$

where $\mathcal{L}_\pm$ denotes the Lie derivatives along the null directions $\ell_\pm$. The location of the apparent horizon is then obtained by solving $\Theta = 0$, where $\Theta = \theta_- \theta_+$. In this particular case, the equation $\Theta = 0$ implies $f(z, v) = 0$. The equation for determining the apparent horizon then yields

$$1 - m(v) z^4 = 0 \quad \Longrightarrow \quad z_{\rm aH} = m(v)^{-1/4} \ . \tag{1.43}$$

Here $z_{\rm aH}$ denotes the apparent horizon. Note that in the future infinity, *i.e.* $v \to \infty$, the apparent horizon coincides with the actual event-horizon.

Note that, during the time-evolution, a global event-horizon exists in the background. This is generated by null geodesics in the background and is

the boundary of a causal set. Since the background (1.35) has three Killing vectors ($\partial/\partial x^i$), the location of the event-horizon is given by a curve $z(v)$. The null geodesic equation in the background (1.35) is given by

$$\frac{dz_{\rm H}(v)}{dv} = -\frac{1}{2} f\left(z_{\rm H}(v), v\right) \ , \tag{1.44}$$

where $z_{\rm H}$ denotes the location of the event-horizon. In the limit $v \to +\infty$, we have $z_{\rm aH} = z_{\rm H}$; however, this is not true in the $v \to -\infty$ limit, *i.e.* the event-horizon lies above the apparent horizon.

It was argued in [55] that, during a time-evolution, it is the apparent horizon rather than the event-horizon that can define a "thermodynamics". Based on an analogy, we can define a "temperature function" and an "entropy function" in terms of the apparent horizon

$$T(v) = -\left.\frac{1}{4\pi}\frac{d}{dz} f(z,v)\right|_{z_{\rm ah}} = \frac{d}{4\pi} m(v)^{1/4} \ , \tag{1.45}$$

$$S(v) = V_3\, m(v)^{-3/4} \ . \tag{1.46}$$

Here V_3 denotes the volume of the $\vec{x}$-directions. The temperature function is obtained by computing the surface gravity at the apparent horizon and the entropy function is obtained as the area of the apparent horizon. Clearly, $T(v)$ and $S(v)$ have well-defined thermodynamic meaning in the limit $v \to +\infty$.

Now, taking derivative of these functions with respect to v, we get

$$\frac{dT(v)}{dv} \sim \frac{dS(v)}{dv} \sim \frac{dm}{dv} \geq 0 \ , \tag{1.47}$$

where we have used the constraint coming from the null energy condition in (1.39). From the perspective of the boundary theory, if it makes sense to talk

about a "temperature function" or an "entropy function" as defined above, the null energy condition implies that these must be monotonically increasing. Thus, we can say that all the above observations are physically equivalent.

1.2.4 Computational tools

1.2.4.1 Two-point functions: the WKB approximation

According to the GKPW prescription (1.11), in order to compute correlation functions we need to solve the classical equation of motion for a bulk field $\phi(t, \vec{x}, z)$ that couples in the boundary to a given gauge invariant operator $\mathcal{O}(t, \vec{x})$, subject to the appropriate boundary conditions [56, 57]. In practice, however, the equations of motion for general time-dependent backgrounds are highly non-linear and only exceptional cases with high amount of symmetry are actually analytically solvable. Here we will provide an alternative recipe which is valid for operators of large conformal dimension Δ.

Recall that for massive scalar fields, in order to have an acceptable near-boundary behavior of (1.11) we must require that $\Delta = 2 + \sqrt{m^2 + 4}$, so large conformal dimension means large mass. In particular, in this limit $\Delta \sim m$ which means that we can make use of the WKB approximation [58, 59]. The Green's function for ϕ is a Green's function of the Klein-Gordon operator $H = -i\partial^2 + m^2 = p^2 + m^2$; we can represent this Green's function as

$$G \equiv \frac{-i}{H} = \int_0^\infty e^{-iNH} dN \,, \tag{1.48}$$

so that using the standard path integral construction, we get

$$\langle x|G|x'\rangle = \int_0^\infty dN \int \mathcal{D}x\,\mathcal{D}p\,\exp\left\{i\int_0^1 \left[\dot{x}p - N(p^2+m^2)\right] d\lambda\right\}. \quad (1.49)$$

We can interpret N as a field in some appropriate gauge-fixing. This can be made explicit by introducing a gauge-fixing condition and determinant:

$$\langle x|G|x'\rangle = \int \mathcal{D}N\,\mathcal{D}x\,\mathcal{D}p\,\Delta(x)\,\exp\left\{i\int_0^1 \left[\dot{x}p - N(p^2+m^2)\right] d\lambda\right\}, \quad (1.50)$$

where now N is a field to be integrated over. Now, in the WKB approximation, we can integrate out the fields N and p by replacing them in the action with their on-shell values. Their equations of motion are:

$$p^2 + m^2 = 0 \qquad \text{and} \qquad \dot{x} - 2Np = 0\,, \quad (1.51)$$

respectively, so their on-shell values are:

$$p = \frac{m\dot{x}}{\sqrt{-\dot{x}^2}} \qquad \text{and} \qquad N = \frac{\sqrt{-\dot{x}^2}}{2m}\,. \quad (1.52)$$

The correlator then becomes

$$\langle x|G|x'\rangle = \int \mathcal{D}x\,(\cdots)\exp\left\{-\int_0^1 \left(m\sqrt{\dot{x}^2}\right) d\lambda\right\}, \quad (1.53)$$

where the dots represent functional determinants that can be neglected at leading order in the WKB approximation. Approximating the path integral over x using the saddle point method, we get

$$\langle x|G|x'\rangle = \exp\left\{-m\,\mathcal{S}[x_0]\right\}, \quad (1.54)$$

where x_0 is a solution to the equations of motion that come from the action

$$\mathcal{S}[x] = \int d\lambda \sqrt{\dot{x}^2} \,. \tag{1.55}$$

This last expression is precisely the action for a geodesic. Since we are interested in a boundary-boundary propagator, the two points x and x' are located at the $z = 0$ hypersurface, and thus the geodesic length is divergent. In order to renormalize one assumes that the two points are located at some finite $z = \epsilon$, and then one subtracts the divergent piece $\mathcal{S} - \mathcal{S}_{\text{div}}$, *i.e.* the terms containing positive powers of ϵ^{-1} and logarithms.

Putting all together, we get that

$$\langle x|G|x'\rangle \equiv \langle \mathcal{O}(x)\mathcal{O}(x')\rangle = e^{-\Delta \mathcal{S}_{\text{ren}}} \,, \tag{1.56}$$

where $\mathcal{O}(x)$ is a gauge invariant operator with conformal dimension Δ and $\mathcal{S}_{\text{ren}}$ is the renormalized geodesic length connecting the points x and x'.

1.2.4.2 Wilson loops

Wilson loops are another relevant set of non-local observables that we will study in some detail. The Wilson loop operator is defined as

$$W(\mathcal{C}) = \frac{1}{N}\text{tr}\left(\mathcal{P}\, e^{\oint_{\mathcal{C}} A}\right) \,, \tag{1.57}$$

where $\mathcal{C}$ is a closed loop in spacetime. It involves the path-ordered integral of the gauge connection along the given contour. The trace is taken over some representation of the gauge group but for our purposes we will only need the

case of the fundamental representation. In this case, we can view the Wilson loop as the phase factor associated to the propagation of a very massive quark in the fundamental representation of the gauge group.

We would like to compute Wilson loops holographically, but in order to do so we first have to add matter in the fundamental representation to the SYM theory. This can be easily achieved by adding a stack of N_f "flavor branes" on top of the original stack of N D3-branes [60]. More specifically, we will consider the following system of D3's and D7's:

	0	1	2	3	4	5	6	7	8	9
D3:	×	×	×	×						
D7:	×	×	×	×	×	×	×	×		

where the numbers denote the spacetime directions and the "×" tell us the directions in which the D-branes lie. Let us assume that the distance of closest approach between the D7's and the D3's is r_m. It can be shown that eight supersymmetries are preserved by such a configuration provided we leave all the branes at zero temperature. Indeed, the dynamics of low-energy excitations is completely determined by the supersymmetry. The difference in this case is that, apart from the D3-D3 string excitations, we also have to take into account the D7-D7 and D3-D7 sectors. The D3-D7 strings, in particular, are described in terms of massive scalars and fermions, *fundamentally* charged under the $SU(N)$ gauge group of the D3-branes. Their mass is just $m = r_m/2\pi l_s^2$, simply because this is the tension of a string with length r_m.

In order to simplify the description of the system we can work in the $N_f \ll N$ limit, so that the backreaction of the D7-branes on the bulk geometry

can be neglected. In this case we can simply replace the D3-branes by the AdS background and then put the stack of D7-branes on top of this geometry. The D7-branes cover the four gauge theory directions x^μ and extend along the radial AdS direction up from the boundary at $z = 0$ to a position $z = z_m$ where they "end" (meaning that the $S^3 \subset S^5$ that they are wrapped on shrinks down to zero size). In particular, in the limit $m \to \infty$ we obtain $z_m \to 0$, so the branes remain arbitrarily close to the boundary.

From the gauge theory perspective, the introduction of the D7-branes in the AdS background is equivalent to the addition of N_f hypermultiplets in the fundamental representation of the $SU(N)$ gauge group and these are the degrees of freedom that we refer to as quarks even though they include both spin 1/2 and spin 0 fields. In particular, a single heavy quark corresponds to an open string that hangs from the boundary of AdS at $z = z_m \to 0$. According to the AdS/CFT dictionary, the expectation value of the Wilson loop operator (1.57) can be identified with the open string partition function [61],

$$\langle W(\mathcal{C}) \rangle = \int \mathcal{D}\Sigma \, e^{-S_{\rm NG}(\Sigma)} \,, \tag{1.58}$$

where the integral runs over all worldsheets Σ with boundary condition $\partial\Sigma = \mathcal{C}$. Here, $S_{\rm NG}$ is the usual Nambu-Goto action,

$$S_{\rm NG} \equiv \int d\tau d\sigma \mathcal{L}_{\rm NG} = \frac{1}{2\pi l_s^2} \int d\tau d\sigma \sqrt{-\det h_{ab}} \,, \tag{1.59}$$

and $h_{ab} = \partial_a x^\mu(\tau,\sigma) \partial_b x^\nu(\tau,\sigma) g_{\mu\nu}$ the induced metric on the worldsheet. Note that the determinant picks up a factor of L^4 from the bulk metric. Therefore,

in the limit of large 't Hooft coupling,

$$\frac{L^2}{l_s^2} = \sqrt{\lambda} \gg 1\,, \tag{1.60}$$

we can make use of the saddle point approximation and (1.58) reduces to

$$\langle W(\mathcal{C})\rangle = e^{-S_{\rm NG}(\Sigma_0)}\,. \tag{1.61}$$

Here Σ_0 is the classical solution to the equations of motion that follow from the Nambu-Goto action, subject to the boundary condition $\partial\Sigma = \mathcal{C}$.

Finally, it is worth pointing out that equation (1.61) generally leads to a divergent result when is evaluated on-shell. This is due to the fact that the worldsheet Σ_0 reaches the boundary of AdS, which has infinite volume. We can easily remove the divergences by means of the minimal subtraction scheme (explained in the previous section). The renormalization method is then equivalent to that of the two point functions in the WKB approximation.

1.2.4.3 Entanglement entropy

Entanglement entropy is our final example of a non-local observable that can be used to probe the evolution of a system. Here we will briefly review its definition and the prescription for computing it holographically.

When we consider an arbitrary quantum field theory with many degrees of freedom, we can ask about the entanglement of the system. To describe the system, we define a density matrix, ρ, which is a self-adjoint, positive semi-definite, trace class operator. Now, on a constant time Cauchy surface we can

imagine dividing the system into two subsystems A and A^c, where A^c is the complement of A. The total Hilbert space then factorizes as $\mathcal{H}_{\text{total}} = \mathcal{H}_A \otimes \mathcal{H}_{A^c}$. For an observer who has access only to the subsystem A, the relevant quantity is the reduced density matrix, which is defined as

$$\rho_A = \text{tr}_{A^c}\, \rho \ . \tag{1.62}$$

The entanglement between A and A^c is measured by the *entanglement entropy*, which is defined as the von Neuman entropy using this reduced density matrix

$$S_A = -\text{tr}_A\, \rho_A \log \rho_A \ . \tag{1.63}$$

In AdS/CFT, Ryu and Takayanagi [62] conjectured a formula to compute the entanglement entropy of quantum systems with a static gravity dual. According to [62], the entanglement entropy of a region A of the quantum field theory is given by

$$S_A = \frac{1}{4G_N} \min \left[\text{Area}\left(\gamma_A\right) \right] \ , \tag{1.64}$$

where G_N is the bulk Newton's constant, and γ_A is the codimension-two area surface such that $\partial \gamma_A = \partial A$. For background with time dependence, this proposal has been successfully generalized by Hubeny, Rangamani and Takayanagi in [63]. In this case

$$S_A = \frac{1}{4G_N^{(d+1)}} \text{ext} \left[\text{Area}\left(\gamma_A\right) \right] \ , \tag{1.65}$$

where now minimal area surface is replaced by extremal surface. Notice the similitude between (1.65), the prescription for computing Wilson loops (1.61) and the prescription for computing two-point functions (1.56). In particular,

notice that all of them involve the computation of geometric quantities in the bulk geometry. In the case of $\mathcal{N} = 4$ SYM, the (non-compact part of the) bulk is 5-dimensional so entanglement entropy is computed extremizing a volume. More generally, in other examples of the $\mathrm{AdS}_{d+1}/\mathrm{CFT}_d$ correspondence in different number of dimensions, entanglement entropy is computed from a $(d-1)$-hypersurface.

Finally, it is well known that entanglement entropy of a spatial region in a quantum field theory is UV-divergent

$$S_A = S_{\text{div}} + S_{\text{finite}} \ . \tag{1.66}$$

Only local physics contributes to the UV-divergent piece S_{div}. On the other hand S_{finite} contains information about the long range entanglement, and is the main quantity we are interested in. In the gravity side, the divergent terms arise from the near-boundary contribution to the area of γ_A. In order to extract the finite piece we can use the minimal subtraction scheme. The renormalization proceeds in a similar way as for Wilson loops or two-point functions, discussed in the previous two sections.

1.3 Outline of the thesis

As mention earlier in Section 1.1, the main goal of this thesis is to develop new computational tools in the framework of the AdS/CFT correspondence in order to gain insight into the subject of out-of-equilibrium quantum field theory. We study a variety of settings, some of them leading to

thermalization, cooling down or coherent oscillations of the quantum fields. Dynamical processes as the ones we study are extremely interesting to explore and learn about, since we do not have a good understanding of the physics governing systems completely out-of-equilibrium, specially at strong coupling. Some of them might even have practical applications, ranging from the physics of heavy-ion collisions to condensed matter physics experiments.

This thesis is organized as follows. In Chapter 2 we study in more dept the physics of gravitational collapse as a model of holographic thermalization. Specifically, we study the effect of a non-vanishing chemical potential on the thermalization time of a strongly coupled gauge theory in $(2+1)$-dimensions, using a specific bottom-up gravity model in asymptotically AdS space [22]. As mentioned in Section 1.2.3, such a process might be phenomenologically described by means of a Vaidya-like geometry; the only difference is that we have to include the effects of the non-vanishing chemical potential, but this can be easily achieved by adding a charge to the collapsing shell. These geometries have been studied in the past by a number of authors, see *e.g.* [64, 65]. The idea here is to go a step forward and study a real collapse of a bulk scalar field. In Section 2.2 we start with a brief motivation of the problem, from the field theory perspective. In Section 2.3 we construct a perturbative solution to the gravity-equations, which dynamically interpolates between two AdS black hole backgrounds with different temperatures and chemical potentials, in a perturbative expansion of a bulk scalar field. In the dual field theory, this corresponds to a quench dynamics by a marginal operator, where the corre-

sponding coupling serves as the small parameter in which the perturbation is carried out. We find that, at the leading order in the perturbation, the solution takes the form of a Vaidya background, thus, validating the Vaidya-based phenomenology [64, 65] from a first principle gravity computation. In Section 2.4 we discuss the thermodynamics of the initial and final states of the field theory. Finally, in section 2.4 we study the evolution of non-local observables. We focus only on entanglement entropy since, as shown in [64, 65], this is the observable that reaches equilibrium at a slower rate, thus setting the relevant time-scale for thermalization. Our results also supports the main observation in [64, 65], namely that for short distances the thermalization time decreases with increasing chemical potential.

In Chapter 3 we study a specific model that leads to hydrodynamic expansion and cooling, in the spirit of the fluid/gravity duality [20]. The motivation here is to model the last stage of the evolution of the quark-gluon plasma, which has been produced experimentally at RHIC and LHC. We recall that, in the framework of gravitational collapse, states that evolve towards the vacuum of the theory are prohibited because they violate the null energy condition. This implies that the physical mechanisms studied here are completely different to the ones leading to thermalization, which makes the analysis more interesting. We start in Section 3.2 with a brief review of hydrodynamics in the AdS/CFT correspondence. We discuss both, the linear response theory and the full non-linear theory, and we show how to construct the dual to an expanding, boost-invariant plasma. At this level we already see various in-

dications that suggest a universal behavior of the relaxation rates in gauge theory plasmas with a gravity dual formulation. In Section 3.3 we turn to the computation of the late-time evolution of various non-local observables. Two-point functions are found to decay exponentially at late times. Moreover, if the points are separated along the collision axis we find that the exponential is modulated by a non-monotonic function of the rapidities and a dimensionless combination of the shear viscosity and proper time. This peculiar behavior constrains the regime of validity of the hydrodynamic approximation. Similar results are also found for certain Wilson loops and entanglement entropies but in all these cases the bound on the hydrodynamic expansion is weaker than in the case of the two-point functions.

Finally, in Chapter 4 we construct and study a family of perturbative solutions in global AdS that are periodic in time [66]. According to the AdS/CFT dictionary, these bulk solutions are dual to states of a strongly interacting boundary CFT that fail to thermalize at late times and hence are candidates to describe "quantum revivals", studied in the condensed matter literature. From the gravity perspective, the backgrounds we find are interesting because they add to the discussion of the nonlinear stability of AdS, a subject that has been debated in recent years. In Section 4.2 we begin with a brief motivation of the problem and we argue that such undamped periodic states must exist, both from the field theory and the gravity perspective. In Section 4.3 we introduce the perturbative formalism and we show how to solve the equations of motion order by order in the perturbation. The general

conclusion here is that we can reabsorb the resonances that would potentially lead to black hole collapse into frequency shifts of the various Fourier modes. In Section 4.4 we study the evolution of entanglement entropy for different regions of the dual CFT. We show that these quantities can be thought of as an infinite set of conserved charges in the state of the theory. Hence, the system is integrable.

Chapter 2

Black hole formation: holographic thermalization

2.1 Introduction

In this Chapter we will study in detail the physics of gravitational collapse as a model of holographic thermalization, using a specific bottom-up gravity model in asymptotically AdS space [22].

A generic thermalization process typically describes the dynamical evolution from a "low temperature" phase to a "high temperature" thermal state, where the evolution is highly non-trivial and, in the case of a black hole formation process, highly non-linear as well. Holographically, such a process in asymptotically AdS space can be set up by turning on a non-normalizable (or a normalizable) mode of a bulk scalar field; as a result a shell of the corresponding field collapses in AdS space. It was shown in [67], using a weak-field perturbation method, that if the boundary non-normalizable mode is chosen to be coordinate independent and only have support over a brief time interval, the collapse of the corresponding homogeneous wave will always lead to black hole formation.

On the other hand, an alternate approach is to phenomenologically

model the black hole formation process with as much simplicity as possible, such that the corresponding geometry can be probed to learn further physics. The hope is to learn at least qualitatively useful lessons which are presumably not heavily dependent on the details of the model. In the present context this can be achieved by exploring the AdS-Vaidya background, which describes a smooth evolving geometry from an empty AdS to an AdS-Schwarzschild background. Gravitationally, this geometry describes the collapse of a null dust in an asymptotically AdS-space. Probing this geometry has already led to numerous interesting results, see *e.g.* [68, 69, 70, 71, 64, 65], where the behavior of various non-local observables in such a dynamical geometry has been explored.

In [67], an interesting bridge between these two approaches has been established. The authors studied a collapse process for a massless scalar field in a so called "weak field approximation" limit, where the amplitude of the perturbation was chosen small and a perturbative solution of the Einstein's equations was obtained. At the leading order, this solution takes the form of an AdS-Vaidya background which is characterized by one mass function that interpolates between an AdS vacuum to an AdS-Schwarzschild geometry. In the dual field theory side, this corresponds to a dynamical evolution from zero temperature ground state to a thermal state of a certain large N gauge theory (such as the $\mathcal{N} = 4$ super Yang-Mills or the ABJM theory). Thus, at least at the leading order, the analysis of [67] validates the AdS-Vaidya-based phenomenology from a first principle gravity computation.

Motivated by this observation, we will explore the possibility of introducing a conserved charge in the boundary theory — the simplest case of an U(1)-charge — in an analogue of the "weak field approximation" limit starting from an effective gravity action. Our motivation is to address how thermalization time is affected in the presence of global conserved charges in a strongly coupled system, with as much analytical control as possible. This may be relevant for understanding the effect of a non-vanishing chemical potential (or a finite-density) on the strong coupling dynamics of out-of-equilibrium QCD at RHIC or at LHC. We will thus generalize the construction of [67] introducing a chemical potential, which — albeit in a suitable approximation — will provide an analytical control on the background. This also provides us with a model in which non-local observables can subsequently be studied to explore the behaviour of thermalization time, in the spirit of [64, 65].

Our results may be of general interest, beyond the QGP physics. For example, a qualitative behaviour, if it is universal, may shed light in condensed matter systems which are typically accompanied by a non-vanishing chemical potential. Moreover, to the best of our knowledge, there is no known field theoretic result about how thermalization time scales in a strongly coupled finite density system. Thus it is useful to explore models where this possibility can be realized.

This chapter is divided in the following parts: we begin with a brief overview and the setup of the problem in section 2.2. In section 2.3 we present the effective gravity model and provide the details of the perturbative solution.

We then discuss the initial and the final states in details in section 2.4, and subsequently discuss the behaviour of the thermalization time in section 2.5. Finally we conclude in section 2.6.

2.2 Setup of the problem

Let us begin with a more specific description of the problem. We will discuss a thermal quench, and for simplicity we will restrict ourselves to a $(2+1)$-dimensional large N gauge theory in the strong coupling regime. Now, consider the Hamiltonian (or the Lagrangian) of the system, denoted by H_0 (or $\mathcal{L}_0$), which is perturbed by a time-dependent perturbation of the form

$$H_\lambda = H_0 + \lambda(t)\delta H_\Delta \quad \Longrightarrow \quad \mathcal{L}_\Delta = \mathcal{L}_0 + \lambda(t)\mathcal{O}_\Delta \ , \tag{2.1}$$

where H_0 (or $\mathcal{L}_0$) describes the Hamiltonian (or the Lagrangian) of the original quantum field theory, $\lambda(t)$ is an external parameter and δH_Δ (or $\mathcal{O}_\Delta$) corresponds to the deformation of the QFT by an operator of dimension Δ.

Here we will restrict ourselves completely on asymptotically locally AdS-spaces, which implies that there is an underlying conformal field theory (CFT) that governs the physics. As a first attempt, we restrict ourselves to the case of $\Delta = d$, which here becomes $\Delta = 3$, *i.e.* an exactly marginal deformation. In principle, it is possible to study the quench dynamics by a relevant operator as well. However, we know that relevant operators can trigger an RG-flow and there may be a new CFT — or perhaps a non-relativistic cousin of it — that emerges in the infrared. In such a situation, unless we

consider a temperature scale much larger than the scale set by the relevant operator, the black hole formation process may be governed by this infrared geometry instead.[1]

To avoid this possible subtlety for relevant operators, we will consider an exactly marginal operator, which does not require a hierarchy between the RG-scale and the temperature-scale. Thus the underlying CFT will remain the same and in the gravitational dual it will suffice for us to specify the asymptotically locally AdS condition with a given radius of curvature as the boundary condition.

Now we need to specify the initial conditions. Typically this is specified at $t \to -\infty$ (in which limit $\lambda \to 0$) as a particular energy eigenstate of the QFT Hamiltonian H_0. As the new coupling is turned on, depending on whether the process is adiabatic or abrupt, the system is expected to evolve differently with the Hamiltonian H_λ. In a quantum mechanical system, under an adiabatic process the system remains in an energy eigenstate whose energy evolves with time following the response of the time-evolution of $\lambda(t)$. On the other hand, for an abrupt quench, the system evolves in a linear superposition of eigenstates of the new Hamiltonian H_λ. Here we will focus on the fast quench only, in which the initial state is macroscopically characterized by $\{E, \langle \mathcal{O}_\phi \rangle, \mu, T\}_{\text{initial}}$ — with E, $\langle \mathcal{O}_\phi \rangle$, μ and T respectively representing the energy, VEV for the marginal operator, chemical potential and the temper-

[1]Note that, quench dynamics of relevant operators have been considered in details in *e.g.* [75, 76, 77].

ature of the state in consideration — and the final state is macroscopically characterized by $\{E, \langle \mathcal{O}_\phi \rangle, \mu, T\}_{\text{final}}$.

To properly account for the scale of measuring dimensionful quantities, we define the following dimensionless parameters:

$$\kappa_E = \frac{E}{T^3} \ , \quad \kappa_{\langle \mathcal{O}_\phi \rangle} = \frac{\langle \mathcal{O}_\phi \rangle}{T^3} \ , \quad \kappa_\mu = \frac{\mu}{T} \ , \tag{2.2}$$

which means that we measure all dimensionful quantities in units of temperature of the corresponding state. Evidently, there can be several hierarchy of scales depending on how κ_E, $\kappa_{\langle \mathcal{O}_\phi \rangle}$ and κ_μ are parametrically separated. Furthermore, there are a couple of dimensionful parameters associated with the quench process itself: the energy injected (denoted by ΔE), and the duration (denoted by δt) or the rapidity of the quench. Thus we can further define

$$\kappa_{\text{quench}} = (\Delta E) \, (\delta t)^3 \quad \text{with} \quad \Delta E = E_{\text{final}} - E_{\text{initial}} \ . \tag{2.3}$$

Now, our initial state is characterized by the following parametric regime

$$\kappa_E^{\text{initial}} \sim \mathcal{O}(1) \ , \quad \kappa_{\langle \mathcal{O}_\phi \rangle}^{\text{initial}} = 0 \ , \quad \kappa_\mu^{\text{initial}} \ll 1 \ . \tag{2.4}$$

The quench process, to be amenable to a perturbative analysis, is characterized by

$$\kappa_{\text{quench}} \ll 1 \quad \text{with} \quad \mathcal{O}\left(\kappa_{\text{quench}}\right) = \mathcal{O}\left(\kappa_\mu^{\text{initial}}\right) \ . \tag{2.5}$$

Finally, the final state is characterized by

$$\kappa_E^{\text{final}} \sim \mathcal{O}(1) \ , \quad \kappa_{\langle \mathcal{O}_\phi \rangle}^{\text{final}} \sim \kappa_\mu^{\text{initial}} \ll 1 \ , \quad \kappa_\mu^{\text{final}} \sim \kappa_\mu^{\text{initial}} \ll 1 \ . \tag{2.6}$$

We remind the reader that the conditions in (2.4)-(2.6) are specific to our perturbative analysis. We further note that, the perturbative solution that we construct is not similar to the AdS-RN-Vaidya geometry described and analyzed in [65] and thus provides a more generic case-study. It is amusing to further note that the regime of parameters outlined in (2.6) physically implies that we are considering a small chemical potential limit, which is qualitatively similar to the QGP-phase at the LHC.

The geometric data describing the corresponding evolution is given by a metric, a gauge field, and a scalar field: $\{G, A, \phi\}$ of the following form

$$\begin{aligned} ds^2 &= G_{\mu\nu}\left(\mathcal{U}_{\rm EF}\right) dX^\mu dX^\nu \ , \\ &= -\frac{2}{z^2} dv dz - g(z,v) dv^2 + f(z,v)^2 \sum_{i=1}^{2} dx_i^2 \ , \qquad (2.7) \\ A &= A_v(z,v) dv \ , \quad \phi = \phi(z,v) \ , \qquad (2.8) \end{aligned}$$

where $\mathcal{U}_{\rm EF}$ denotes the ingoing Eddington-Finkelstein (EF) patch, $g(z,v)$ and $f(z,v)$ are two functions that are determined by solving the equations, z is the radial coordinate (in which the boundary is located at $z \to 0$) and v is the EF-ingoing null direction. We obtain a dynamical evolution that can be summarized as:

$$\begin{aligned} \{G, A, \phi\}|_{v \to -\infty} &= {\rm AdS} - {\rm RN}_{\rm initial}\left(\mu_i, T_i, \phi = 0\right) \ , \qquad (2.9) \\ \{G, A, \phi\}|_{v \gg \delta t} &= {\rm AdS} - {\rm BH}_{\rm final}\left(\mu_f, T_f, \phi \neq 0\right) \ . \qquad (2.10) \end{aligned}$$

Let us now comment on the evolution of the event-horizon and the apparent horizon. We begin with the notion of the apparent horizon. Following [65], let

us define the tangent vectors to the ingoing and outgoing null geodesics

$$\ell_- = -\partial_z \ , \quad \ell_+ = -z^2\partial_v + \frac{g(z,v)}{2} z^4 \partial_z \ , \tag{2.11}$$

which satisfy

$$\ell_- \cdot \ell_- = 0 \ , \quad \ell_+ \cdot \ell_+ = 0 \ , \quad \ell_- \cdot \ell_+ = -1 \ . \tag{2.12}$$

The co-dimension two spacelike surface, which is orthogonal to the tangent vectors above, has the following volume element

$$\Sigma = f\left(z,v\right)^2 \ . \tag{2.13}$$

The expansion of this volume element along the ingoing and outgoing null directions are given by

$$\theta_\pm = \mathcal{L}_\pm \log\Sigma = \ell^\mu_\pm \partial_\mu \left(\log\Sigma\right) \ . \tag{2.14}$$

Here $\mathcal{L}_\pm$ denotes the Lie derivatives along the null direction corresponding to $\ell^\mu_\pm$. Now, we can define the invariant expansion by $\Theta = \theta_+\theta_-$ which is given by

$$\begin{aligned} &\Theta = \frac{\left(\partial_z f(z,v)\right)}{f(z,v)} \left[2z^2 \frac{\left(\partial_v f(z,v)\right)}{f(z,v)} - z^4 \frac{\left(\partial_z f(z,v)\right)}{f(z,v)} g(z,v)\right] \ , \quad \text{with} \\ &\Theta\left(z = z_{\rm aH}\right) = 0 \ . \end{aligned} \tag{2.15}$$

Here $z_{\rm aH}$ denotes the location of the apparent horizon.

On the other hand, the event horizon is a null surface in the background (2.7):

$$\mathcal{N} = z - z_{\rm H}(v) \quad \text{obeying} \quad G^{\mu\nu}\left(\partial_\mu \mathcal{N}\right)\left(\partial_\nu \mathcal{N}\right) = 0 \ , \tag{2.16}$$

which gives

$$\partial_v z_{\rm H}(v) = -\frac{1}{2} z_{\rm H}^2 g\left(z_{\rm H}, v\right) \ . \tag{2.17}$$

Thus, solving (2.15) and (2.17) gives the time-evolution of the apparent and the event horizon, respectively. Evidently, at the initial and the final states they coincide: $z_{\rm H} = z_{\rm aH}$. During the evolution, since the collapse is sourced by a physically reasonable matter field, the apparent horizon lies behind the event horizon, *i.e.* $z_{\rm aH} > z_{\rm H}$ in our choice of the radial coordinate. One way to summarize our perturbative solution is to state that the evolution of *e.g.* the event-horizon can be obtained in a series expansion as follows:

$$\begin{aligned} \text{Given that} \quad g(z,v) &= \sum_{n=0} \varepsilon^{2n} g_{(2n)}\left(z_{\rm H}, \frac{v}{\delta t}\right) \ , \\ \text{construct} \quad z_{\rm H} &= z_{\rm H}^{(0)} \left[1 + \sum_{n=1} \varepsilon^{2n} \Upsilon_{(2n)}\left(\frac{v}{\delta t}\right)\right] \ , \end{aligned} \tag{2.18}$$

where Υ_{2n} can be determined from a first order differential equation of the form

$$\partial_v \Upsilon_{(2n)} = \Xi\left[\left\{\Upsilon_{(2n)}\right\}, \left\{\partial^n_{z_{\rm H}} g_{(2m)}\right\}\right] \ , \tag{2.19}$$

where Ξ is a functional of

$$\left\{\Upsilon_{(2n)}\right\} = \left\{\Upsilon_{(2p)} \,|\, 1 \leq p \leq n\right\} \ , \quad \left\{\partial^n_{z_{\rm H}} g_{(2m)}\right\} = \left\{\partial^p_{z_{\rm H}} g_{(2q)} \,|\, 0 \leq (p,q) \leq n\right\} \tag{2.20}$$

and, finally, $\varepsilon \sim \kappa_{\rm quench}^{1/2} \ll 1$. In section 2.5, we will present a pictorial representation of how the apparent and the event-horizons evole.

It is clear from (2.18) that the asymptotic series captures the physics as long as $||\varepsilon^{2n}\Upsilon_{(2n)}|| \ll 1$. It will be shown In section 2.3.3, that this

imposes a constraint and our perturbative analysis is valid up to a time-scale $t_{\rm pert} \sim 1/\left(\Delta E\right)^{1/3}$. For $t \gg t_{\rm pert}$, we will need to solve the system of equations numerically, which we will not pursue here. Written in terms of the duration of the pulse, the perturbative treatment is valid up to a time-scale $t_{\rm pert}$ which is given by

$$t_{\rm pert} = \mathcal{O}\left(\frac{\delta t}{\varepsilon^{2/3}}\right) \ . \tag{2.21}$$

Thus, by tuning $\varepsilon \ll 1$, we parametrically separate $t_{\rm pert}$ and δt at will, and in this sense our approach is equivalent to considering an "fast quench". In the strict fast quench limit, *i.e.* $t_{\rm pert}/(\delta t) \to \infty$, the $t > t_{\rm pert}$ dynamics is completely frozen and we are left with the perturbative solution for all times.

To measure thermalization time, we need to identify suitable observables, which primarily fall in two classes: local and non-local. Note that, unlike the Vaidya-construction, for gauge-invariant local observables thermalization is not instantaneous in this case. This is buried in the details of the solution in (2.7), since as time varies, the scalar field dynamically acquires a non-zero expectation value. However, such local operators thermalize over a time-scale of $\mathcal{O}(\delta t)$, and does not contain the information about long-range correlations. On the other hand, non-local operators provide a more global information and we will explore the evolution of entanglement entropy in this chapter.

Now, let us comment on a naìve expectation about the scaling of the thermalization time. It is known that for integrable systems, which contains an infinite number of conserved charges, thermalization does not happen. This is

intuitively clear, since it becomes unlikely to populate the entire phase space. Furthermore, for a single U(1)-charge, if we consider a bosonic system, increasing the chemical potential will enhance Bose-Einstein condensation and thus will inhibit thermalization. For fermionic degrees of freedom, a higher value of chemical potential is associated with a higher Fermi surface which will subsequently need to be populated to achieve a thermal state. Thus, introducing a conserved charge is likely to have a slowing down of the thermalization time.

However, contrary to the expectation outlined in the above paragraph, we gather evidence that thermalization speeds up for increasing chemical potential in the regime $\mu/T \ll 1$. Thus, modulo the caveats of an effective gravity description and the approximate measures of the thermalization time, we are lead to think that the strong coupling dynamics perhaps gives rise to qualitatively new physics. Furthermore, since the thermalization time is unlikely to vanish for arbitrarily high chemical potential, we expect it to either saturate or turn back. In both cases, the scaling of the thermalization time seems to group the dynamics in two qualitatively different regimes: $\mu/T \ll 1$ and $\mu/T \gg 1$, much like what was observed in [65]. Now we will turn to discussing the details of our model.

2.3 Einstein-Maxwell-Dilaton system

We begin with the following action

$$S = \frac{1}{8\pi G_N^{(4)}} \int d^4x\sqrt{-G}\left[\frac{1}{2}\left(R + 6 - \frac{1}{2}(\partial\phi)^2\right) - \frac{h(\phi)}{4}F_{\mu\nu}F^{\mu\nu}\right] , \qquad (2.1)$$

which leads to the following equations of motion

$$R_{\mu\nu} - \frac{1}{2} G_{\mu\nu} \left(R + 6 \right) = T_{\mu\nu} \ , \tag{2.2}$$

$$\nabla^2 \phi - \frac{1}{2} F_{\mu\nu} F^{\mu\nu} \frac{\partial h(\phi)}{\partial \phi} = 0 \ , \tag{2.3}$$

$$\nabla_\nu \left(h(\phi) F^{\mu\nu} \right) = 0 \ , \tag{2.4}$$

where

$$T_{\mu\nu} = T_{\mu\nu}^{(\text{scalar})} + T_{\mu\nu}^{(\text{Maxwell})} \ , \tag{2.5}$$

$$T_{\mu\nu}^{(\text{scalar})} = \frac{1}{2} (\partial_\mu \phi \partial_\nu \phi) - \frac{1}{4} G_{\mu\nu} (\partial \phi)^2 \ , \tag{2.6}$$

$$T_{\mu\nu}^{(\text{Maxwell})} = h(\phi) F_{\mu\sigma} F_\nu^\sigma - \frac{1}{4} G_{\mu\nu} h(\phi) F_{\rho\sigma} F^{\rho\sigma} \ . \tag{2.7}$$

Let us now specify our ansatz which consists of the metric field, the Maxwell field and the scalar field: $\{G, A, \phi\}$. We will assume translational invariance and we choose the ingoing Eddington-Finkelstein patch to represent our ansatz data:

$$ds^2 = -\frac{2}{z^2} dv dz - g(z,v) dv^2 + f(z,v)^2 dx_i^2 \ , \tag{2.8}$$

$$\phi = \phi(z,v) \ , \tag{2.9}$$

$$A = A_v(z,v) dv \ . \tag{2.10}$$

We need two more sets of data: the boundary conditions and the initial conditions. The boundary conditions simply impose that the geometry is asymp-

totically locally AdS, which is represented by

$$g(z,v) = \frac{1}{z^2}\left(1+\mathcal{O}\left(z^2\right)\right) \qquad \text{as} \qquad z\to 0\ , \tag{2.11}$$

$$f(z,v) = \frac{1}{z}\left(1+\mathcal{O}\left(z\right)\right) \qquad \text{as} \qquad z\to 0\ , \tag{2.12}$$

$$\phi(z,v) = \phi(v)+\mathcal{O}(z) \qquad \text{as} \quad z\to 0\ , \qquad \text{and} \tag{2.13}$$

$$A_v(z,v) = \text{const}+\mathcal{O}(z) \qquad \text{as} \quad z\to 0\ . \tag{2.14}$$

This choice fixes the gauge completely.[2]

Let us specify the initial condition now. Our initial state in the dual field theory corresponds to a thermal state with a non-vanishing chemical potential. This is represented by

$$\lim_{v\to-\infty} g(z,v) = \frac{1}{z^2}\left(1-Mz^3+\frac{Q^2}{2}z^4\right)\ , \tag{2.15}$$

$$\lim_{v\to-\infty} f(z,v) = \frac{1}{z}\ , \tag{2.16}$$

$$\lim_{v\to-\infty} \phi(z,v) = 0\ , \tag{2.17}$$

$$\lim_{v\to-\infty} A_v(z,v) = \mu_i+Qz\ . \tag{2.18}$$

Our goal now is to find a solution of the system of equations in (2.2)-(2.4) subject to the initial conditions in (2.11)-(2.13) and with the asymptotically locally AdS boundary condition in (2.15)-(2.18). We want to introduce dynamics in the system by exciting a time-dependent non-normalizable mode for

[2]Demanding that $f(z,v)\sim\frac{1}{z}+\mathcal{O}(1)$ fixes the gauge redundancy which remains after choosing Eddington-Finkelstein gauge $g_{zz}=0,\ g_{vx}=0,\ g_{zv}=1$. See *e.g.* [67].

the scalar field near the boundary, which can be represented by

$$\phi_{\rm b}(v) = \begin{cases} 0 & v < 0 \\ \epsilon\ \phi_1(v) & 0 < v < \delta t \\ 0 & v > \delta t\ , \end{cases} \tag{2.19}$$

where $\phi_1(v)$ is now a function[3] of $\mathcal{O}(1)$ and the dimensionless parameter $\epsilon \ll 1$ will eventually serve as the expansion parameter. To connect with the discussion in section 2.2, we note that: $\epsilon = \kappa_{\rm quench}^{1/2}$. Note that, the energy-momentum tensor in (2.6), (2.7) evaluated on (2.19) is not of a null-dust-type, as considered in *i.e.* [65], and thus we will not encounter potential subtleties associated with violating null energy condition[11].

Before proceeding further, let us comment on the particular coordinate patch. To incorporate the dynamics, we have chosen the Eddington-Finkelstein coordinates, collectively denoted by $\mathcal{U}_{\rm EF}$, which is well-defined everywhere. On the other hand, in order to read off the stress-energy tensor of the dual field theory, it is very useful to express all data in terms of the Fefferman-Graham patch, which we denote by $\mathcal{U}_{\rm FG}$. We can define a map $\varphi : \mathcal{U}_{\rm EF} \to \mathcal{U}_{\rm FG}$, such that

$$\begin{aligned} ds^2_{\rm EF} &= -\frac{2}{z^2} dz dv - g(z,v) dv^2 + f(z,v)^2 dx_i^2 \\ &= \frac{dr^2}{r^2} + \frac{\gamma_{ab}(x,r)}{r^2} dx^a dx^b = ds^2_{\rm FG}\ , \quad a,b = 0,\ldots 2 \end{aligned} \tag{2.20}$$

[3]Note that the symmetry and boundary behavior requirements allow the scalar ϕ to be an arbitrary function of time at the boundary.

with $\varphi \equiv \{z(t,r), v(t,r)\}$ satisfying

$$\begin{aligned} \dot{v}z' + v'\dot{z} + z^2\dot{v}v' &= 0 \ , & (2.21)\\ \frac{2}{z^2}v'z' + g(z,v)v'^2 &= -\frac{1}{r^2} \ , & (2.22)\\ -r^2\left(\frac{2}{z^2}\dot{v}\dot{z} + g(z,v)\dot{v}^2\right) &= \gamma_{00} \ , & (2.23) \end{aligned}$$

where $' \equiv \partial_r$ and $\dot{} \equiv \partial_t$. Near the boundary we have

$$\gamma_{ab}(x,r) = \gamma_{ab}(x) + r^3\gamma^{(3)}_{ab}(x) + \dots \ . \tag{2.24}$$

After appropriate holographic renormalization, and using the GKPW recipe, the stress-energy tensor of the dual field theory is obtained to be [46, 47]

$$\langle T_{ab}\rangle = \frac{3}{16\pi G_N^{(4)}}\gamma^{(3)}_{ab} \ . \tag{2.25}$$

Evidently, once we obtain a solution in the $\mathcal{U}_{\rm EF}$-patch, we can use the map $\varphi : \mathcal{U}_{\rm EF} \to \mathcal{U}_{\rm FG}$ by solving equations in (2.21)-(2.23) and finally using (2.24), (2.25) we can read off the field theory stress-tensor of the corresponding state. In practice though, for the initial and the final states, the boundary energy-momentum tensor can be obtained by analyzing the thermodynamics of the corresponding state.

2.3.1 Asymptotic, $z \to 0$, expansion

Let us first investigate the near boundary behavior of the solution to (2.2)-(2.4) to ensure the asymptotically locally AdS criterion. As $z \to 0$, we

introduce the formal expansion

$$\begin{aligned} f(z,v) &= \frac{1}{z} + \sum_{n=0} z^n \mathfrak{f}_n(v) \ , \\ g(z,v) &= \frac{1}{z^2} + \sum_{n=0} z^n \mathfrak{g}_n(v) \ , \\ \phi(z,v) &= \phi_{\rm b}(v) + \sum_{n=1} z^n \mathfrak{p}_n(v) \ , \\ A_v(z,v) &= \sum_{n=0} z^n \mathfrak{a}_n(v) \ , \end{aligned} \tag{2.26}$$

where $\phi_{\rm b}(v)$, as introduced in (2.19) before, denotes the source which we are turning on at the boundary and the set of functions $\{\mathfrak{f}_n, \mathfrak{g}_n, \mathfrak{p}_n, \mathfrak{a}_n\}$ can be systematically determined from the equations of motion at each order in z-expansion.

For illustrative purpose, we provide below explicit formulae up to $\mathcal{O}(z^5)$-term

$$\begin{aligned} g(z,v) &= \frac{1}{z^2}\left[1 - \frac{3\phi_{\rm b}'(v)^2 z^2}{4} + M(v) z^3 + \frac{c^2 z^4}{2h(\phi_{\rm b})} \right. \\ &\qquad \left. + \frac{L(v)\phi_{\rm b}'(v) z^4}{2} - \frac{\phi_{\rm b}'(v)^4 z^4}{24} + \mathcal{O}(z^5)\right] , \end{aligned} \tag{2.27}$$

$$f(z,v) = \frac{1}{z}\left[1 - \frac{\phi_{\rm b}'(v)^2 z^2}{8} - \frac{L(v)\phi_{\rm b}'(v) z^4}{8} - \frac{\phi_{\rm b}'(v)^4 z^4}{384} + \mathcal{O}(z^5)\right] , \tag{2.28}$$

$$\begin{aligned} \phi(z,v) &= \phi_{\rm b}(v) + \phi_{\rm b}'(v) z + L(v) z^3 - \frac{c^2\, \dot{h}(\phi_{\rm b})}{4h(\phi_{\rm b})^2} z^4 + \phi_{\rm b}'(v) L'(v) z^4 \\ &\quad + \frac{\phi_{\rm b}'(v)}{4}\left(M(v) + \phi_{\rm b}'(v)\phi_{\rm b}''(v)\right) z^4 + \mathcal{O}(z^5) , \end{aligned} \tag{2.29}$$

$$\begin{aligned} A_v(z,v) &= \mu(v) + \frac{cz}{h(\phi_{\rm b})} - \frac{c\,\dot{h}(\phi_{\rm b})\phi_{\rm b}'(v)^2}{2h(\phi_{\rm b})^2} + \frac{c\,\phi_{\rm b}'(v)^2 z^3}{12h(\phi_{\rm b})} \\ &\quad + \frac{c\,\phi_{\rm b}'(v)^2}{6h(\phi_{\rm b})^3}\left(2\dot{h}(\phi_{\rm b})^2 - h(\phi_{\rm b})\ddot{h}(\phi_{\rm b})\right) z^3 + \mathcal{O}(z^4) , \end{aligned} \tag{2.30}$$

where c is a free parameter, $' \equiv \partial_v$ and $\dot{} \equiv \partial_\phi$. Furthermore, $L(v)$ and $M(v)$ are undetermined functions which satisfy

$$M'(v) = -\frac{1}{8}\phi_{\rm b}'(v)\left(3\phi_{\rm b}'^3(v) - 4\phi_{\rm b}'''(v) - 12L(v)\right) \ . \tag{2.31}$$

The two time-dependent functions $M(v)$ and $L(v)$, which are not determined by the asymptotic expansion above, physically correspond to the mass of the black hole and the VEV of the marginal operator, respectively. Note that, the solutions in (2.27)-(2.30) represent an asymptotic solution of the full geometry.

So far, we have imposed the asymptotically locally AdS condition in details. In order to carry out a perturbative treatment, we need to identify the "correct" initial state around which it is meaningful to carry out a perturbation order by order. We will answer this question *a priori*: it turns out that one choice for which such a perturbative treatment works is to start from an AdS-RN geometry with a "small" mass and a "small" charge. Thus, instead of arbitrary M and Q in (2.15), we rewrite them as

$$\{M, Q\} = \epsilon_1^2 \{m, q\} \ , \quad \text{with} \quad \{m, q\} \sim \mathcal{O}(1) \ , \tag{2.32}$$

where $\epsilon_1 \ll 1$ is another small parameter. We can identify $\epsilon_1 = \kappa_\mu^3$ to connect to the discussion in section 2.2. Clearly, ϵ and ϵ_1 are hitherto independent parameters.

Thus, the initial state can be written as

$$g(z,v) = \frac{1}{z^2}\left(1 - m\epsilon_1^2 z^3 + \frac{q^2\epsilon_1^4}{2} z^4\right) \qquad (v<0)\ , \tag{2.33}$$

$$f(z,v) = \frac{1}{z} \qquad (v<0)\ , \tag{2.34}$$

$$A_v(z,v) = \mu_i + q\epsilon_1^2 z \qquad (v<0)\ . \tag{2.35}$$

Here μ_i can be fixed by demanding regularity of the gauge field at the event horizon.

2.3.2 Expansion in amplitude of $\phi_{\rm b}(v)$

To solve the equations of motion, we now work with the following formal expansion

$$f(z,v) = \sum_{n=0} \epsilon^n f_n(z,v)\ , \tag{2.36}$$

$$g(z,v) = \sum_{n=0} \epsilon^n g_n(z,v)\ , \tag{2.37}$$

$$\phi(z,v) = \sum_{n=0} \epsilon^n \Phi_n(z,v)\ , \tag{2.38}$$

$$A_v(z,v) = \sum_{n=0} \epsilon^n A_{v_n}(z,v)\ , \tag{2.39}$$

where the data $\{f_n, g_n, \Phi_n, A_{v_n}\}$ are to be systematically determined from the equations of motion.

In order to perturbatively solve the equations of motion and motivated by convenience, we will treat ϵ_1 as a parameter of $\mathcal{O}(\epsilon)$. Thus,

$$\epsilon_1 = k\,\epsilon\ , \quad \text{with} \quad k \sim \mathcal{O}(1)\ . \tag{2.40}$$

Note that the above relation is akin to the condition $\mathcal{O}(\kappa_\mu) = \mathcal{O}(\kappa_{\rm quench})$. It is clear that in this regime we regroup the dynamical contributions at various unrelated orders involving ϵ and ϵ_1. Physically this corresponds to linearly combining processes which occur at *e.g.* $\mathcal{O}(\epsilon^2)$ and $\mathcal{O}(\epsilon_1^2)$, and hence there is only one expansion parameter at the end.

We will be able to check two independent limits of setting $\epsilon \to 0$ and $\epsilon_1 \to 0$ using (2.40). Solving the dilaton equation of motion requires $\dot{h}(0) = 0$. Similarly, from Einstein field equation we obtain $h(0) = 1$. To present the explicit solution up to, *e.g.* $\mathcal{O}(\epsilon^4)$, we first define the following functions

$$C_2(v) = -\frac{1}{2}\int_{-\infty}^{v} \phi_1'(x)\phi_1'''(x)dx \ , \tag{2.41}$$

$$C_4(v) = \frac{3}{8}\int_{-\infty}^{v} \phi_1'(x)\left(-\phi_1'(x)^3 + \int_{-\infty}^{x}(B(y) - mk^2\phi_1'(y))dy\right)dx \ , \tag{2.42}$$

$$B(x) = \phi_1'(x)\left(C_2(x) + \phi_1'(x)\phi_1''(x)\right) \ , \tag{2.43}$$

$$P(v) = \frac{1}{4}\int_{-\infty}^{v}\left(-mk^2\phi_1'(x) + B(x)\right)dx \ , \tag{2.44}$$

$$a_4(v) = -qk^2\int_{-\infty}^{v}\phi_1(x)\phi_1'(x)\ddot{h}(0)dx \ . \tag{2.45}$$

In order to properly account for the powers of ϵ, let us write the ϵ-dependence of $C_4(v), P(v)$ and $a_4(v)$ explicitly. From (2.42), (2.44) and (2.45) we have,

$$C_4(v) = c_4(v) + mk^2\mathfrak{c}_4(v) \ , \tag{2.46}$$

$$P(v) = p(v) + mk^2\mathfrak{p}(v) \ , \tag{2.47}$$

$$a_4(v) = qk^2\mathfrak{a}_4(v) \ , \tag{2.48}$$

where now neither c_4, p nor $\mathfrak{c}_4, \mathfrak{p}, \mathfrak{a}_4$ depend on ϵ. With these definitions the

solution can now be written as:[4]

$$
\begin{aligned}
g(z,v) = \frac{1}{z^2} - mz\epsilon_1^2 + \frac{q^2\epsilon_1^4}{2}z^2 - \left(zC_2(v) + \frac{3}{4}\phi_1'(v)^2\right)\epsilon^2 \\
+ \left[zc_4(v) + \frac{z^2}{24}\left(12p(v)\phi_1'(v) - \phi_1'(v)^4\right)\right. \\
\left. + \frac{z^3}{12}\left(3p(v)\phi_1''(v) - p'(v)\phi_1'(v) - C_2(v)\phi_1'(v)^2\right)\right]\epsilon^4 \\
+ m\left[z\mathfrak{c}_4(v) + \frac{z^2}{2}\mathfrak{p}(v)\phi_1'(v)\right. \\
\left. + \frac{z^3}{12}\left(3\mathfrak{p}(v)\phi_1''(v) - \mathfrak{p}'(v)\phi_1'(v) - \phi_1'(v)^2\right)\right]\epsilon_1^2\epsilon^2 + \mathcal{O}\left(\epsilon^6\right) \ , \qquad (2.49)
\end{aligned}
$$

$$
\begin{aligned}
f(z,v) = \frac{1}{z} - \frac{1}{8}z\phi_1'(v)^2\epsilon^2 + \frac{z^3}{384}\left(\phi_1'(v)^4 - 48p(v)\phi_1'(v)\right)\epsilon^4 \\
- \frac{z^3}{8}\mathfrak{p}(v)\phi_1'(v)\epsilon_1^2\epsilon^2 + \mathcal{O}\left(\epsilon^6\right) \ , \qquad (2.50)
\end{aligned}
$$

$$
\Phi(z,v) = (\phi_1(v) + z\phi_1'(v))\epsilon + z^3p(v)\epsilon^3 + z^3m\mathfrak{p}(v)\epsilon_1^2\epsilon^2 + \mathcal{O}\left(\epsilon^5\right) \ , \qquad (2.51)
$$

$$
\begin{aligned}
A(z,v) = \mu(v) + qz\epsilon_1^2 + \frac{q}{12}\left[12z\mathfrak{a}_4(v) - 6z^2\phi_1(v)\phi_1'(v)\ddot{h}(0)\right. \\
\left. + z^3\phi_1'(v)^2(1 - 2\ddot{h}(0))\right]\epsilon_1^2\epsilon^2 + \mathcal{O}\left(\epsilon^4\right) \ . \qquad (2.52)
\end{aligned}
$$

We can now relate the boundary quantities $\{M(v),\ L(v),\ c\}$ appearing in (2.27), (2.29) to the amplitude expansion:

$$
M(v) = -\left(mk^2 + C_2(v)\right)\epsilon^2 + \left(c_4(v) + mk^2\mathfrak{c}_4(v)\right)\epsilon^4 + \mathcal{O}(\epsilon^6) \ , \qquad (2.53)
$$

$$
L(v) = \left(p(v) + mk^2\mathfrak{p}(v)\right)\epsilon^3 + \mathcal{O}(\epsilon^5) \ , \qquad (2.54)
$$

$$
\frac{c}{h(\phi_b(v))} = qk^2\epsilon^2 + qk^2\mathfrak{a}_4(v)\epsilon^4 + \mathcal{O}(\epsilon^5) \ . \qquad (2.55)
$$

Before going further, let us check a couple of trivial limits: (i) First, note that setting $\epsilon = 0$ keeping $\epsilon_1 \neq 0$, we kill off the entire dynamics and get

[4]We are retaining the factors of ϵ and ϵ_1 separately as a bookkeeping device.

back the initial AdS-RN state in (2.33)-(2.35). In other words, this limit is equivalent to taking $v \to -\infty$. (ii) Secondly, if we set $\epsilon_1 = 0$ keeping $\epsilon \neq 0$, our initial state reduces to empty AdS. It is straightforward to check that this case reduces to the one with a vanishing chemical potential[67]. However, the non-trivial dynamics remain. (iii) Third, if we set both $\epsilon_1 = 0 = \epsilon$, then we are left in the empty AdS-background with no dynamics. This is the most trivial limit of the solution described above. As alluded in (2.40), we will consider $\epsilon_1 \neq 0$ and $\epsilon \neq 0$, with the constraint that $k = \epsilon_1/\epsilon \sim \mathcal{O}(1)$.

At late times, *i.e.* $v \gg \delta t$, the final state is given by

$$g(z,v) = \frac{1}{z^2} - z\left[\epsilon^2\left(mk^2 + \tilde{C}_2\right) - \epsilon^4\,\widetilde{c}_4\right] + z^2\frac{\epsilon^4 k^4 q^2}{2} + \mathcal{O}\left(\epsilon^6\right)\ , \tag{2.56}$$

$$f(z,v) = \frac{1}{z} + \mathcal{O}\left(\epsilon^6\right)\ , \tag{2.57}$$

$$\Phi(z,v) = z^3\,\widetilde{p}\,\epsilon^3 + \mathcal{O}\left(\epsilon^5\right)\ , \tag{2.58}$$

$$A(z,v) = \mu_f + q\,z\,k^2\epsilon^2\ . \tag{2.59}$$

Here the tilde denotes the function evaluated at any $v \gg \delta t$. Since ϕ_1 is of compact support, this is equal to the value of the function at infinity, $\widetilde{C}_2 = C_2(\infty) = -\frac{1}{2}\int_{-\infty}^{\infty}\phi_1'(x)\phi_1'''(x)dx$, *etc.* Note that to fourth order, the mass of the black hole has increased by an amount $\widetilde{C}_2\,\epsilon^2 + \widetilde{c}_4\,\epsilon^4$ as compared to the initial state, similarly to [67]. Exploring the solution at higher order we find that at sixth order $g(z,v)$ has a dependence on $\ddot{h}(0)$ that survives at late time and gives a subleading contribution to the mass of the final black hole. Note also that the gauge field at late times differs from the original gauge field only by a shift in the chemical potential. This is consistent with our expectations

since the charge of the black hole remains the same. However, the position of the horizon changes and thus — as we will see in section 2.4 — the chemical potential also changes due to the boundary condition on the gauge field. We will analyze the resulting thermodynamics in Section 2.4.

2.3.3 Analytic structure and regime of validity

Let us briefly investigate the analytic structure and regime of validity of the perturbative solution for $v > \delta t$. We can systematically find the solution to arbitrary order in ϵ. Then, following a similar approach as in [67], we can inductively show that, among the functions that appear in (2.36)-(2.39),

$$g_{2n+1} = 0 \ , \quad f_{2n+1} = 0 \ , \quad \phi_{2n} = 0 \ , \quad A_{v_{2n+1}} = 0 \ , \quad \forall n \in \mathbb{Z}_+ \ . \tag{2.60}$$

Thus the non-trivial information about the dynamics is contained in the set of functions: $\mathbb{G} \equiv \{\mathbb{G}_n\} = \{g_{2n}, f_{2n}, \phi_{2n+1}, A_{v_n}\}$ and they take the following general form

$$\begin{aligned}
\phi_{2n+1}(z,v) &= \sum_{k=0}^{2n-2} z^{2n+1-k} \phi_{2n+1}^k(v) \ , \qquad n \geq 2 \\
f_{2n}(z,v) &= \frac{1}{z} \sum_{k=0}^{2n-4} z^{2n-k} f_{2n}^k(v) \ , \qquad n \geq 3 \\
g_{2n}(z,v) &= z C_{2n}(v) + \frac{1}{z} \sum_{k=0}^{2n-3} z^{2n-k} g_{2n}^k(v) \ , \qquad n \geq 3 \\
A_{v_{2n}}(z,v) &= \mu_{2n}(v) + \sum_{k=0}^{2n-2} z^{2n-1-k} A_{v_{2n}}^k(v) \ . \qquad n \geq 3
\end{aligned} \tag{2.61}$$

In general $\mathbb{G}$ is a function of v and a functional of $\phi_1(v)$ and its derivatives: $\mathbb{G} = \mathbb{G}\left(v, \phi_1, \phi_1', \ldots\right)$. Note that even powers of ϵ are absent in $\phi(z,v)$ and

odd powers are absent in $g(z,v)$, $f(z,v)$ and $A_v(z,v)$. Likewise, the odd derivatives of the coupling function, $h(\phi)$, evaluated at $\phi = 0$ should vanish, $0 = \dot{h}(0) = \dddot{h}(0) = h^{(5)}(0)... = 0$.[5]

For $v > \delta t$ the functions $\tilde{\mathbb{G}} = \{g_{2n}, f_{2n}, \phi_{2n+1}\}$ consists of polynomials in v of a degree that grows with n [6]. In particular ϕ_{2n+1} is at most of degree $(n+k-1)$, f_{2n} is at most of degree $(n+k-3)$ and g^k_{2n} of degree $(n+k-4)$. Thus we have

$$\max\left\{\deg\left[\tilde{\mathbb{G}}_n\right]\right\} = (n+k-1)\ . \tag{2.62}$$

The fact that the functions $\tilde{\mathbb{G}}_n$ are polynomials in v whose degree grows with n implies that the series expansion will break down at late times. In order to characterize the regime of validity lets focus on $\phi(z,v)$, which has the maximum degree in v:

$$\phi(z,v) = \sum_{n,k} \epsilon^{2n+1} \phi^k_{2n+1}\, z^{2n+1-k}\ . \tag{2.63}$$

It can further be checked that for late times

$$\phi^k_{2n+1} \sim \frac{v^{n+k-1}}{\delta t^{3n}}\ . \tag{2.64}$$

It would suffice for our purposes, if the perturbative solution is valid up to the event-horizon of the geometry. Recall that the event-horizon is given by, up

[5] As stated previously, the equations of motion demand that $h(0) = \dot{h}(0) = 0$. The requirement that the odd higher derivatives vanish ($\dddot{h}(0) = h^{(5)}(0) = h^{(2j+1)}... = 0$) comes from assuming a series of the form 2.61 for the dilaton and the gauge field.

[6] The late time behavior of A_v is different; all terms of order ϵ^4 or higher go to zero at late times. Thus, at $v > \delta t$ we recover the original gauge field and A_v does not enter in the analysis of the late time validity of the solution.

to the leading order in ϵ,

$$z_{\rm H} \sim \frac{1}{\epsilon^{2/3}(k^2 m + \tilde{C}_2)^{1/3}} \ . \tag{2.65}$$

Also recall that k and m are $\mathcal{O}(1)$ numbers while $\tilde{C}_2 \sim \frac{1}{\delta t^3}$. Thus we get: $z_{\rm H} \sim \frac{\delta t}{\epsilon^{2/3}}$. Therefore, close to the horizon and for late times, the term with labels n, k in (2.63) will scale approximately as $(\epsilon^{2/3}\frac{v}{\delta t})^{n-1+k}\epsilon$. This implies that if $\epsilon^{2/3}\frac{v}{\delta t} \ll 1$ the small values of $\{n, k\}$ dominate the series and larger values are subleading. However if $\epsilon^{2/3}\frac{v}{\delta t} \gg 1$ it is the larger values of $\{n, k\}$ that dominate and the perturbation series breaks down. Thus, our series solution is good only up to times $v \sim \mathcal{O}\left(\frac{\delta t}{\epsilon^{2/3}}\right)$ which to leading order in ϵ corresponds to $1/\left(\Delta E\right)^{1/3}$ (see eq. (2.33)).

2.4 Thermodynamics of the states

We will now briefly discuss the initial and the final states which are interpolated by the evolution described in (2.49)-(2.52). Both our initial and the final states are characterized by a non-vanishing temperature and a chemical potential, both of which have dimension length^{-1}. It is also accompanied by the VEV of the marginal operator, denoted by $\langle \mathcal{O}_\phi \rangle \sim$ length^{-3}, which is being quenched *via* the dynamics. Thus the state is specified by the following data:

$$\text{QFT} \ni \{\mu, T, \langle \mathcal{O}_\phi \rangle\} \quad \Longleftrightarrow \quad \{G, A, \phi\} \in \text{Gravity} \ . \tag{2.1}$$

Furthermore, note that from the full solution in (2.52) it is clear that the normalizable mode of the gauge field does not have any dynamics associated

and thus

$$\lim_{z\to 0} \partial_v F_{zv} = \partial_v \left(q k^2 \epsilon^2 \right) = 0 \ , \tag{2.2}$$

which implies that the charge density in the dual field theory is kept fixed. Thus, we are considering the dynamical evolution in a "canonical ensemble". We will now discuss the initial and the final states in more detail.

The regularized on-shell Euclidean action corresponds to the Gibbs free energy, which characterizes the grand-canonical ensemble. If we denote the Gibbs free energy by W, then the Helmholtz free energy, which we denote by F, characterizes the canonical ensemble and is obtained by a Legendre transformation of the Gibbs potential

$$F = W - \mu\, Q \ , \tag{2.3}$$

where μ and Q are respectively the chemical potential and the charge density.

2.4.1 Initial state

Here we will reinstate ϵ_1 where they originally appear. According to (2.33)-(2.35), in the limit $v \to -\infty$, we get:

$$f(z) = \frac{1}{z} , \tag{2.4}$$

$$g(z) = \frac{1}{z^2}\left(1 - \epsilon_1^2 m z^3 + \frac{\epsilon_1^4 q^2 z^4}{2}\right) , \tag{2.5}$$

$$A_v(z) = \mu_i + \epsilon_1^2 q z \, , \tag{2.6}$$

$$\phi(z) = 0 \, . \tag{2.7}$$

With the scalar field turned off, the geometry reduces to the usual AdS-RN black hole. For the above solution, the corresponding mass M and charge Q are given by

$$M = \epsilon_1^2 m \quad \text{and} \quad Q^2 = \epsilon_1^4 q^2 \,. \tag{2.8}$$

Alternatively, the mass can also be given as

$$M = \frac{1}{z_{\rm H}^3} + \frac{Q^2}{2} z_{\rm H} \,, \tag{2.9}$$

where $z_{\rm H}$ is the location of the event horizon, given by the smallest real positive positive root of the algebraic equation $g(z) = 0$. For small ϵ_1 we obtain,[7]

$$z_{\rm H} = \frac{1}{\epsilon_1^{2/3} m^{1/3}} \left(1 + \frac{\epsilon_1^{4/3} q^2}{6 m^{4/3}} + \mathcal{O}(\epsilon_1^{8/3}) \right) . \tag{2.10}$$

On the other hand, the one-form A_v must be regular at the horizon such that $||A||$ remains finite at the bifurcation point of the Kruskal-extended patch. This imposes a constraint, relating the chemical potential to the charge and the mass:

$$\lim_{z \to z_{\rm H}} A = 0 \quad \Longrightarrow \quad \mu_i = -\epsilon_1^2 q z_{\rm H} = -\frac{\epsilon_1^{4/3} q}{m^{1/3}} \left(1 + \frac{\epsilon_1^{4/3} q^2}{6 m^{4/3}} + \mathcal{O}(\epsilon_1^{8/3}) \right) . \tag{2.11}$$

The subscript i in all subsequent physical quantities will stand for the initial state. To calculate the Hawking temperature of the initial state T_i, we first perform a Wick rotation obtained as usual by the replacement $t \to i\tau$. Since the Euclidean time direction shrinks to zero size at $z = z_{\rm H}$, we must require

[7] For concreteness, we will evaluate all physical quantities in two leading order terms in ϵ_1.

that τ be periodically identified with appropriate period β_i, *i.e.* $\tau \sim \tau + \beta_i$. A simple calculation shows that

$$\begin{aligned} T_i &= -\frac{1}{4\pi}\frac{d}{dz}g(z)\Big|_{z_{\rm H}} = \frac{3}{4\pi z_{\rm H}}\left(1-\frac{1}{6}Q^2 z_{\rm H}^4\right) \\ &= \frac{3\epsilon_1^{2/3}m^{1/3}}{4\pi}\left(1-\frac{\epsilon_1^{4/3}q^2}{3m^{4/3}}+\mathcal{O}(\epsilon_1^{8/3})\right), \end{aligned} \tag{2.12}$$

or equivalently,

$$\beta_i \equiv \frac{1}{T_i} = \frac{4\pi}{3\epsilon_1^{2/3}m^{1/3}}\left(1+\frac{\epsilon_1^{4/3}q^2}{3m^{4/3}}+\mathcal{O}(\epsilon_1^{8/3})\right). \tag{2.13}$$

It is convenient to invert the relations $\mu_i(m,q)$ and $\beta_i(m,q)$ given in (2.11)-(2.13) to obtain $m(\mu_i,\beta_i)$ and $q(\mu_i,\beta_i)$. However, we have to proceed with some care given that $\mu_i \sim \mathcal{O}(\epsilon_1^{4/3})$ whereas $\beta_i \sim \mathcal{O}(\epsilon_1^{-2/3})$. First we define rescaled quantities $\tilde{\mu}_i = \epsilon_1^{-4/3}\mu_i$ and $\tilde{\beta}_i = \epsilon_1^{2/3}\beta_i$ such that they both are of order $\mathcal{O}\left(\epsilon_1^0\right)$. Then, an expansion in ϵ_1 is reliable and the inversions can be found perturbatively. To our order of approximation we find,

$$m = \frac{64\pi^3}{27\tilde{\beta}_i^3}\left(1+\frac{9\epsilon_1^{4/3}\tilde{\beta}_i^2\tilde{\mu}_i^2}{16\pi^2}+\mathcal{O}(\epsilon_1^{8/3})\right) \approx \frac{64\pi^3}{27\epsilon_1^2\beta_i^3}\left(1+\frac{9\beta_i^2\mu_i^2}{16\pi^2}\right), \tag{2.14}$$

and

$$q = -\frac{4\pi\tilde{\mu}_i}{3\tilde{\beta}_i}\left(1+\frac{3\epsilon_1^{4/3}\tilde{\beta}_i^2\tilde{\mu}_i^2}{32\pi^2}+\mathcal{O}(\epsilon_1^{8/3})\right) \approx -\frac{4\pi\mu_i}{3\epsilon_1^2\beta_i}\left(1+\frac{3\beta_i^2\mu_i^2}{32\pi^2}\right). \tag{2.15}$$

To study the thermodynamics of these solutions, we first evaluate the Euclidean action I on-shell which defines the grand canonical (Gibbs) potential $W = I/\beta_i$ (see for instance [92]). With our conventions, the full Euclidean action is given by analytically continuing (2.1). Moreover, when the space is

asymptotically AdS the Gibbons-Hawking boundary term gives a vanishing contribution.

As usual, the action diverges upon integration, given that the volume of any asymptotically AdS geometry goes to infinity near the boundary. These divergences can be eliminated by subtracting the pure AdS contribution, obtaining

$$I = -\frac{\mathrm{Vol}(\mathbb{R}^2)\beta_i}{\kappa^2}\left[\int_0^{z_\mathrm{H}} \frac{\epsilon_1^4 q^2}{2} dz - \int_{z_\mathrm{H}}^{\infty} \frac{3}{z^4} dz\right], \tag{2.16}$$

$$= -\frac{\mathrm{Vol}(\mathbb{R}^2)\beta_i m \epsilon_1^2}{\kappa^2}\left(1 + \frac{\epsilon_1^{8/3} q^4}{4m^{8/3}} + \mathcal{O}\left(\epsilon_1^4\right)\right). \tag{2.17}$$

This may be rewritten entirely in terms of β_i and μ_i as

$$I = -\frac{64\pi^3 \mathrm{Vol}(\mathbb{R}^2)\epsilon_1^{4/3}}{27\kappa^2 \tilde{\beta}_i^2}\left(1 + \frac{9\epsilon_1^{4/3}\tilde{\beta}_i^2\tilde{\mu}_i^2}{16\pi^2} + \mathcal{O}(\epsilon_1^{8/3})\right), \tag{2.18}$$

$$\approx -\frac{64\pi^3 \mathrm{Vol}(\mathbb{R}^2)}{27\kappa^2 \beta_i^2}\left(1 + \frac{9\beta_i^2\mu_i^2}{16\pi^2}\right). \tag{2.19}$$

The grand canonical potential is given by $W = E_i - T_i S_i - \mu_i Q_i$. Using the expression given in (2.19), we may compute the state variables of the system. At leading order we get:[8]

$$E_i = \left(\frac{\partial I}{\partial \beta_i}\right)_{\mu_i} - \frac{\mu_i}{\beta_i}\left(\frac{\partial I}{\partial \mu_i}\right)_{\beta_i} \approx \frac{2\mathrm{Vol}(\mathbb{R}^2)\epsilon_1^2 m}{\kappa^2}, \tag{2.20}$$

$$S_i = \beta_i\left(\frac{\partial I}{\partial \beta_i}\right)_{\mu_i} - I \approx \frac{4\pi \mathrm{Vol}(\mathbb{R}^2)\epsilon_1^{4/3} m^{2/3}}{\kappa^2}, \tag{2.21}$$

$$Q_i = -\frac{1}{\beta_i}\left(\frac{\partial I}{\partial \mu_i}\right)_{\beta_i} \approx -\frac{2\mathrm{Vol}(\mathbb{R}^2)\epsilon_1^2 q}{\kappa^2}. \tag{2.22}$$

[8] In RN black holes $S \to$ constant as $T \to 0$, indicating the degeneracy of the ground state. This can be seen at our order of approximation from (2.21) and (2.14). A brief computation leads to $S_i \sim \mu_i^2$ as $T_i \to 0$.

Together, they indeed satisfy the first law of thermodynamics, $dE_i = T_i dS_i + \mu_i dQ_i$. Moreover, the free energy $W = I/\beta_i$ is always negative, indicating stability of the solutions. Notice that we could have alternatively worked in the canonical ensemble, which is characterized by the Helmholtz free energy $F = E - ST$. A brief computation shows that, at the same order of approximation,

$$F \approx -\frac{64\pi^3 \mathrm{Vol}(\mathbb{R}^2)}{27\kappa^2\beta_i^3}\left(1 - \frac{9\beta_i^2\mu_i^2}{16\pi^2}\right) . \tag{2.23}$$

Let us now comment on the identification of the field theory quantity corresponding to the putative small parameter ϵ_1. From (2.12), (2.11) and (2.20), it is clear that parametrically $T_i/E_i \sim \mathcal{O}(1)$. However,

$$\frac{\mu_i}{T_i} = -\left(\frac{4\pi}{3}\right)\frac{q}{m^{2/3}}\epsilon_1^{2/3} \quad \Longrightarrow \quad \epsilon_1 = \left(\frac{\mu_i}{T_i}\right)^{3/2}\mathcal{O}(1) . \tag{2.24}$$

Thus, we are considering an initial state in which the chemical potential is small compared to the temperature. It also becomes clear that, in obtaining the perturbative solution outlined in (2.49)-(2.52), we have set the expansion parameter $\epsilon \sim \left(\frac{\mu_i}{T_i}\right)^{3/2}$. By analyzing the final state, we will now observe that ϵ corresponds to an otherwise independent parameter in the dual field theory.

2.4.2 Final state

Let us now consider the final state. For $v \to \infty$ (in practice for $v \gg \delta t$) the bulk solution in (2.56)-(2.59) can be written as:

$$f(z) = \frac{1}{z} + \mathcal{O}(\epsilon^6)\,, \tag{2.25}$$

$$g(z) = \frac{1}{z^2}\left[1 - \epsilon^2\left(k^2 m + \widetilde{C}_2\right) z^3 + \epsilon^4\left(\widetilde{c}_4 z^3 + \frac{k^4 q^2}{2} z^4\right)\right] + \mathcal{O}\left(\epsilon^6\right) \tag{2.26}$$

$$A_v(z) = \mu_f + \epsilon^2 k^2 q z\,, \tag{2.27}$$

$$\phi(z) = z^3 \widetilde{p} \epsilon^3 + \mathcal{O}\left(\epsilon^5\right)\,, \tag{2.28}$$

where $k = (\epsilon_1/\epsilon)$ and all the tildes denote the corresponding functions evaluated at $v \to \infty$, which are of order $\mathcal{O}\left(\epsilon^0\right)$.

The mass and charge of the final background are now

$$M_f = \epsilon^2(k^2 m + \widetilde{C}_2) - \epsilon^4 \widetilde{c}_4 \quad \text{and} \quad Q_f^2 = \epsilon^4 k^4 q^2 = Q_i^2\,, \tag{2.29}$$

which gives

$$\Delta M = M_f - M_i = \epsilon^2 \widetilde{C}_2 - \epsilon^4 \widetilde{c}_4\,. \tag{2.30}$$

The new horizon lies at

$$z_{\rm H}^{(f)} = \frac{1}{\epsilon^{2/3} m_2^{1/3}}\left(1 + \frac{\epsilon^{4/3} k^4 q^2}{6 m_2^{4/3}} + \mathcal{O}\left(\epsilon^2\right)\right)\,. \tag{2.31}$$

For convenience, we have defined $m_2 = k^2 m + \widetilde{C}_2$. Regularity of the gauge field at the horizon now yields

$$\lim_{z \to z_{\rm H}^{(f)}} A = 0 \quad \Longrightarrow \quad \mu_f = -\frac{\epsilon^{4/3} k^2 q}{m_2^{1/3}}\left(1 + \frac{\epsilon^{4/3} k^4 q^2}{6 m_2^{4/3}} + \mathcal{O}\left(\epsilon^2\right)\right)\,. \tag{2.32}$$

On the other hand, the inverse temperature is given by

$$\beta_f \equiv \frac{1}{T_f} = \frac{4\pi}{3\epsilon^{2/3} m_2^{1/3}} \left(1 + \frac{\epsilon^{4/3} k^4 q^2}{3 m_2^{4/3}} + \mathcal{O}\left(\epsilon^{8/3}\right) \right) . \tag{2.33}$$

Defining $\tilde{\mu}_f = \epsilon^{-4/3} \mu_f$ and $\tilde{\beta}_f = \epsilon^{2/3} \beta_f$, we can invert (2.32)-(2.33) as follows

$$m_2 = \frac{64\pi^3}{27 \tilde{\beta}_f^3} \left(1 + \frac{9\epsilon^{4/3} \tilde{\beta}_f^2 \tilde{\mu}_f^2}{16\pi^2} + \mathcal{O}\left(\epsilon^{8/3}\right) \right) \approx \frac{64\pi^3}{27\epsilon^2 \beta_f^3} \left(1 + \frac{9\beta_f^2 \mu_f^2}{16\pi^2} \right) \tag{2.34}$$

and

$$q = -\frac{4\pi \tilde{\mu}_f}{3k^2 \tilde{\beta}_f} \left(1 + \frac{3\epsilon^{4/3} \tilde{\beta}_f^2 \tilde{\mu}_f^2}{32\pi^2} + \mathcal{O}\left(\epsilon^{8/3}\right) \right) \approx -\frac{4\pi \mu_f}{3\epsilon^2 k^2 \beta_f} \left(1 + \frac{3\beta_f^2 \mu_f^2}{32\pi^2} \right) . \tag{2.35}$$

After subtracting the AdS contribution, the Euclidean on-shell action evaluates to:

$$\begin{aligned} I &= -\frac{\mathrm{Vol}(\mathbb{R}^2) \beta m_2 \epsilon^2}{\kappa^2} \left(1 - \frac{3\epsilon^2 (k^2 m\widetilde{\mathfrak{p}} + \widetilde{p})^2}{4 m_2^2} + \mathcal{O}\left(\epsilon^{8/3}\right) \right) , \\ &\approx -\frac{64\pi^3 \mathrm{Vol}(\mathbb{R}^2)}{27\kappa^2 \beta_f^2} \left(1 + \frac{9\beta_f^2 \mu_f^2}{16\pi^2} \right) . \end{aligned} \tag{2.36}$$

Finally, we can compute the state variables for the final state. At leading order we get:

$$\begin{aligned} E_f &= \left(\frac{\partial I}{\partial \beta_f} \right)_{\mu_f} - \frac{\mu_f}{\beta_f} \left(\frac{\partial I}{\partial \mu_f} \right)_{\beta_f} \approx \frac{2\mathrm{Vol}(\mathbb{R}^2) \epsilon^2 m_2}{\kappa^2} , \\ S_f &= \beta_f \left(\frac{\partial I}{\partial \beta_f} \right)_{\mu_f} - I \approx \frac{4\pi \mathrm{Vol}(\mathbb{R}^2) \epsilon^{4/3} m_2^{2/3}}{\kappa^2} , \\ Q_f &= -\frac{1}{\beta_f} \left(\frac{\partial I}{\partial \mu_f} \right)_{\beta_f} \approx -\frac{2\mathrm{Vol}(\mathbb{R}^2) \epsilon^2 k^2 q}{\kappa^2} . \end{aligned} \tag{2.37}$$

Again, these quantities satisfy the first law of thermodynamics, $dE_f = T_f dS_f + \mu_f dQ_f$. Note that, upon integration by parts, we get that $\widetilde{C}_2 = \frac{1}{2} \int_{-\infty}^{\infty} \phi_1''(x)^2 dx >$

0 so we always have $m_2 > m$. Both the energy and entropy increase but the charge remains the same, as expected. Moreover, for this final state, the Helmholtz free energy is given by

$$F \approx -\frac{64\pi^3 \text{Vol}(\mathbb{R}^2)}{27\kappa^2\beta_f^3}\left(1 - \frac{9\beta_f^2\mu_f^2}{16\pi^2}\right) . \tag{2.38}$$

Before concluding this section, let us comment on the parameter ϵ. It is straightforward to check that

$$\begin{aligned} \widetilde{C}_2 &\sim \frac{1}{(\delta t)^3} , \quad \text{and} \\ \Delta E &= (E_f - E_i) \sim \frac{\epsilon^2}{(\delta t)^3} \quad \Longrightarrow \quad \epsilon \sim (\delta t)^{3/2} (\Delta E)^{1/2} . \end{aligned} \tag{2.39}$$

Note that, this scaling is in keeping with the scaling behaviour obtained in [78, 79, 80], which follows from dimensional analysis in our case. Evidently, (2.39) provides us with a natural meaning for the expansion parameter in gravity purely in terms of the field theory data. What is more, we observe that the perturbative solution is consistent as long as we impose

$$\epsilon_1 \sim \epsilon \quad \Longrightarrow \quad \left(\frac{\mu_i}{T_i}\right)^3 \sim (\delta t)^3 (\Delta E) . \tag{2.40}$$

2.5 Thermalization time

Given the background that we obtained in the previous section, we will now explore how the thermalization time behaves with relevant parameters for the system. We will measure thermalization time by measuring non-local observables, specially entanglement entropy and define our thermalization time

according to the behavior of this non-local probe. Via the AdS/CFT correspondence, this exercise amounts to computing an extremal area surface in the bulk geometry. For this purpose, we will only require the solution for the metric (2.8), which is given explicitly in (2.56)-(2.59). The specific form of $f(z,v)$ and $g(z,v)$ will not be important for now.

The metric (2.8) is asymptotically AdS. To make this manifest, let us rescale the metric functions such that

$$ds^2 = \frac{1}{z^2}\left[-2dvdz - \tilde{g}(z,v)dv^2 + \tilde{f}^2(z,v)\left(dx^2+dy^2\right)\right] , \tag{2.1}$$

where we have defined $\tilde{f}(z,v) \equiv zf(z,v)$ and $\tilde{g}(z,v) \equiv z^2 g(z,v)$. These new functions satisfy that $\tilde{f} \to 1$ and $\tilde{g} \to 1$ as $z \to 0$. Also, the boundary time coordinate is related to the Eddington-Finkelstein coordinates in (2.1) through [9]

$$dv = dt - \frac{dz}{\tilde{g}(z,v)} . \tag{2.2}$$

This relation will be important below, for the computation of the thermalization time.

2.5.1 Entanglement entropy

We will compute entanglement entropy in this background for a particular shape: namely a "rectangular strip" which can be parametrized by $\{x \in (-\ell/2, \ell/2)\} \cup \{y \in (-\ell_\perp/2, \ell_\perp/2)\}$. In a quantum system, entanglement

[9] Here we neglect the redshift effect indicated in [72]. In the thin-shell limit for $v_0 \to 0$, the redshift factor will reduce to one for the regime outside the shell. Note that the $t_{\rm crit}$ introduced in (2.29) will be slightly longer when incorporating the redshift effect.

(or geometric) entropy of a region A with its complement B is defined using the reduced density matrix *a la* von Neuman: $S_A = -\mathrm{tr}_A\, \rho_A \log \rho_A$, where ρ_A is obtained by tracing over the degrees of freedom in B, $\rho_A = \mathrm{tr}_B\, \rho$. As reviewed in section 1.2.4, entanglement entropy can be holographically computed by means of the Ryu-Takayanagi prescription [62] or, more generally, its covariant generalization [63]. Before delving into the computation, let us flesh out the approximation in which we will be working for the rest of this chapter.

The perturbative solution that we have obtained in (2.49)-(2.52) can be numerically subtle to handle, specially since we have a small parameter ϵ. Instead, we make use of the small parameter in the following manner: The metric data can be summarized as follows:

$$G_{\mu\nu} = G^{(0)}_{\mu\nu} + \epsilon^2 G^{(1)}_{\mu\nu} + \epsilon^4 G^{(2)}_{\mu\nu} + \dots \ , \tag{2.3}$$

Subsequently the geodesics and the entanglement entropy can also be determined by a similar expansion

$$\gamma_A = \gamma_A^{(0)} + \epsilon^2 \gamma_A^{(1)} + \epsilon^4 \gamma_A^{(2)} + \dots \ , \tag{2.4}$$

$$S_A = S_A^{(0)} + \epsilon^2 S_A^{(1)} + \epsilon^4 S_A^{(2)} + \dots \ . \tag{2.5}$$

It can be checked that upon using the equations of motion at the first non-trivial order in ϵ, which in this case happens to be at $\mathcal{O}(\epsilon^2)$, $\gamma_A^{(0)}$ determines $S_A^{(1)}$ completely [81]. Thus, if we limit ourselves to results at the first non-trivial order in ϵ, the task of determining geodesics simplifies significantly. On the

other hand, it is clear from the metric in *e.g.* (2.49), the effect of the charge enters at $\mathcal{O}(\epsilon^4)$, at which order there is no such simplification. For simplicity, we will keep our discussions limited to $\mathcal{O}(\epsilon^2)$. We therefore emphasize that, our numerical results should be taken as *indications* of a certain physics rather than an *observation*. On the other hand, it is possible to go beyond $\mathcal{O}(\epsilon^2)$ systematically, which we leave for future work.

Also note that, as we are measuring the *response* of the system at the first non-trivial order in ϵ, so we will measure the *external dial*. In our case, the *external dial* is a combination of *e.g.* $(\mu/T) \sim \mathcal{O}(\epsilon^{2/3})$. Thus, effectively we are using a different precision for measuring the response-observables as compared to the parameters of the system. In a very precise sense, the subsequent dynamics that we analyze is primarily determined by the temperature-scale of the system.

Now let us discuss the details. We will now compute S_A in the limit $\ell_\perp \to \infty$, so that the construction becomes invariant under translations in y. We can parameterize the extremal surfaces with functions $z(x)$, $v(x)$ subject to the boundary conditions

$$z(\pm\ell/2) = z_0 \quad \text{and} \quad v(\pm\ell/2) = t \ , \tag{2.6}$$

where z_0 is the usual UV cut-off needed to regularize the on-shell acion. These boundary conditions impose that the boundary of γ_A coincides with the boundary of A along the temporal evolution. The area functional is given by

$$\mathcal{A} = \text{Area}(\gamma_A) = \ell_\perp \int_{-\ell/2}^{\ell/2} dx \frac{\tilde{f}(z,v)}{z^2} \sqrt{\tilde{f}(z,v)^2 - \tilde{g}(z,v) v'^2 - 2v'z'} \ , \tag{2.7}$$

where $' \equiv d/dx$. Since there is no explicit x-dependence, there is a corresponding conservation equation given by

$$\tilde{f}^2(z,v) - \tilde{g}(z,v)v'^2 - 2v'z' = \tilde{f}^6(z,v)\left(\frac{z_*}{z}\right)^4 \ . \tag{2.8}$$

In this expression, z_* is defined through $z(0) = z_*$. Now, the right hand side of (2.2) in empty AdS is identically zero. In our case it is of order $\mathcal{O}(\epsilon^4)$, which we can safely neglect since we are working to order $\mathcal{O}(\epsilon^2)$. Thus, we have

$$v' + \frac{z'}{\tilde{g}(z,v)} \sim 0 \ . \tag{2.9}$$

Combining (2.8) and (2.9) we get

$$z' = \sqrt{\left(\tilde{f}^4(z,v)\left(\frac{z_*}{z}\right)^4 - 1\right)\tilde{f}(z,v)^2\tilde{g}(z,v)} \ . \tag{2.10}$$

In practice we solve the above system as follows. First, we rewrite (2.9) as

$$\dot{v} + \frac{1}{\tilde{g}(z,v)} = 0 \ , \tag{2.11}$$

where $\dot{} \equiv d/dz$ and we solve for $v(z)$ subject to the boundary condition: $v(z_0) = t_{\text{boundary}}$. With this function at hand and given a value of z_*, we can then obtain a solution for $z(x)$ by direct integration of (2.10). However, note that this last step is not necessary if we only want to extract the values of ℓ and $\mathcal{A}$ for a given z_*. More specifically, these values can be obtained from

$$\ell = 2\int_{z_0}^{z_*} \frac{dz}{z'} \quad \text{and} \quad \mathcal{A} = 2\ell_\perp \int_{z_0}^{z_*} dz \frac{\tilde{f}(z,v)^4 z_*^2}{z^4 z'} \ , \tag{2.12}$$

respectively. In particular, the last equation in (2.12) arises upon substituting (2.9)-(2.10) in (2.7) and then changing the integration variable $dx \to dz/z'$.

On the other hand, the area in (2.12) is divergent as the UV cut-off $z_0 \to 0$ and must be regularized. The divergence comes from the fact that the volume of any asymptotically AdS background is infinite and the spatial surface γ_A reaches the boundary. In particular, near the boundary it is clear that $\tilde{f}(z \to 0) \to 1$, $z'(z \to 0) = z_*^2/z^2$ and therefore

$$\mathcal{A}_{\text{div}} = 2\ell_\perp \int_{z\sim z_0} \frac{dz}{z^2} = \frac{2}{z_0} \ . \tag{2.13}$$

Subtracting this divergence, we obtain the finite term of the area which is the quantity we are interested in:

$$\mathcal{S} \equiv \mathcal{A} - \mathcal{A}_{\text{div}} = 2\ell_\perp \left(\int_{z_0}^{z_*} dz \frac{\tilde{f}(z,v)^4 z_*^2}{z^4 z'} - \frac{1}{z_0} \right) \ . \tag{2.14}$$

2.5.2 Toy model and choice of parameters

Before proceeding to the numerical results, we must specify the system we want to study. First, notice that at $\mathcal{O}(\epsilon^4)$ the computation of entanglement entropy does not rely on the specific form of the coupling $h(\phi)$. Then, for the purposes of this section it is enough to set $h(0) = 1$ and $\dot{h}(0) = 0$, as required by the perturbative solution. For the scalar profile, we choose for simplicity a Gaussian function of the form

$$\phi_1(v) = \lambda e^{-v^2/v_0^2} \ , \tag{2.15}$$

where λ and v_0 are numerical parameters that control the amplitude and the width. With this choice, the leading-order amplitude of the dilaton scales as $\phi \sim \epsilon\lambda$. Note that the perturbative expansion requires each order in to be

at most of order $\mathcal{O}(1)$ in ϵ. Here we have introduced the extra parameter λ for convenience, which could yield $(\frac{\tilde{C}_2}{m}) \sim \mathcal{O}(1)$ with a proper choice of its numerical value. We will come back to this point below. One advantage of the above profile is that it can be integrated analytically to obtain the explicit form of $C_2(v)$, $C_4(v)$ and $P(v)$. A brief computation leads to:

$$C_2(v) = \frac{\lambda^2}{8v_0^6}\left[4ve^{-2v^2/v_0^2}\left(4v^2 - 3v_0^2\right) + 3\sqrt{2\pi}v_0^3\left(2 - \mathrm{erf}(\sqrt{2}v/v_0)\right)\right], \quad (2.16)$$

$$\begin{aligned} C_4(v) = -\frac{3\lambda^2}{16}e^{-2v^2/v_0^2}k^2m + \frac{\lambda^4}{1536v_0^6}\Bigg[&12ve^{-4v^2/v_0^2}\left(72v^2 + 25v_0^2\right) \\ &+108\sqrt{2\pi}v_0^3e^{-2v^2/v_0^2}\left(1 + \mathrm{erf}(\sqrt{2}v/v_0)\right) + 9\sqrt{\pi}v_0^3\Big(1 + \mathrm{erf}(2v/v_0)\Big) \\ &-128\sqrt{3\pi}v_0^3e^{-v^2/v_0^2}\left(1 + \mathrm{erf}(\sqrt{3}v/v_0)\right)\Bigg], \end{aligned} \quad (2.17)$$

and

$$\begin{aligned} P(v) = -\frac{\lambda}{4}e^{-v^2/v_0^2}k^2m + \frac{\lambda^3}{288v_0^6}\Bigg[&27\sqrt{2\pi}v_0^3e^{-v^2/v_0^2}\left(1 + \mathrm{erf}(\sqrt{2}v/v_0)\right) \\ &-12ve^{-3v^2/v_0^2}\left(12v^2 + v_0^2\right) - 16\sqrt{3\pi}v_0^3\left(1 + \mathrm{erf}(\sqrt{3}v/v_0)\right)\Bigg]. \end{aligned} \quad (2.18)$$

Here $\mathrm{erf}(x)$ denotes the error function. Furthermore, we only need derivatives of $\phi_1(v)$ and $P(v)$ to compute the analytic forms of $\tilde{f}(z,v)$ and $\tilde{g}(z,v)$ according to (2.56)-(2.59).

Next, we have to select values for the various parameters in order to be consistent with the perturbative expansion. First, we set $m = 1$ and $v_0 = 0.01$. The first choice fixes a reference scale for the initial energy whereas the second

guarantees that we are dealing with the thin shell limit. Then, we must fix λ in order to have $m_2 \sim \mathcal{O}(1)$ for the final state. Note that $\tilde{C}_2$ evaluates to

$$\tilde{C}_2 = \frac{3\sqrt{2\pi}\lambda^2}{4v_0^3} \,. \tag{2.19}$$

Then, a good choice for λ is

$$\lambda = \frac{2^{3/4} v_0^{3/2}}{\sqrt{3}\pi^{1/4}} \approx 7.3 \times 10^{-4} \,, \tag{2.20}$$

so that $\tilde{C}_2 = 1$. We further set $k = 1$ so $\epsilon = \epsilon_1$ and $m_2 = k^2 m + \tilde{C}_2 = 2$. In Figure 2.1 we plot both the gaussian profile for the scalar field and the mass function $m_2(v) \equiv k^2 m + \tilde{C}_2(v)$ for the parameters given above. The remaining functions $C_4(v)$ and $P(v)$ are of order $\mathcal{O}\left(10^{-7}\right)$ and $\mathcal{O}\left(10^{-4}\right)$, respectively. Note that the mass function does not increase monotonically in time, in stark

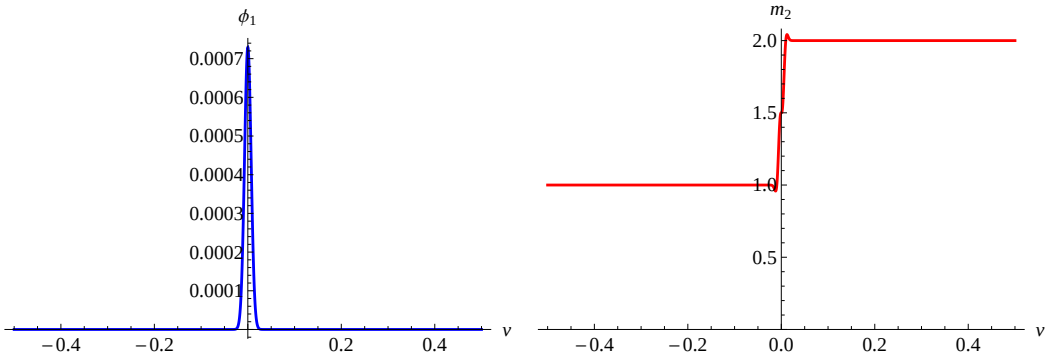

(a) (b)

Figure 2.1: (a) Gaussian profile for the scalar field $\phi_1(v)$ and (b) mass function $m_2(v)$ according to (2.15) and (2.16), respectively. For the plots we chose $m = 1$, $v_0 = 0.01$, $k = 1$ and λ given by (2.20).

contrast with the usual behavior of collapsing Vaidya geometries. Nevertheless, our field content is physically sensible and all the energy conditions are

satisfied. Following the arguments of [11], then, we expect reasonable results for the thermalization process in the boundary theory.[10] Another reason to argue that this must be true is that, although the *apparent* horizon (2.15) also shows this non-monotonic behavior, the *event* horizon (2.17), on the other hand, always increases along the temporal evolution.[11] Figure 2.2 shows representative behaviors of these two quantities. At any rate, it is worth pointing out that such non-monotonic behavior disappears as we take the thin shell limit, which is the case we are focusing on. In this limit both $m_2(v)$ and $z_{\rm aH}(v)$ take the form of a step function.

The expansion parameter ϵ should be a small number. We observe that the first and second corrections to the functions $\tilde{f}(z,v)$ and $\tilde{g}(z,v)$ over AdS are of order $\mathcal{O}(\epsilon^2)$ and $\mathcal{O}(\epsilon^4)$, respectively. A reasonable choice for ϵ is then $\epsilon = 0.1$. Finally, the value of q can be tuned in order to vary the temperature and the chemical potential of the solutions. There are two requirements for this quantity: (i) we must impose that $q \sim \mathcal{O}(1)$ to be consistent with the perturbative expansion and (ii) we cannot exceed the maximum value allowed in order to avoid a naked singularity at early times. Regarding this last point, recall that to our order of approximation, the initial state is characterized by

$$T_i = \frac{3\epsilon^{2/3} m^{1/3}}{4\pi}\left(1 - \frac{\epsilon^{4/3} q^2}{3m^{4/3}}\right) \ , \quad \mu_i = -\frac{\epsilon^{4/3} q}{m^{1/3}}\left(1 + \frac{\epsilon^{4/3} q^2}{6m^{4/3}}\right) \ . \tag{2.21}$$

[10] We thank Esperanza Lopez for a discussion on this point.

[11] If we truncate the metric at order $\mathcal{O}(\epsilon^4)$, we find that for $v_0 \sim 10$ or larger the event horizon also presents signs of non-monotonic behavior. This issue is corrected as we consider higher order corrections in ϵ.

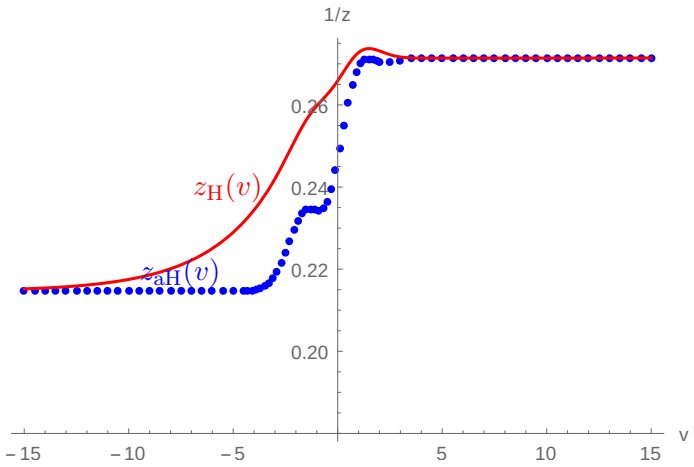

Figure 2.2: Evolution of the the apparent horizon $z_{\rm aH}(v)$ (blue) vs. the event horizon $z_{\rm H}(v)$ (red) according to (2.15) and (2.17), respectively. For the plots we chose $m = 1$, $q = 0.7$, $v_0 = 2$, $k = 1$ and λ given by (2.20). Notice that for this example we have chosen v_0 away from the thin shell limit in order to observe the non-monotonicity of the apparent horizon. If we let $v_0 \to 0$, this non-monotonic behavior is smoothed out and $z_{\rm aH}(v)$ approaches to a step function.

Therefore, from (2.21) it follows that the condition (ii) for not having a naked singularity sets a maximum value

$$|q|_{\rm max} = \frac{\sqrt{3}m^{2/3}}{\epsilon^{2/3}} \simeq 8.04 \ , \tag{2.22}$$

above which $T_i < 0$ and with no real roots of $g(z_{\rm H}) = 0$. Fortunately, notice that (2.22) is also within the acceptable range for satisfying item (i).

The final state, on the other hand, is characterized by

$$T_f = \frac{3\epsilon^{2/3}m_2^{1/3}}{4\pi}\left(1 - \frac{\epsilon^{4/3}q^2}{3m_2^{4/3}}\right) \ , \quad \mu_f = -\frac{\epsilon^{4/3}q}{m_2^{1/3}}\left(1 + \frac{\epsilon^{4/3}q^2}{6m_2^{4/3}}\right) \ , \tag{2.23}$$

where

$$m_2 = m + \frac{3\sqrt{2\pi}\lambda^2}{4v_0^3} \ . \tag{2.24}$$

It is easy to check that for values of q in the range allowed by (2.22), the final states are also free of naked singularities. Of course, this is directly related to the fact that the mass of the black hole is increased while the charge is kept fixed.

Now, we have both temperature and chemical potential in our system and we need to construct a dimensionless ratio which would be our tunable parameter. Notice that both temperature and chemical potential has inverse length dimensions. Then, we can consider [65]

$$\chi \equiv \frac{1}{4\pi}\left(\frac{\mu_f - \mu_i}{T_f - T_i}\right) \tag{2.25}$$

to be the relevant parameter that we will vary. In practice, we can vary χ by tuning the parameter $q \in [-8.04, 8.04]$. In particular, it is found that for this range of values, $\chi(q) \in [-0.42, 0.42]$ and increases almost linearly with q. Thus, within the perturbative approximation and for the choices of the various parameters, we are restricted to small values of χ as compared to [65].

2.5.3 Regimes of thermalization

Now we will discuss the numerical results. In Figure 2.3 (a) we plot sample solutions for the embedding functions $z(x)$ for a fixed ℓ as the boundary times t is varied. Some of them cross the shell, located at $v = 0$, and refract. This refraction is suppressed by a factor of ϵ^2 given that the energy-momentum of the shell is itself of order $\mathcal{O}(\epsilon^2)$. Nevertheless, the aforementioned effect is noticeable to the naked eye for large enough distances, $(4\pi\Delta T)\,\ell \gtrsim 1$. We also

show in (b) the behavior of entanglement entropy as a function of time, for a fixed distance ℓ. In order to compare the results for various values of χ we subtract the entropy of the initial state $\Delta S(t) = S(t) - S(-\infty)$, and focus on the entanglement growth over time.[12] We note some general properties of the behavior of $\Delta S(t)$ as we change the value of χ. Qualitatively, our results agree with those of [82, 83] (see also [84, 85, 86]) obtained in the context of Vaidya geometries. At early times, *i.e.* the "pre-local-equilibration" regime, the evolution is almost quadratic in time and is weakly dependent on the size ℓ. This stage is followed by a linear growth phase at intermediate times and, finally, a saturation is reached at late times, $t \geq t_{\rm sat}$, where the entropy abruptly flattens out.

Let us explain these regimes in more details. First, in Figure 2.4, we have shown the functional dependence of entanglement entropy growth in various regimes. Following [82] we can introduce a "local equilibrium scale", denoted by $\ell_{\rm eq}$, which means that a local thermodynamic description applies at length scales$\sim \mathcal{O}(\ell_{\rm eq})$ even though the global description is out-of-equilibirum. For early times, which can be represented by the regime $t \ll \ell_{\rm eq}$, the rate of entanglement entropy growth is expected to be proportional to the area of the entangling surface. Furthermore, we can assume that the growth is proportional to a characteristic energy scale of the system. Note that, at the

[12]The divergent piece of the entanglement entropy is independent of the legth. Here we are subtracting also a finite piece that depends on ℓ but does not display temporal evolution. With this subtraction, the entanglement entropy $\Delta S(t)$ starts at zero in the infinite past for all values of ℓ.

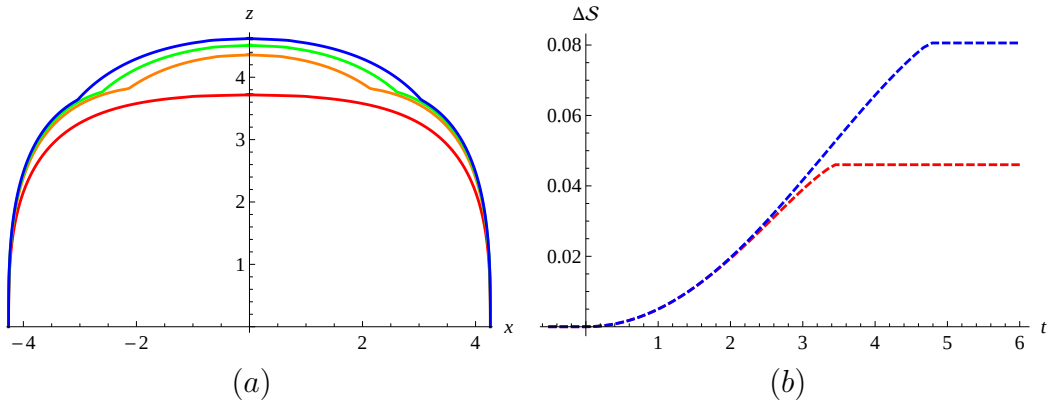

Figure 2.3: (a) Sample embedding functions $z(x)$ for $\chi = 0.2$ ($q \simeq 3.651$), $4\pi\Delta T\ell = 2$ ($\ell \simeq 8.524$) and $t = \{5.6, 6.8, 8, 9.2\}$ from top to bottom. (b) Entanglement growth $\mathcal{S}(t)$ for $\chi = 0.002$ (blue) and $\chi = 2$ (red) with fixed $4\pi\Delta T\ell = 1$. In both plots we have set the AdS radius to unity $L = 1$.

initial stage, we have the energy of the initial state, denoted by E_{initial}, and the energy which is being injected to induce the dynamics, denoted by ΔE. Thus the typical energy-scale should be identified as

$$E_{\text{typical}} = \max\left\{E_{\text{initial}}, \Delta E\right\} \ . \tag{2.26}$$

A priori, E_{initial} and ΔE are independent. However, in our case, we already demanded $E_{\text{initial}} \sim \Delta E$ and thus, using dimensional analysis, we can arrive at

$$\Delta S(t) = \left(\alpha_1 E_{\text{initial}}\mathcal{A}\right) t^2 = \left(\alpha_2 \Delta E\mathcal{A}\right) t^2 \ , \tag{2.27}$$

where $\alpha_{1,2}$ are two constants and $\mathcal{A}$ denotes the area of the entangling surface.

On the other hand, in the regime $t \gg \ell_{\text{eq}}$, we have a notion of a thermal entropy density which is denoted by S_{thermal}. If we further assume that the

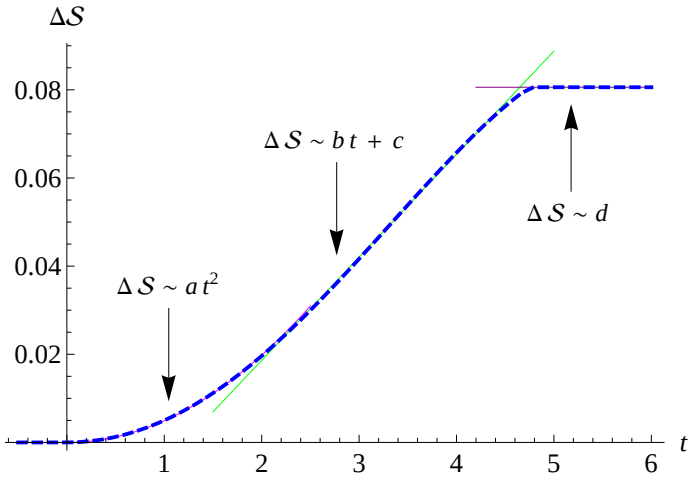

Figure 2.4: Functional dependence of entanglement entropy as a function of time in the various regimes of thermalization. For this example we fixed $\chi = 0.002$ and $4\pi\Delta T\ell = 1$, and the best fits yielded the following constants: $a = 0.00496$, $b = 0.02338$, $c = -0.02813$ and $d = 0.08059$. The time here is measured in units of the AdS radius which has been set to unity $L = 1$.

entanglement entropy is proportional to the area of the entangling surface and the local thermal entropy density, then by dimensional analysis we get

$$\Delta S(t) = (v_{\rm E} \mathcal{A} S_{\rm thermal})\, t \ , \tag{2.28}$$

where $v_{\rm E}$ is the entanglement production rate which has been analyzed in [82, 83]. Evidently, our numerical data agrees very well with the intuition outlined in (2.27) and (2.28). It is intriguing to further note that, although we are not starting from a vacuum state, the analysis of [82, 83] continues to hold.[13] Finally, since we are considering the "rectangular" shaped entangling

[13]The issue of state dependence was further studied in [15] for the case of hyperbolic AdS-Vaidya black holes, finding qualitative agreement with the results of [82, 83].

surface, we expect that the saturation will be accompanied by an abrupt jump in the corresponding extremal area geodesic.

Now we will discuss the scaling of thermalization time. From the time-evolution of entanglement entropy, we can extract $t_{\rm sat}$ for a given length ℓ. Alternatively, we can define another time-scale $t_{\rm crit}$ as a measure of the thermalization time. Recall that the shell is densely peaked around $v = 0$ for $v_0 \ll 1$. Thus, we can define $t_{\rm crit}$ to be the time at which the corresponding extremal surface grazes the shell at $v = 0$. By definition from (2.2), we get

$$t_{\rm crit} = \int_{z_0}^{z_*} \frac{dz}{\tilde{g}(z, v = 0)} \ . \tag{2.29}$$

In practice, it is easier to extract $t_{\rm crit}$ rather than $t_{\rm sat}$.[14] Furthermore, in the limit $v_0 \to 0$ these two quantities are found to agree. For the case of finite thickness, they only differ by a factor of order $\mathcal{O}(v_0)$ so we expect similar results for the thermalization time as long as v_0 is not too large. We thus focus on the critical time $t_{\rm crit}$.

Let us, however, clarify a further caveat regarding $t_{\rm crit}$. Precisely speaking, $t_{\rm crit}$ measure the time a null ray takes to reach the AdS-boundary starting from the bulk point z_*. Thus, for a given boundary length ℓ, the corresponding extremal area geodesic will indeed graze the shell at $t_{\rm crit}$ provided the shell propagates at the speed of light. However, as can be checked from (2.6)

[14]Note, however, the approach to equilibrium is expected to be abrupt in the case of a rectangular entangling region[82]. Thus, strictly speaking, $t_{\rm crit}$ may not be the correct measure of thermalization time. However, in our case, we have checked that $t_{\rm sat}$ and $t_{\rm crit}$ exhibit qualitatively similar behaviour. Since we are only concerned with qualitative features, we do not attempt to make this more precise here.

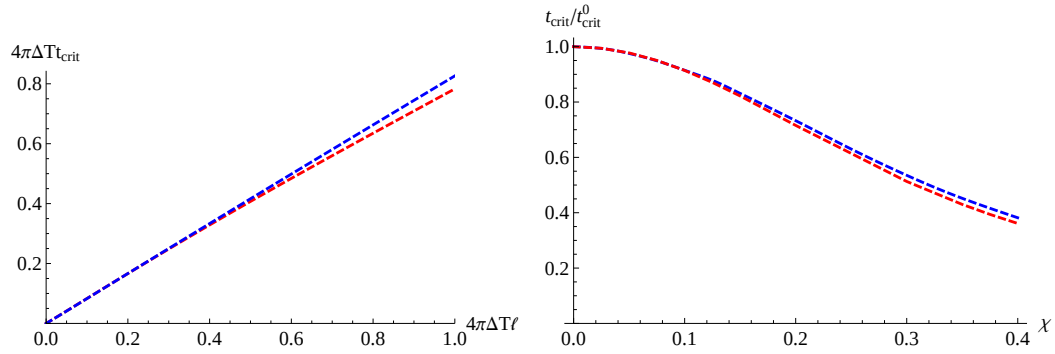

(a) (b)

Figure 2.5: (a) Critical time as a function of length for fixed $\chi = 0.04$ (red) and $\chi = 0.4$ (blue). (b) Critical time as a function of χ for a fixed length $4\pi\Delta T\ell = 0.1$ (red) and $4\pi\Delta T\ell = 1$ (blue). The AdS radius has been set to unity $L = 1$.

and (2.7), the matter field is non-null and thus propagates slower than the speed of light. Thus, in reality t_{crit} will serve as a lower bound for the actual thermalization time.

The dependence of t_{crit} with ℓ is shown in Figure 2.5 (a), which approximates a linear growth similar to the one observed in [69, 70]. Generally, we can represent the dependence as

$$\Delta T t_{\text{crit}} = A\left(\chi\right)\left(\Delta T\ell\right) + B\left(\chi\right)\left(\Delta T\ell\right)^{\alpha(\chi)} \ , \tag{2.30}$$

where $A(\chi)$ represents the slope of the linear regime, *i.e.* the velocity at which thermalization propagates in the system. Numerically we find

$$A(\chi) = 0.83 \quad \text{for blue} \tag{2.31}$$

$$= 0.79 \quad \text{for red} \ , \tag{2.32}$$

which implies that thermalization is super-critical (faster than speed of light).

At larger length-scales, the deviation from linearity is characterized by the second term above, where $\alpha(\chi)$ is an index which can, in principle, depend on χ.

On the other hand $t_{\rm crit}$ monotonically decreases with χ for fixed ℓ (in the allowed range for χ), which means that thermalization is faster in the presence of a chemical potential. We have shown a representative behaviors in Figure 2.5 (b). Our findings agree qualitatively with the results of [65], in the regime of validity of our solutions.

Let us now comment on what may happen beyond the validity of our perturbative solutions. It is unlikely that the thermalization time keep decreasing with increasing chemical potential. Hence there are two possibilities: (i) thermalization time plateaus or (ii) thermalization time eventually turns around and starts increasing with increasing chemical potential. Either way, it implies a qualitatively different scaling behaviour of thermalization time in two regimes: when $\chi \ll 1$ and when $\chi \gg 1$, *i.e.* which has an obvious interpretation as a "classical" and a "quantum" regime respectively. The latter observation is similar to the one made in [65].

2.5.4 A remark on the scrambling time

Before closing this section, we wish to make a few comments.[15] Our initial state is thermal, and thus is represented in the gravity description by an

[15]We thank Diego Trancanelli for bringing this point to our attention.

AdS black hole. It is generally believed that black holes are endowed with the special property of "fast scrambling" [87, 88]. In particular, this implies that the time scale associated to the process of thermalization grows logarithmically with the number of degrees of freedom of the system

$$t_* \sim \beta \log N \ , \tag{2.33}$$

where β is independent of N. In our case, we can count N by evaluating the thermal entropy of the initial state S^i_{Thermal}, or of the final state S^f_{Thermal}, or of their difference $\Delta S_{\text{Thermal}}$.

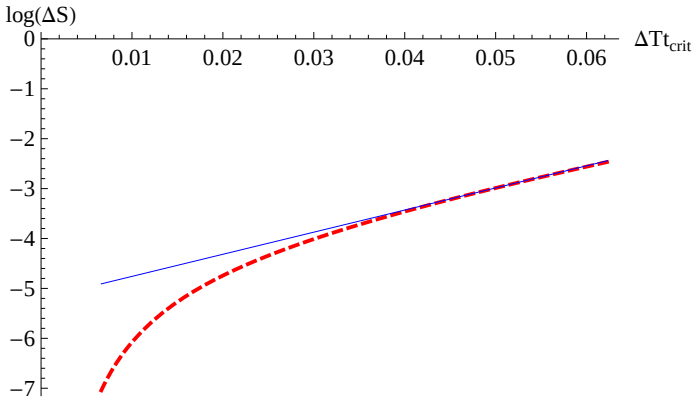

Figure 2.6: Behavior of entanglement entropy vs. saturation time for a fixed $\chi = 0.04$. The plot is generated by joining the points $\{\Delta S(\ell), \Delta T t_{\text{crit}}(\ell)\}$ corresponding to different values of ℓ. The blue line represent the best fit in the farthermost region, for which the values of length are of order $\Delta T \ell \sim 1$.

Now, in order to make contact with the scrambling property of the black hole, we have to focus on the regime $\Delta T \ell \gg 1$ where entanglement entropy approaches the thermal entropy, $S(\Delta T \ell \gg 1) \sim S_{\text{Thermal}}$. In this same limit,

we can identify $t_{\rm crit} \sim t_*$ since $t_{\rm crit}(\Delta T \ell \gg 1)$ serves as a measure of "global" equilibration. In Figure 2.6 we show the behaviour of $\log \Delta S$ as a function of the $\Delta T t_{\rm crit}$ for a fixed value of chemical potential χ. To generate the plot, we vary the length ℓ to generate pair of points $\{\Delta S(\ell), \Delta T t_{\rm crit}(\ell)\}$ and then we join them. Larger values of ℓ correspond to larger $t_{\rm crit}(\ell)$ for a fixed ΔT (see Figure 2.5), so we are interested in the rightmost part of Figure 2.6. It is worth pointing out that, due to limitations of the numerical accuracy and the validity of our perturbative solution, we can only go as far as $\Delta T \ell \sim 1$. This is because in order to increase the length of the boundary strip we have to reduce $z_{\rm H} - z_*$ accordingly, which needs to be fine-tuned to high precision in order to increase $\Delta T \ell$. However, it is intriguing that in the region around $\Delta T \ell \sim 1$ the curve smoothly approaches a straight line, in concordance with (2.33). It would be remarkable if this statement holds true as $\Delta T \ell$ is increased. If it does, this may lead to important clues on how the effective degrees of freedom interact towards the process of thermalization[89, 7]. It will be interesting to investigate this issue further and make contact with other approaches within the framework of AdS/CFT (see, *e.g.* [90]).

2.6 Conclusions

We have considered here the thermal quench of a marginal operator in a prototypical large N-gauge theory. In order to establish the scaling of the thermalization time on a more robust ground, there are many directions which we intend to explore in near future.

First, we can generalize our perturbative analysis when the quench is being carried out for a relevant operator. This will correspond to introducing a non-trivial scalar potential and it will be interesting to check to what extent our observations are universal. In turn, it is easier to embed such effective gravity descriptions within 11-dimensional supergravity. Subsequently it will also be interesting to understand the specific embedding of our effective gravity description, in which the scalar potential is vanishing, in string theory. Note that, our model is unlikely to be realized within ABJM, since the latter does not have any marginal scalar-deformation.[16]

To test the robustness of our qualitative observation, it will be interesting to model a similar dynamical background in the presence of more than one global U(1)-charge, by *e.g.* coupling the STU-model with a neutral massless scalar.[17] The quench of this scalar field will correspond to the quench of a marginal or relevant operator in the dual field theory. It will be very interesting to check how thermalization behaves in this case.

We have considered only $(3+1)$-dimensional bulk theory which corresponds to a $(2+1)$-dimensional boundary theory. It is well-known that the dynamics in asymptotically locally AdS_{d+1} differs qualitatively for even vs. odd d, see *e.g.* [67]. Thus generalizing our results for the asymptotically AdS_5-background will be an interesting avenue to pursue.

[16] All scalars have a non-vanishing mass around the corresponding AdS-fixed point.

[17] Note that charged black hole solutions for STU-models possess a very rich phase diagram[92].

Intuitively a generic charged-system is much richer than the neutral case and one can consider various possibilities. In our study, we considered the quench by a neutral scalar. One can also consider a charged-scalar field. In the latter, depending on the temperature of the system, the ground state of the system can be described by a Reissner-Nordstorm black hole or a hairy black hole, corresponding to a "normal" phase and a superconducting phase of the field theory. Clearly, this corresponds to a more complicated dynamical process and it will be worthwhile to check how much physics can be accessed *via* a perturbative approach analogous to what we have adopted here.

Generalizing on this theme, it will be interesting to catalogue the possibilities in which Einstein equations admit such perturbative analyses. A bottom-up approach can be followed with various matter content in an Einstein-gravity theory with a negative cosmological constant. We can further relax the asymptotically AdS-condition, by using an asymptotically Lifshitz or Hyperscaling-Violating geometries.

The importance of a complete numerical evolution can hardly be over-estimated. It is very crucial that eventually we have access to the entire evolution process in the full parameter space. As outlined above, there are numerous physically inequivalent real-time phenomena that can be captured within Einstein gravity with Maxwell and (charged or uncharged) scalar fields in various dimensions, which needs extensive numerical explorations. This is a long-term goal which we leave for future.

Chapter 3

Fluid/gravity duality: hydrodynamic expansion and cooling

3.1 Introduction

As studied in Chapter 2, black hole collapse is a useful tool to explore the physics of holographic thermalization, where the system evolves from a "low temperature" phase to a "high temperature" thermal state. However, in many circumstances the relevant physics is described by the opposite process: the system might start in a thermalized state and then evolve towards a lower temperature, or vacuum state of the theory. One of such examples is the quark-gluon plasma, a new phase of quantum chromo-dynamics (QCD) recently discovered in heavy-ion collision experiments at RHIC and LHC. According to the current paradigm, the colliding matter creates a soup of deconfined quarks and gluons that thermalizes fast, expands, cools down and finally hadronizes. At the relevant energies achieved in these experiments, QCD is still strongly-coupled and standard perturbative techniques are inadequate, creating a demand for new theoretical tools. In recent years, the discovery of the AdS/CFT correspondence [25, 26, 27] has granted us access to the study of a large class of strongly-coupled gauge theories, providing us with a variety of tools to tackle this problem.

In this Chapter we will study a model that describes the physics of the quark-gluon plasma in the stage of hydrodynamic expansion and cooling, using using the tools of the AdS/CFT correspondence [20]. We will then compute various observables in order to characterize the process. The goal is to gain insight into the physics of expanding fluids and, if possible, to uncover possible universal signatures of strongly-coupled systems.

Experimentally, it is well-known that, in the last stage of the evolution, various observables of the quark-gluon plasma are well described in terms of hydrodynamics [93] and, to a good extent, it seems that it behaves approximately as a perfect fluid [94]. In the context of AdS/CFT, the first steps towards understanding the late-time evolution of the plasma were given in [95], assuming boost-invariance along the collision axis (which is believed to hold in the mid-rapidity region [94]) and homogeneity/isotropy in the transverse plane. Of course, these simplifying assumptions were vital for having an analytical handle on the problem but one ultimately wants to relax these conditions in order to model a more realistic plasma, e.g. including anisotropic effects generated by off-center collisions [96] and radial flow due to finite size nuclei [97]. Going beyond the hydrodynamical description requires one to overcome several challenges, as it requires a full numerical solution to the initial value problem in asymptotically AdS spaces [98].

One way to characterize the evolution of the plasma in a time-dependent setup is by studying the behavior of non-local observables and analyzing the way in which they reach equilibrium. Indeed, this approach has been used

with great success in the program of holographic thermalization [99], where the system is excited by the injection of a spatially uniform density of energy and eventually equilibrates. On the gravity side, such quenches are described in terms of the gravitational collapse of a shell of matter that leads to the formation of a black hole. These are toy models that describe the early-time evolution of the quark-gluon plasma, before entering the regime of expansion and cooling. The idea here is to extend these results to another regime of interest that is analytically tractable, namely the stage in which the plasma is described by hydrodynamics.

In the framework of non-linear hydrodynamics, the fluid/gravity duality [111, 112] provides us with full control of the bulk geometry in a wide variety of scenarios. For concreteness, we will assume boost-invariance along the axis of expansion and translational/rotational symmetry in the transverse plane as in [95]. We will phrase our discussion in terms of the simplest theory with a known gravity dual, i.e. $\mathcal{N} = 4$ supersymmetric Yang-Mills at large N and 't Hooft coupling λ but, appealing to universality, we expect our results to hold under more general circumstances.

This Chapter is organized as follows. In Section 3.2 we start with a brief review of hydrodynamics in the AdS/CFT correspondence. First, we show how compute the transport coefficients of the strongly-coupled plasma in the linear response theory. This is achieved by weakly perturbing a state in thermal equilibrium and then computing the relevant correlators of the stress-energy tensor. We then discuss how to study out-of-equilibrium configurations,

focusing specifically on Bjorken or boost-invariant hydrodynamics, which directly applies to our problem. Next, in Section 3.3 we study the relaxation of non-local probes in the expanding medium, including two-point functions of operators with large conformal dimension, Wilson loops and entanglement entropy. We close in Section 3.4 with conclusions and future directions.

3.2 Hydrodynamics in AdS/CFT

3.2.1 Linear response theory

While thermodynamics describes static properties of a system in perfect thermal equilibrium, hydrodynamics is the effective theory that describes long-wavelength, small-amplitude perturbations around thermal equilibrium. Unlike the familiar effective field theories (for example, the chiral perturbation theory), it is normally formulated in the language of equations of motion instead of an action principle. The reason for this is the presence of dissipation in thermal media.

In the simplest case, the hydrodynamic equations are just the laws of conservation of energy and momentum,

$$\partial_\mu T^{\mu\nu} = 0\,. \tag{3.1}$$

To close the system of equations, we must reduce the number of independent elements of $T^{\mu\nu}$. This is done through the assumption of local thermal equilibrium: if perturbations have long wavelengths, the state of the system, at a given time, is determined by the temperature as a function of coordinates

$T(x)$ and the local fluid velocity u^μ, which is also a function of coordinates $u^\mu(x)$. Because $u_\mu u^\mu = -1$, only three components of u^μ are independent. The number of hydrodynamic variables is four, equal to the number of equations.

In hydrodynamics we express $T^{\mu\nu}$ through $T(x)$ and $u^\mu(x)$ through the so-called constitutive equations. Following the standard procedure of effective field theories, we can expand in powers of spatial derivatives. To zeroth order, $T^{\mu\nu}$ is given by the familiar formula for perfect fluids,

$$T^{\mu\nu}_{\text{perfect}} = (\varepsilon + p)u^\mu u^\nu + p g^{\mu\nu}\,, \tag{3.2}$$

where ε is the energy density, and p is the pressure. Normally one would stop at this leading order, but qualitatively new effects appear in the next order. Indeed, from equation (3.2) and the thermodynamic relations (1.31), one finds that entropy is conserved

$$\partial_\mu(s u^\mu) = 0\,. \tag{3.3}$$

Thus, to have entropy production, one needs to go to the next order in the derivative expansion.

At the next order, we can write

$$T^{\mu\nu} = T^{\mu\nu}_{\text{perfect}} + \sigma^{\mu\nu}\,, \tag{3.4}$$

where $\sigma^{\mu\nu}$ is proportional to derivatives of $T(x)$ and $u^\mu(x)$. The more general form of $\sigma^{\mu\nu}$ is

$$\sigma^{\mu\nu} = -\eta(\triangle^{\mu\sigma}\partial_\sigma u^\nu + \triangle^{\nu\sigma}\partial_\sigma u^\mu - \tfrac{2}{3}\triangle^{\mu\nu}\partial_\sigma u^\sigma) - \zeta\triangle^{\mu\nu}\partial_\sigma u^\sigma\,, \tag{3.5}$$

where η and ζ are the first order hydrodynamical coefficients best known as the shear viscosity and the bulk viscosity, respectively, and $\triangle^{\mu\nu} = g^{\mu\nu} + u^\mu u^\nu$ is the projection operator onto the directions perpendicular to u^μ. To simplify things, let us work in the proper frame (or comoving frame) that is attached to a fixed point x. In this frame we have that $u^i(x) = 0$ and in principle one may expect dissipative corrections to the energy-momentum density $T^{0\mu}$. However, one recalls that the choice of T and u^μ is arbitrary, and thus one can always redefine them so that these corrections vanish, $\sigma^{00} = \sigma^{0i} = 0$, and so at a point x,

$$T^{00} = \varepsilon\,, \qquad T^{0i} = 0\,. \tag{3.6}$$

The only nonzero elements of the dissipative energy-momentum tensor are σ_{ij}. Furthermore, if we restrict our attention to conformal invariant field theories, there appear two constrains. At zeroth order we get the usual equation of state $\varepsilon = 3p$, while at first order we get the condition $\zeta = 0$. This means that, at the level of approximation we are considering, the only non-vanishing hydrodynamical coefficient for a CFT is just the shear viscosity η.

We can compute the value of η in various ways. The easiest one is to assume that the system is very close thermal equilibrium, in which case the linear response theory does the work. This can be done as follows: we start with a thermal state and we couple some sources $J_a(x)$ to a set of operators $\mathcal{O}_a(x)$, so that the new action is

$$S = S_0 + \int_x J_a(x)\mathcal{O}_a(x)\,, \tag{3.7}$$

then the source will introduce a perturbation in the system. In particular, the expectation values of $\mathcal{O}_a$ will differ from the equilibrium values, which we can assume to be constant. If the sources J_a are small, the perturbations are given by the linear response theory as

$$\langle \mathcal{O}_a(x) \rangle = -\int_y G^R_{ab}(x-y) J_b(y)\,, \tag{3.8}$$

where G^R_{ab} is the retarded Green's function

$$iG^R_{ab}(x-y) = \theta(x^0-y^0)\langle [\mathcal{O}_a(x), \mathcal{O}_b(y)] \rangle\,. \tag{3.9}$$

The fact that the linear response is determined by the retarded (and not by any other) Green's function is obvious from causality: the source can influence the system only after it has been turned on.

Now, in order to determine the correlation functions of $T^{\mu\nu}$, we need to couple a weak source to $T^{\mu\nu}$, *i.e.* we have to perturb the background metric $g_{\mu\nu}$, and determine the response of $T^{\mu\nu}$ after this source is turned on. One must generalize the hydrodynamic equations to curved space-time and from it determine the response of the thermal medium to a weak perturbation of the metric. If we focus on the particular case when the metric perturbation is homogeneous in space but time dependent,

$$\begin{aligned} g_{ij}(t,x) &= \delta_{ij} + h_{ij}(t)\,, \qquad h_{ij} \ll 1\,, \\ g_{00}(t,x) &= -1\,, \qquad g_{0i}(t,x) = 0\,, \end{aligned} \tag{3.10}$$

and we assume the perturbation to be traceless, $h_{ii} = 0$, we can find that the spatial component of $\sigma_{\mu\nu}$ is

$$\sigma_{xy} = \eta \partial_t h_{xy}\,. \tag{3.11}$$

By comparison with the expectation from the linear response theory, this equation means that we have found the zero spatial momentum, low-frequency limit of the retarded Green's function of T_{xy}:

$$G^R_{xy,xy}(\omega,0) = \int d^4x e^{i\omega t}\theta(t)\langle[T_{xy}(x),T_{xy}(0)]\rangle = -i\eta\omega + O(\omega^2) \tag{3.12}$$

(modulo contact terms). Then, we can relate the value of η to the retarded Green's function as

$$\eta = -\lim_{\omega\to 0}\frac{1}{\omega}\mathrm{Im}\, G^R_{xy,xy}(\omega,0)\,, \tag{3.13}$$

which is known as the Kubo's formula for the shear viscosity.

The fact that the viscosity is given by a formula like (3.13) is not surprising. The correlator G^R measures the response at a point x to a perturbation at a point $x = 0$. Evaluating the zero-momentum, low-frequency limit of this correlator corresponds to the long-wavelength limit of hydrodynamics. The imaginary part is associated to a diffusion-like process, in this case of momentum density.

With the formula (3.13) at hand it is a simple problem to calculate the viscosity of the $\mathcal{N} = 4$ SYM plasma at large N and large λ using the supergravity description. However, this is a slightly technical calculation and here we will only sketch the basic steps.

In order to extract the viscosity using the formula (3.13) we must compute the two point function of the stress tensor. This can be obtained by taking two functional derivatives of the gauge theory generating functional with respect to the source that couples to the energy-momentum tensor, *i.e.*

the boundary metric. As mentioned in section 1.2.2, the AdS/CFT dictionary identifies the generating functional of the gauge theory with that of string theory — see equation (1.11) — which in the supergravity approximation reduces to (1.12). Moreover, the energy-momentum tensor $T_{\mu\nu}$ of the gauge theory is dual to the metric $g_{\mu\nu}$ on the gravity side. Therefore the desired correlator is schematically given by

$$\langle TT \rangle \sim \frac{\delta^2}{\delta h^2} S_{\text{sugra}}\left[g+h\right]\Big|_{h=0}\,, \tag{3.14}$$

where S_{sugra} is the on-shell supergravity action, g is the metric (1.14) and h is an infinitessimal metric perturbation. Since one is only interested in a second derivative, it suffices to consider the supergravity action expanded to quadratic order in this perturbation, which leads to a linear equation of motion. Once this is solved, the result can be substituted back into the action and then the derivative in (3.14) evaluated. The final result for the viscosity is given by

$$\eta = \frac{\pi}{8} N^2 T^3\,. \tag{3.15}$$

Now, the hydrodynamic behavior of a system is better characterized by the ratio of the shear viscosity to the entropy density, η/s, rather than by η itself, since this ratio is a measure of the viscosity per degree of freedom. From the result above it follows that for $\mathcal{N}=4$ SYM [114]:

$$\frac{\eta}{s} = \frac{1}{4\pi}\,. \tag{3.16}$$

This formula became known as one the most important results of the AdS/CFT correspondence, since explicit computations as the one sketched

above as well as general arguments have shown that it is a universal property of large N, strongly-coupled, finite temperature gauge theories with a gravity dual [115, 116]. These include theories in different numbers of dimensions, with or without a chemical potential, with or without fundamental matter, etc. Presumably, the reason for the universality of η/s is that both the entropy density and the shear viscosity are related to universal properties of black hole horizons. Using the AdS/CFT prescription, for instance, one can show that under very general conditions the shear viscosity is given by [117]

$$\eta = \frac{\sigma_{\rm abs}(\omega \to 0)}{16\pi G}\,, \tag{3.17}$$

where $\sigma_{\rm abs}(\omega \to 0)$ is the zero-fequency limit of the absorption cross-section of the black hole for a minimally coupled scalar. Similarly, under very general conditions one can show that this quantity is precisely equal to the area of the black hole horizon, $\sigma_{\rm abs}(\omega \to 0) = a$ [118, 119]. Since the entropy density is $s = a/4G$ we obtain (3.16), as expected.

3.2.2 Bjorken hydrodynamics

We can go a step forward and take the fluid/gravity duality more seriously. The idea here is to describe holographically states of the dual CFT that are described by hydrodynamics but are, nevertheless, far-from-equilibrium. We will focus exclusively on describing the dual of an expanding, boost-invariant plasma, which is sometimes referred to as a Bjorken expansion [94]. First we will start with some field theory considerations of boost-invariant kinematics and then we will discuss the dual holographic description [95].

3.2.2.1 Boost-invariant kinematics

After thermalization, the QGP undergoes a regime of expansion and cooling which is approximately boost-invariant along the collision axis. In spite of the strong interactions, in this regime the plasma behaves like a liquid of very low viscosity (almost a perfect fluid!), which makes a hydrodynamic description reliable.

Let us parameterize the spacetime by coordinates $(t, \vec{x})$ and lets imagine that the collision takes places along the x_3-axis. Assuming boost-invariance, then, it is convenient to define new coordinates $(\tau, y, \vec{x}_\perp)$ where the symmetry becomes manifest,

$$t = \tau \cosh y \,, \quad x_3 = \tau \sinh y \,. \tag{3.18}$$

These are known as proper time and rapidity coordinates, respectively. The Minkowski metric becomes

$$ds^2 = -d\tau^2 + \tau^2 dy^2 + d\vec{x}_\perp^2 \,. \tag{3.19}$$

In order to simplify the problem, we assume isotropy and homogeneity in the plane spanned by $\vec{x}_\perp = (x_1, x_2)$, which is valid in the case of central collisions and under the assumption that the colliding nuclei are large. Thus, given these symmetries, the number of independent components of the stress-energy tensor $T_{\mu\nu}$ reduce to three. In addition, we have two constraints imposed by the conservation of energy and momentum, $\nabla_\mu T^{\mu\nu} = 0$, and the traceless condition for conformal fluids, $T^\mu_\mu = 0$, reducing the number of components to

one. Specifically, in the local rest frame we can write

$$T_{\mu\nu} = \begin{pmatrix} \varepsilon & 0 & 0 & 0 \\ 0 & \frac{1}{\tau^2}\left(-\varepsilon - \tau\dot{\varepsilon}\right) & 0 & 0 \\ 0 & 0 & \varepsilon + \frac{1}{2}\tau\dot{\varepsilon} & 0 \\ 0 & 0 & 0 & \varepsilon + \frac{1}{2}\tau\dot{\varepsilon} \end{pmatrix}, \tag{3.20}$$

where $\dot{\varepsilon} = d\varepsilon/d\tau$. Note that we chose the energy density $\varepsilon = \varepsilon(\tau)$ as the only dynamical variable and we wrote the remaining components as functions of the above. The explicit form of $\varepsilon(\tau)$ can be obtained order by order in an hydrodynamical expansion. In the perfect fluid approximation, for instance, we can write the stress-energy tensor in the standard form (3.2). Tracelessness of the stress-energy tensor implies the equation of state for conformal fluids, $\varepsilon = 3p$. Finally, conservation of energy and momentum implies

$$\dot{\varepsilon} = -\frac{4}{3}\frac{\varepsilon}{\tau}\,, \tag{3.21}$$

which can be solved to obtain [94]

$$\varepsilon(\tau) = \frac{\varepsilon_0}{\tau^{4/3}} \qquad \varepsilon_0 \equiv \text{constant}\,. \tag{3.22}$$

In first order hydrodynamics we consider an additional contribution that is of first order in gradients (3.4). At this order we get further constraints. First, from the tracelessness condition we obtain $\zeta = 0$, which is valid for any conformal fluid. And second, from the conservation equation we get

$$\varepsilon = \frac{\varepsilon_0}{\tau^{4/3}}\left(1 - \frac{2\hat{\eta}}{\tau^{2/3}}\right), \qquad \hat{\eta} \equiv \text{constant}\,. \tag{3.23}$$

The relation between $\hat{\eta}$ and the shear viscosity η is found to be

$$\eta \equiv \frac{\hat{\eta}}{\tau}\,. \tag{3.24}$$

The time dependence in equation (3.24) follows from thermodynamical considerations. Recall that in conformal fluids, the Stefan-Boltzmann law implies that $\varepsilon \sim T^4$. Therefore, by dimensional analysis it follows that $\eta \sim T^3$ and hence $\eta \sim \varepsilon^{3/4} \sim 1/\tau$.

Finally, higher order hydrodynamics can be considered in a similar way by generalizing $T^{\mu\nu}$ to contain terms of higher order in gradients. At each order we obtain a correction to the energy density that is suppressed by a factor of order $\mathcal{O}(\tau^{-2/3})$ with respect to the previous order. Therefore, the hydrodynamic expansion can be thought of as a late proper time expansion.

3.2.2.2 Holographic description

We will now discuss the bulk dual to an expanding $\mathcal{N} = 4$ SYM plasma from the point of view of 10-dimensional supergravity [101]. The starting point is the bosonic part of the type-IIB low-energy action in 10-dimensions. In Einstein frame this is given by

$$I_{10} = \frac{1}{2\kappa_{10}^2} \int d^{10}\xi \sqrt{-\tilde{g}} \left[\mathcal{R} - \frac{1}{2} \left(\partial\phi\right)^2 - \frac{1}{4 \cdot 5!} F_5^2 \right] . \tag{3.25}$$

We take the ansatz:

$$\begin{aligned} d\tilde{s}^2 &= \tilde{g}_{MN} d\xi^M d\xi^N = \sigma^{-2}(x) g_{\mu\nu}(x) dx^\mu dx^\nu + \sigma^{6/5}(x) \left(dS^5\right)^2 , \\ \phi &= \phi(x) , \end{aligned} \tag{3.26}$$

where $M, N = 0, ..., 9$ and $\mu, \nu = 0, ..., 4$, and $(dS^5)^2$ is the line element for a 5-dimensional unit sphere. For the 5-form F_5 we assume

$$F_5 = \mathcal{F}_5 + \star\mathcal{F}_5 , \qquad \mathcal{F}_5 = -4Q\, \omega_{S^5} , \tag{3.27}$$

where ω_{S^5} is the 5-sphere volume form and Q is a constant.

Alternatively, from the point of view of a 5-dimensional effective description, the same system can be described by the following action [101]

$$I_5 = \frac{1}{2\kappa_5^2}\int d^5x\sqrt{-g}\left[R - \frac{1}{2}\left(\partial\phi\right)^2 - \frac{24}{5}\left(\partial\alpha\right)^2 - \mathcal{P}(\alpha)\right], \tag{3.28}$$

with

$$\kappa_5^2 = \frac{\kappa_{10}^2}{\mathrm{vol}\left\{S^5\right\}}. \tag{3.29}$$

In the above we have defined the scalar field $\alpha(x)$ through $\sigma(x) \equiv e^{\alpha(x)}$, $\mathcal{P}(\alpha)$ is the potential[1]

$$\mathcal{P}(\alpha) = -20\, e^{-16\alpha/5} + 8Q^2\, e^{-8\alpha}, \tag{3.30}$$

and R is the Ricci scalar for the 5-dimensional metric $g_{\mu\nu}$.

Either, from (3.25) or (3.28) we obtain the following field equations:

$$\begin{aligned} R_{\mu\nu} &= \frac{24}{5}\left(\partial_\mu\alpha\right)\left(\partial_\nu\alpha\right) + \frac{1}{2}\left(\partial_\mu\phi\right)\left(\partial_\nu\phi\right) + \frac{1}{3}g_{\mu\nu}\mathcal{P}(\alpha), \\ \Box\alpha &= \frac{5}{48}\frac{\partial\mathcal{P}}{\partial\alpha}, \\ \Box\phi &= 0. \end{aligned} \tag{3.31}$$

In Fefferman-Graham coordinates, the most general bulk metric for the symmetries of a boost-invariant plasma takes the following form:

$$ds^2 = g_{\mu\nu}dx^\mu dx^\nu = \frac{1}{z^2}\left[-e^{a(\tau,z)}d\tau^2 + e^{b(\tau,z)}\tau^2 dy^2 + e^{c(\tau,z)}dx_\perp^2 + dz^2\right], \tag{3.32}$$

[1]We choose $Q = 1$ so that the minimum of the potential is $\mathcal{P}_{\min} = -12$. This sets the AdS radius to unity.

where $dx_\perp^2 \equiv dx_1^2 + dx_2^2$. We further assume $\alpha = \alpha(\tau, z)$ and $\phi = \phi(\tau, z)$. The equations of motion (3.31) are solved asymptotically as a late-time expansion in powers of $\tau^{-2/3}$. For this purposes, we define the scaling variable

$$v \equiv \frac{\epsilon^{1/4} z}{\tau^{1/3}}\,, \tag{3.33}$$

where ϵ is a dimensionful constant, and take the limit $\tau \to \infty$ with v fixed.[2] Such a scaling is motivated by the fact that, after holographic renormalization [104], the energy density of the boundary theory $\langle T_{00}(\tau)\rangle \equiv \varepsilon(\tau)$ evaluates to

$$\varepsilon(\tau) = -\lim_{z\to 0} \frac{N_c^2}{2\pi^2}\frac{a(z,\tau)}{z^4} = -\epsilon \lim_{v\to 0} \frac{N_c^2}{2\pi^2}\frac{a(v,\tau)}{v^4\tau^{4/3}}\,, \tag{3.34}$$

leading to a late-τ expansion that matches the expected behavior from conformal Bjorken hydrodynamics. We then expand the coefficients $a(z,\tau)$, $b(z,\tau)$, $c(z,\tau)$, $\alpha(z,\tau)$ and $\phi(z,\tau)$ as series of the form[3]

$$a(\tau, v) = a_0(v) + \frac{1}{\tau^{2/3}} a_1(v) + \frac{1}{\tau^{4/3}} a_2(v) + \mathcal{O}(\tau^{-2})\,, \tag{3.35}$$

$$b(\tau, v) = b_0(v) + \frac{1}{\tau^{2/3}} b_1(v) + \frac{1}{\tau^{4/3}} b_2(v) + \mathcal{O}(\tau^{-2})\,, \tag{3.36}$$

$$c(\tau, v) = c_0(v) + \frac{1}{\tau^{2/3}} c_1(v) + \frac{1}{\tau^{4/3}} c_2(v) + \mathcal{O}(\tau^{-2})\,, \tag{3.37}$$

$$\alpha(\tau, v) = \alpha_0(v) + \frac{1}{\tau^{2/3}} \alpha_1(v) + \frac{1}{\tau^{4/3}} \alpha_2(v) + \mathcal{O}(\tau^{-2})\,, \tag{3.38}$$

$$\phi(\tau, v) = \phi_0(v) + \frac{1}{\tau^{2/3}} \phi_1(v) + \frac{1}{\tau^{4/3}} \phi_2(v) + \mathcal{O}(\tau^{-2})\,. \tag{3.39}$$

[2] Since ϵ is the only dimensionful constant, we can set it to one and measure all quantities in units of ϵ. We can then restore it using dimensional analysis, if desired.

[3] While it is possible to go to arbitrary high orders in powers of $\tau^{-2/3}$, for concreteness we will truncate the series at the given order. This will suffice to study second order hydrodynamics.

The equations of motion (3.31) are then solved, imposing the standard AdS boundary conditions

$$\left\{a_i(v), b_i(v), c_i(v), \alpha_i(v), \phi_i(v)\right\}\Big|_{v\to 0} = 0\,, \tag{3.40}$$

and requiring the absence of curvature singularities order by order. In order to present the solutions it is convenient to define

$$\tilde{b}_i(v) \equiv b_i(v) + 2c_i(v)\,. \tag{3.41}$$

The coefficients for $i = 0, 1, 2$ encode the perfect fluid approximation, first and second order dissipative hydrodynamics, respectively. These are given by

$$a_0 = \ln\frac{\left(1-v^4/3\right)^2}{1+v^4/3}\,, \quad \tilde{b}_0 = 3c_0 = \ln\left(1+v^4/3\right)^3\,. \tag{3.42}$$

$$a_1 = \frac{2\hat{\eta}\,(9+v^4)\,v^4}{9-v^8}\,, \quad \tilde{b}_1 = -\frac{6\hat{\eta}v^4}{3+v^4}\,, \quad c_1 = -\frac{2\hat{\eta}v^4}{3+v^4} - \hat{\eta}\ln\frac{3-v^4}{3+v^4}\,, \tag{3.43}$$

and

$$\begin{aligned}
a_2 &= \frac{(9+5v^4)v^2}{6(9-v^8)} - \frac{C(9+v^4)v^4}{36(9-v^8)} + \frac{\hat{\eta}^2(-1053-171v^4+9v^8+7v^{12})v^4}{3(9-v^8)^2} \\
&\quad + \frac{1}{4\sqrt{3}}\ln\frac{\sqrt{3}-v^2}{\sqrt{3}+v^2} - \frac{3\hat{\eta}^2}{2}\ln\frac{3-v^4}{3+v^4}\,, \\
\tilde{b}_2 &= \frac{v^2}{2(3+v^4)} + \frac{Cv^4}{12(3+v^4)} + \frac{\hat{\eta}^2(39+7v^4)v^4}{(3+v^4)^2} + \frac{1}{4\sqrt{3}}\ln\frac{\sqrt{3}-v^2}{\sqrt{3}+v^2} \\
&\quad + \frac{3\hat{\eta}^2}{2}\ln\frac{3-v^4}{3+v^4}\,, \\
c_2 &= -\frac{\pi^2}{144\sqrt{3}} + \frac{v^2(9+v^4)}{6(9-v^8)} + \frac{Cv^4}{36(3+v^4)} - \frac{\hat{\eta}^2(-9+54v^4+7v^8)v^4}{3(3+v^4)(9-v^8)} \\
&\quad + \frac{1}{4\sqrt{3}}\ln\frac{\sqrt{3}-v^2}{\sqrt{3}+v^2} + \frac{1}{36}(C+66\hat{\eta}^2)\ln\frac{3-v^4}{3+v^4} \\
&\quad + \frac{1}{12\sqrt{3}}\left(\ln\frac{\sqrt{3}-v^2}{\sqrt{3}+v^2}\ln\frac{(\sqrt{3}-v^2)(\sqrt{3}+v^2)^3}{4(3+v^4)^2} - \mathrm{li}_2\left(-\frac{(\sqrt{3}-v^2)^2}{(\sqrt{3}+v^2)^2}\right)\right)\,,
\end{aligned} \tag{3.44}$$

with

$$\hat{\eta} = \frac{1}{2^{1/2}3^{3/4}}\,, \qquad C = \frac{6\ln 2 - 17}{\sqrt{3}}\,. \tag{3.45}$$

Furthermore, the coefficients α_i and ϕ_i are found to vanish for $i = 0, 1, 2$ which suggest a universality of the relaxation times from second order hydrodynamics in gauge theory plasmas at (infinitely) strong 't Hooft coupling. This is further supported by the equivalence of relaxation rates in other superconformal theories [101], in which metric warp factors $\{a_i, b_i, c_i\}$ agree with those for the $\mathcal{N} = 4$ plasma (3.42)-(3.44) but, in addition, have other fields turned on at order $\mathcal{O}(\tau^{-4/3})$.

3.3 Relaxation of non-local probes

The metric (3.32) is dual to a plasma that is expanding along the x_3-direction, with the transverse plane spanned by $\vec{x}_\perp = \{x_1, x_2\}$. Given this geometry, with the coefficients (3.42)-(3.44), we would like to study the evolution of non-local observables such as two-point functions, Wilson loops and entanglement entropy. As studied in section 1.2.4, this problem amounts to the computation of certain extremal surfaces with fixed boundary conditions.

Before proceeding further, let us make some general remarks. For $v \to 0$ the metric (3.32) reduces to pure AdS and, therefore, in this limit we expect to recover the known results for the various observables in the vacuum of the CFT [107]. According to the UV/IR connection [108], the bulk coordinate z maps into a length scale $L \sim z$ in the boundary theory. Therefore, in the late-time regime $L\tau^{-\frac{1}{3}}\epsilon^{\frac{1}{4}} \to 0$, we expect all the probes to relax to their corresponding

AdS solution. Our goal is then to extract the leading order correction in the small parameter $\chi \equiv L\tau^{-\frac{1}{3}}\epsilon^{\frac{1}{4}}$, which is valid in the final stage of the evolution. Within this regime, we can explore the behavior as the other dimensionless parameter, $\xi \equiv \tau^{-\frac{2}{3}}\hat{\eta}$, is varied bearing in mind that ξ must be small enough so that the hydrodynamical description still applies. Finally, note that for an expanding plasma there is no notion of thermodynamics given that we are dealing with an out-of-equilibrium configuration. However, at late times, the system can be consider near-equilibrium and the energy density provides a definition of an *effective* temperature

$$T \equiv \left(8\varepsilon/(3\pi^2 N^2)\right)^{\frac{1}{4}} \sim \tau^{-\frac{1}{3}}\epsilon^{\frac{1}{4}} \,. \tag{3.46}$$

Thus, as expected, we have the gravity dual of a plasma undergoing cooling during expansion.[4] The regime we are interested in corresponds to the low temperature regime $LT \ll 1$. Hence, we are looking at approximate solutions in the same spirit as in [109] for the case of a static plasma.

3.3.1 Equilibrium results at late-times

From the holographic point of view, the non-local observables we want to study involve the computation of extremal surfaces anchored to the boundary. In this section we will review the standard results in AdS_5 [107], which are expected to hold in the $\tau \to \infty$ limit. In the Poincare patch the AdS

[4]Indeed, with the definition (3.46), and taking onto account the thermodynamic relations (1.31), one finds that $s = \hat{\eta}\tau^{-1}/4\pi$, leading to the well-know result of $1/4\pi$ for the ratio of the shear viscosity over the entropy density

metric is given by

$$ds^2 = \frac{1}{z^2}\left(-dt^2 + d\vec{x}^2 + dz^2\right) . \tag{3.47}$$

We define a boundary region A to be an n-dimensional strip with $x_1 \in [-\frac{\Delta x}{2}, \frac{\Delta x}{2}]$ and $x_i \in [-\frac{\ell}{2}, \frac{\ell}{2}]$ for $i = 2, ..., n$. We assume $\ell \to \infty$, so there is translation invariance along the transverse directions. We want to find the extremal surface Γ_A in the bulk that is anchored on ∂A. For the cases in consideration, $n = 1$, 2 and 3, Γ_A corresponds to a geodesic, a minimal area and a minimal volume, respectively. Choosing the coordinates on Γ_A to be $\sigma^1 = x_1 \equiv x$ and $\sigma^i = x_i$ for $i = 2, ..., n$ and parameterizing the surface by a single function $z(x)$ we get that the area functional is given by

$$\mathcal{A} \equiv \text{Area}(\Gamma_A) = \ell^{n-1} \int_{-\frac{\Delta x}{2}}^{\frac{\Delta x}{2}} \frac{\sqrt{1+z'^2}}{z^n} dx \, . \tag{3.48}$$

Since there is no explicit dependence on x, the Hamiltonian is conserved,

$$\mathcal{H} = \frac{\partial \mathcal{L}}{\partial z'} z' - \mathcal{L} = \frac{-1}{z^n \sqrt{1+z'^2}} \equiv \frac{-1}{z_*^n} \, , \tag{3.49}$$

where z_* is defined through $x(z_*) = 0$. This allows us to obtain an explicit expression for $x(z)$:

$$\pm\, x(z) = \frac{\Delta x}{2} - \frac{z^{n+1}}{(n+1) z_*^n} {}_2F_1\left[\tfrac{1}{2}, \tfrac{n+1}{2n}, \tfrac{3n+1}{2n}, \tfrac{z^{2n}}{z_*^{2n}}\right] , \tag{3.50}$$

from which we can obtain

$$z_* = \frac{n\Gamma(\frac{2n+1}{2n})}{\sqrt{\pi}\Gamma(\frac{n+1}{2n})} \Delta x \ . \tag{3.51}$$

Finally, the area of the extremal surface can be computed evaluating (3.48) on-shell,

$$\mathcal{A} = 2\ell^{n-1} \int_{z_0}^{z_*} \frac{dz}{z^n \sqrt{1-(z/z_*)^{2n}}} \, . \tag{3.52}$$

This quantity is UV divergent given that in the limit $z_0 \to 0$ the surface reaches the boundary of AdS. The divergent piece can be isolated by studying the near-boundary behavior of (3.52):

$$\mathcal{A}_{\rm div} = 2\ell^{n-1}\int_{z_0}\frac{dz}{z^n} = \begin{cases} -2\log z_0\,, & n=1\,, \\ \dfrac{2\ell^{n-1}}{(n-1)z_0^{n-1}}\,, & n>1\,. \end{cases} \tag{3.53}$$

Subtracting this divergence, we obtain the finite term which is the main quantity we are interested in:

$$\mathcal{A}_{\rm ren} = \begin{cases} 2\log\Delta x\,, & n=1\,, \\ -\dfrac{8\pi^3}{\Gamma(\frac{1}{4})^4}\dfrac{\ell}{\Delta x}\,, & n=2\,, \\ -\dfrac{4\pi^{3/2}\Gamma(\frac{4}{6})^3}{\Gamma(\frac{1}{6})^3}\dfrac{\ell^2}{(\Delta x)^2}\,, & n=3\,. \end{cases} \tag{3.54}$$

With the above results at hand, we can now proceed to compute the late-time $\tau \to \infty$ expectation value of the various non-local observables. Using (1.56), (1.61) and (1.64) we find that

$$\langle G^{(0)}\rangle = \frac{1}{|x-x'|^{2\Delta}}\,, \tag{3.55}$$

$$\langle W^{(0)}\rangle = \exp\left(\frac{4\pi^2\sqrt{\lambda}\ell}{\Gamma(1/4)^4|x-x'|}\right)\,, \tag{3.56}$$

and

$$\langle S_A^{(0)}\rangle = -\frac{2\sqrt{\pi}\Gamma(\frac{4}{6})^3\ell^2N^2}{\Gamma(\frac{1}{6})^3|x-x'|^2}\,, \tag{3.57}$$

respectively. In these formulas, the subindex "(0)" is just a reminder that these are the expectation values in the vacuum of the SYM theory.

3.3.2 Results for first and second order hydrodynamics

In order to extract the first correction at late-times of the various non-local observables we proceed in the following way. Consider the Lagrangian density $\mathcal{L}[x(z);\lambda]$ for the extremal surfaces, where $x(z)$ is the embedding function and λ is a dimensionless parameter such that $\lambda \ll 1$. Of course, here $\mathcal{L}$ is proportional to Area(Γ_A) in the full geometry (3.32). We can expand both $\mathcal{L}$ and $x(z)$ as follows:

$$\begin{aligned} \mathcal{L}[x(z);\lambda] &= \mathcal{L}^{(0)}[x(z)] + \lambda \mathcal{L}^{(1)}[x(z)] + \mathcal{O}(\lambda^2)\,, \\ x(z) &= x^{(0)}(z) + \lambda x^{(1)}(z) + \mathcal{O}(\lambda^2)\,. \end{aligned} \tag{3.58}$$

In principle, the functions $x^{(n)}(z)$ could be obtained by solving the equations of motion order by order in λ. However, these equations are in general highly non-linear so in practice it is very difficult (and in most cases impossible) to obtain analytic results. The key observation is that at first order in λ,

$$\begin{aligned} \mathcal{S}_{\text{on-shell}}[x(z)] = &\int dz\, \mathcal{L}^{(0)}[x^{(0)}(z)] + \lambda \int dz\, \mathcal{L}^{(1)}[x^{(0)}(z)] \\ &+ \lambda \int dz\, x^{(1)}(z) \left[\cancel{\frac{d}{dz} \frac{\partial \mathcal{L}^{(0)}}{\partial x'(z)}} - \cancel{\frac{\partial \mathcal{L}^{(0)}}{\partial x(z)}} \right]_{x^{(0)}} + \mathcal{O}(\lambda^2). \end{aligned} \tag{3.59}$$

Therefore, we only need $x^{(0)}(z)$ to obtain the first correction to the on-shell action. Fortunately, this is the solution to the embedding in pure AdS, which is know anallitically. The parameter λ is related to the expansion parameter in the gauge theory side $\chi \equiv L\tau^{-\frac{1}{3}}\epsilon^{\frac{1}{4}}$. More specifically, we will see that $\lambda \sim \chi^4 \sim v^4$ so in order to extract the first order corrections we need the action up to the order $\mathcal{O}(v^4)$. Let us now specialize to the various non-local observables and make the above derivation more explicit.

3.3.2.1 Two-point functions

As a first step let us consider a space-like geodesic connecting two boundary points separated in the transverse plane: $(\tau, x) = (\tau_0, -\frac{\Delta x}{2})$ and $(\tau', x') = (\tau_0, \frac{\Delta x}{2})$, where $x \equiv x_1$ and all other spatial directions are identical. Such a geodesic can be parameterized by two functions $\tau(z)$ and $x(z)$, satisfying the following boundary conditions:

$$\tau(0) = \tau_0 \ , \quad x(0) = \pm \frac{\Delta x}{2} \ . \tag{3.60}$$

For such a geodesic, the action is given by

$$\mathcal{S} = 2 \int_0^{z_*} \frac{dz}{z} \sqrt{1 + e^c x'^2 - e^a \tau'^2} \, . \tag{3.61}$$

Of course, in the strict limit $v \to 0$ we expect to recover the action for a geodesic in AdS. Expanding around $v = 0$, we get $\mathcal{S} = \mathcal{S}^{(0)} + \mathcal{S}^{(4)} + \mathcal{O}(v^6)$ where[5]

$$\mathcal{S}^{(0)} = 2 \int_0^{z_*} \frac{dz}{z} \sqrt{1 + x'^2 - \tau'^2} \, , \tag{3.62}$$

$$\mathcal{S}^{(4)} = \frac{1}{3} \int_0^{z_*} \frac{dz}{z} \frac{[x'^2 + 3\tau'^2 - 6 \, \tau'^2 \, \xi - (x'^2 - 3\tau'^2)\tilde{\xi}^2] v^4}{\sqrt{1 + x'^2 - \tau'^2}} \, , \tag{3.63}$$

where

$$\xi \equiv \frac{\hat{\eta}}{\tau^{2/3}} \, , \qquad \tilde{\xi}^2 \equiv \frac{1}{2}(1 + \log(4))\xi^2 \, . \tag{3.64}$$

Clearly, the terms in $\mathcal{S}^{(4)}$ proportional to ξ and $\tilde{\xi}^2$ encode the first and second order dissipative hydrodynamics, respectively. At zeroth order, it can be

[5]Because $v = v(z)$ is a dynamical variable, we introduce a (dimensionless) scaling parameter through $v \to \zeta v$ and perform a Taylor expansion around $\zeta = 0$. Then, we simply restore $\zeta = 1$.

checked that the AdS solution $\tau(z) = \tau_0$ and $x(z)$ given in (3.50) (for $n = 1$) is indeed a solution to the equations of motion derived from $\mathcal{S}^{(0)}$. In this limit the renormalized geodesic length evaluates to:

$$\mathcal{S}^{(0)}_{\text{ren}} = 2 \log L \,, \quad L \equiv \Delta x \,. \tag{3.65}$$

Taking into account the next-to-leading order term in the action changes the equations of motion for $\tau(z)$ and $x(z)$. However, it is easy to see that the corrections in these functions will only contribute at higher order in v when the action is evaluated *on-shell*. Therefore, at our order of approximation it is still valid to evaluate $\mathcal{S}^{(4)}$ in the AdS solutions. A brief calculation leads to

$$\mathcal{S}^{(4)} = \frac{1}{90} \chi (1 - \tilde{\xi}^2) \,, \quad \chi \equiv L^4 \tau_0^{-\frac{4}{3}} \epsilon \,. \tag{3.66}$$

Putting all together, we find that the late time behavior of the two-point correlator decays exponentially as

$$\langle G(x_1, x_1') \rangle = \langle G^{(0)} \rangle \exp \left\{ - \frac{\epsilon \Delta |x_1 - x_1'|^4}{90 \tau^{4/3}} \left(1 - \frac{1}{2} (1 + \log(4)) \xi^2 \right) \right\} \,, \tag{3.67}$$

where $\langle G^{(0)} \rangle$ is vacuum result given in (3.55). Note that ξ must be bounded from above in order for the hydrodynamic description to be valid. Indeed, from (3.67) we can already see that the approximation breaks down unless

$$\xi < \sqrt{\frac{2}{1 + \log(4)}} \simeq 0.915 \,. \tag{3.68}$$

If ξ is bigger than this value, the exponential flips sign and the vacuum value is reached from below. We will see, however, that the behavior of other observables constrain even further the maximum value of ξ.

For longitudinal separation we can proceed in a similar way. In this case we are interested in a space-like geodesic connecting the two boundary points (τ_0, x_3) and (τ_0, x_3'). We can make use of the invariance under translations in y and parameterize the geodesic by functions $\tau(z)$ and $y(z)$ with boundary conditions

$$\tau(0) = \tau_0 \ , \quad y(0) = \pm\frac{\Delta y}{2} \ . \tag{3.69}$$

At the end, we can simply shift our rapidity coordinate $y \to y + y_0$ and express our results in terms of

$$x_3 = \tau_0 \sinh(y_0 + \tfrac{\Delta y}{2}) \, , \quad x_3' = \tau_0 \sinh(y_0 - \tfrac{\Delta y}{2}) \, . \tag{3.70}$$

The action for this geodesic reads

$$\mathcal{S} = 2 \int_0^{z_*} \frac{dz}{z} \sqrt{1 + e^b \tau^2 y'^2 - e^a \tau'^2} \, . \tag{3.71}$$

Again, expanding in v we get $\mathcal{S} = \mathcal{S}^{(0)} + \mathcal{S}^{(4)} + \mathcal{O}(v^6)$, where

$$\mathcal{S}^{(0)} = 2 \int_0^{z_*} \frac{dz}{z} \sqrt{1 + \tau^2 y'^2 - \tau'^2} \, , \tag{3.72}$$

$$\mathcal{S}^{(4)} = \frac{1}{3} \int_0^{z_*} \frac{dz}{z} \frac{[\tau^2 y'^2 + 3\tau'^2 - 6(\tau^2 y'^2 + \tau'^2)\xi + (5\tau^2 y'^2 + 3\tau'^2)\tilde{\xi}^2] v^4}{\sqrt{1 + \tau^2 y'^2 - \tau'^2}} \tag{3.73}$$

The term $\mathcal{S}^{(0)}$ is the action of a geodesic in AdS written in proper time and rapidity coordinates. It is straightforward to check that the following embedding is a solution at zeroth order:

$$\tau(z) = \sqrt{t_0^2 - x(z)^2} \, , \quad y(z) = \operatorname{arccosh}\left(\frac{t_0}{\tau(z)}\right) \, , \tag{3.74}$$

where t_0 is a constant and $z(x)$ is the function given in (3.50) (for $n = 1$). The relation between $(t_0, \Delta x_3)$ and $(\tau_0, \Delta y)$ is[6]

$$t_0 = \tau_0 \cosh(\tfrac{\Delta y}{2}) \,, \quad \Delta x_3 = 2\tau_0 \sinh(\tfrac{\Delta y}{2}) \,. \tag{3.75}$$

Of course, at zeroth order we have translation invariance in x_3 and the on-shell action reduces to

$$\mathcal{S}^{(0)}_{\rm ren} = 2 \log L \,, \quad L \equiv \Delta x_3 \,. \tag{3.76}$$

In this case, the first correction to the action is given by

$$\mathcal{S}^{(4)} = f(\Delta y, \xi) \times L^4 \tau_0^{-\frac{4}{3}} \epsilon \,, \tag{3.77}$$

where $f(\Delta y, \xi)$ is given by the dimensionless integrals

$$\begin{aligned} f(\Delta y, \xi) = & \int_0^1 \frac{x^5[3x^2 + (4 - 3x^2)\cosh(\Delta y) - 2]}{96(1-x^2)^{1/2}[x^2 \sinh^2(\frac{\Delta y}{2}) + 1]^{5/3}} dx \\ & - \xi \int_0^1 \frac{x^5[x^2 + (2 - x^2)\cosh(\Delta y)]}{16(1-x^2)^{1/2}[x^2 \sinh^2(\frac{\Delta y}{2}) + 1]^{2}} dx \\ & + \tilde{\xi}^2 \int_0^1 \frac{x^5[3x^2 + (8 - 3x^2)\cosh(\Delta y) + 2]}{96(1-x^2)^{1/2}[x^2 \sinh^2(\frac{\Delta y}{2}) + 1]^{7/3}} dx \,. \end{aligned} \tag{3.78}$$

The two-point correlator for longitudinal separation evaluates to

$$\langle G(x_3, x_3') \rangle = \langle G^{(0)} \rangle \exp\left\{ - \frac{\epsilon \Delta |x_3 - x_3'|^4}{\cosh^4(y_0) \tau^{4/3}} f(\Delta y, \xi) \right\} \,, \tag{3.79}$$

which is manifestly not invariant under translations.

The function $f(\Delta y, \xi)$ can be evaluated in terms of hypergeometric functions but we refrain from writing out the explicit result here since it is

[6] More in general $\Delta x_3 = 2\tau_0 \cosh(y_0) \sinh(\frac{\Delta y}{2})$ for $y_0 \neq 0$.

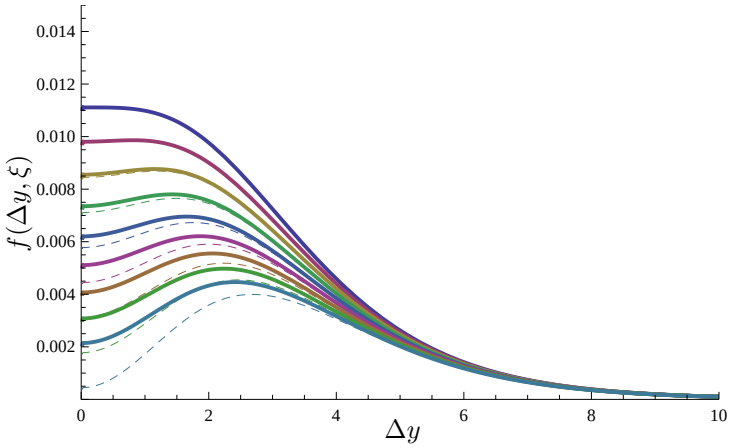

Figure 3.1: Contours of $f(\Delta y, \xi)$ for fixed $\xi = \{0, ..., 0.16\}$ with increments of 0.02, from top to bottom, respectively. The solid lines correspond to the results for second order hydrodynamics, while the dashed lines correspond to the results for first order hydrodynamics. In the latter case, we are neglecting terms of order $\mathcal{O}(\xi^2)$.

not particularly illuminating. In figure 3.1 we plot f as a function of Δy for some fixed values of ξ. A few comments are in order. First, notice that for a fixed value of Δy, f decreases as ξ is increased. This is consistent with the fact that the viscosity damps the dynamics of the plasma and, therefore, we expect faster decorrelation when ξ is decreased. For $\xi = 0$, the function is monotonically decreasing in Δy, and interpolates from the $1/90$ coefficient found for the transverse case (3.66) to $f(\Delta y, \xi) \sim \mathcal{O}(e^{-\frac{2\Delta y}{3}}) \to 0$ at large Δy. For finite ξ, the function is non-monotonous and the small Δy behavior is modified to

$$f(\Delta y, \xi) = \frac{1}{90}\left(1 - 6\xi + \frac{5}{2}(1 + \log(4))\xi^2\right) + \mathcal{O}((\Delta y)^2)\,. \tag{3.80}$$

In order to have a correct physical behavior of the correlator we must impose

that $f(\Delta y, \xi) > 0$ for all values of Δy and ξ, so we see here that the behavior for small Δy in (3.80) constrain further the maximum value of ξ. If we take into account first order hydrodynamics we can neglect the ξ^2 term. In this case, we obtain the bound

$$\xi^{(1)} < \frac{1}{6} \simeq 0.167\,. \tag{3.81}$$

On the other hand, for second order hydrodynamics we obtain

$$\xi^{(2)} < \frac{6 - \sqrt{26 - 10\log(4)}}{5(1 + \log(4))} \simeq 0.211\,, \tag{3.82}$$

which, as expected, increases the range of validity of the hydrodynamic approximation. Finally, notice that the bound (3.82) is much stronger than the bound found from the transverse correlator (3.68). Therefore, if $\xi < \xi^{(2)}$ then (3.68) is automatically satisfied.

3.3.2.2 Wilson loops and entanglement entropy

From the point of view of the bulk, Wilson loops and entanglement entropy are natural generalizations of the two-point functions considered above. In particular, they involve the computation of extremal surfaces of higher dimensions and therefore, the results of Section 3.3.1 (for $n = 2, 3$) will now become handy. We will only deal with some loop contours $\mathcal{C}$ and regions A that can be treated analytically in the same way as the two-point correlators. For such cases, the computations proceed identically as before so we will just state the final results.

For the Wilson loop we consider two cases. The first case consists of a rectangular loop in the transverse plane, where $x_1 \in [-\frac{\Delta x}{2}, \frac{\Delta x}{2}]$, $x_2 \in [-\frac{\ell}{2}, \frac{\ell}{2}]$ and $\ell \to \infty$. We will call this case $W_\perp$. The second case is also a rectangular loop but in this case one side is along the longitudinal direction, $y \in [-\frac{\Delta y}{2}, \frac{\Delta y}{2}]$, $x_1 \in [-\frac{\ell}{2}, \frac{\ell}{2}]$ and $\ell \to \infty$. We will refer to this one as $W_\parallel$. For the first case we find an exponential decay

$$\langle W_\perp \rangle = \langle W^{(0)} \rangle \exp\left\{ -\frac{\epsilon\sqrt{\lambda}\ell(\Delta x_1)^3}{15\Gamma(\frac{3}{4})^4\tau^{4/3}} \left(1 - \frac{1}{2}(1+\log(4))\xi^2\right)\right\}, \tag{3.83}$$

where $\langle W^{(0)} \rangle$ is the vacuum expectation value of the Wilson loop given in (3.56). As we can see, the constraint imposed on ξ by this observable is similar to that imposed by the transverse two-point function (3.68). For the second case, we find that the exponential is modulated by a new function $g(\Delta y, \xi)$,

$$\langle W_\parallel \rangle \sim \langle W^{(0)} \rangle \exp\left\{ -\frac{\epsilon\sqrt{\lambda}\ell(\Delta x_1)^3}{\cosh^3(y_0)\tau^{4/3}} g(\Delta y, \xi)\right\}. \tag{3.84}$$

In the regime $\Delta y \ll 1$, the function g behaves as

$$g(\Delta y, \xi) = \frac{1}{60\Gamma(\frac{3}{4})^4}\left(4 - 9\xi + \frac{5}{2}(1+\log(4))\xi^2\right) + \mathcal{O}((\Delta y)^2), \tag{3.85}$$

which imposes weaker constraints with respect to the longitudinal two-point function. For first order hydrodynamics we obtain

$$\xi^{(1)} < \frac{4}{9} \simeq 0.444\,. \tag{3.86}$$

For second order hydrodynamics the bound is shifted to

$$\xi^{(2)} < \frac{9}{5(1+\log(4))} \simeq 0.754\,, \tag{3.87}$$

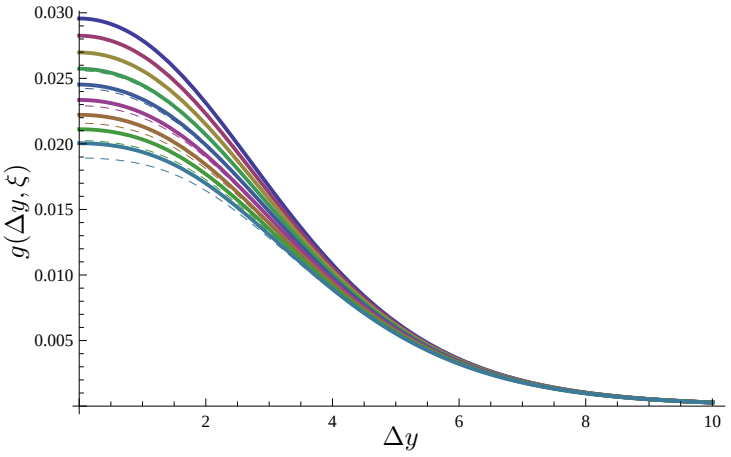

Figure 3.2: Contours of $g(\Delta y, \xi)$ for fixed $\xi = \{0, ..., 0.16\}$ with increments of 0.02, from top to bottom, respectively. The solid lines correspond to the results for second order hydrodynamics, while the dashed lines correspond to the results for first order hydrodynamics. In the latter case, we are neglecting terms of order $\mathcal{O}(\xi^2)$.

At large Δy, we find $g(\Delta y, \xi) \sim \mathcal{O}(e^{-\frac{2\Delta y}{3}})$. Some contours of g for fixed values of ξ (in the range allowed by the longitudinal two-point function) are given in figure 3.2. Notice that, contrary to the two-point function, in this range the function g always decreases monotonically in Δy.

For entanglement entropy we only consider the case where the region A is a 3-dimensional strip with $y \in [-\frac{\Delta y}{2}, \frac{\Delta y}{2}]$, $x_i \in [-\frac{\ell}{2}, \frac{\ell}{2}]$ $(i = 1, 2)$ and $\ell \to \infty$. A brief computation leads to

$$\langle S_A \rangle = \langle S_A^{(0)} \rangle \left(1 - \frac{\epsilon (\Delta x_3)^4 h(\Delta y, \xi)}{\cosh^2(y_0) \tau^{4/3}} \right) , \tag{3.88}$$

where $\langle S_A^{(0)} \rangle$ is the entanglement entropy of region A in the vacuum state given in (3.57). The function $h(\Delta y, \xi)$ behaves in a similar way as $g(\Delta y, \xi)$, with

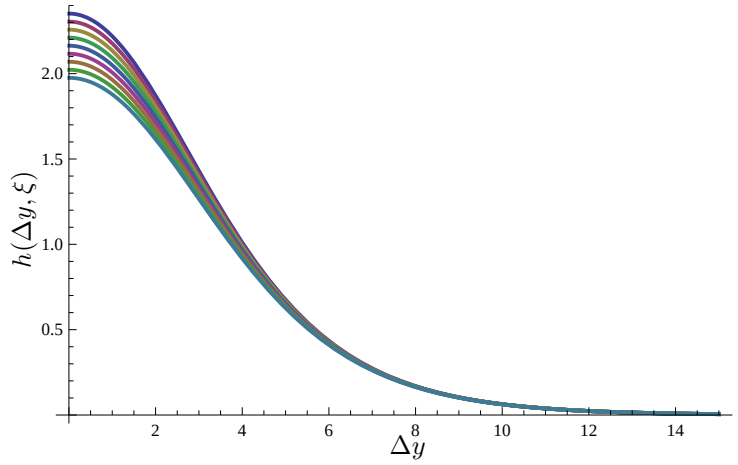

Figure 3.3: Contours of $h(\Delta y, \xi)$ for fixed $\xi = \{0, ..., 0.16\}$ with increments of 0.02, from top to bottom, respectively. The solid lines correspond to the results for second order hydrodynamics. We are also plotting the results for first order hydrodynamics on top, but the differences are so small that they are indistinguishable to the naked eye.

slightly less sensitivity with respect to the viscosity. For small Δy we find

$$h(\Delta y, \xi) = \frac{\Gamma(\frac{1}{6})^9}{1280\pi^{13/2}}(1-\xi) + \mathcal{O}((\Delta y)^2)\,, \tag{3.89}$$

whereas for large Δy, $h(\Delta y, \xi) \sim \mathcal{O}(e^{-\frac{2\Delta y}{3}})$. The constraint on ξ is even weaker in this case. For first order hydrodynamics we obtain $\xi^{(1)} < 1$, and since there is no correction of order $\mathcal{O}(\xi^2)$ in (3.89), the bound for second order hydrodynamics is equal to the one imposed by first order hydrodynamics $\xi^{(2)} < 1$. The full function $h(\Delta y, \xi)$ have corrections of order $\mathcal{O}(\xi^2)$ for finite Δy, but they are very small and basically indistinguishable to the naked eye. Some contours of h for fixed ξ are given in figure 3.3.

3.4 Conclusions

In this Chapter we have studied a hydrodynamical model of heavy-ion collisions in the framework of the AdS/CFT correspondence. This model differs from the one studied in the previous Chapter because the system here evolves towards the vacuum of the theory, instead of a thermalized state. We paid particular attention to the late-time behavior of various non-local observables, including effects of first and second order dissipative hydrodynamics. More specifically, we gave analytic expressions for the evolution of certain two-point functions, Wilson loops and entanglement entropies in the regime $\chi = L\tau^{-\frac{1}{3}}\epsilon^{\frac{1}{4}} \ll 1$ (where L is the typical size of the probe) as a function of $\xi = \tau^{-\frac{2}{3}}\eta_0$. Our results lead to universal formulas for the relaxation of such probes in conformal field theories with a gravity dual formulation in the limit of infinite coupling.

The two-point correlators and Wilson loops are found to relax exponentially in χ whereas the entanglement entropy equilibrates at a much slower rate (as a power of χ). Hence, it is the entanglement that sets the relevant timescale for the approach to equilibrium, which is consistent with the known results of [99]. Another interesting result is the dependence of the observables on the longitudinal variables. We find that, in such cases, the leading behaviour of the observables is modulated by functions of Δy and ξ. For fixed Δy, these functions decrease monotonically in ξ, which is consistent with the dissipative nature of the viscosity. For fixed ξ we also find a monotonic behavior for the Wilson loop and entanglement entropy, but not for the two-point function.

This is interpreted as a non-trivial prediction from AdS/CFT. Indeed, one would naively expect a higher correlation for points with similar rapidities, which is does not hold for some range of the parameter space. Finally, it is worth pointing out that our results point to a break down of the first order hydrodynamics for $\xi > 0.211$, which is set by the behavior of the longitudinal two-point function at small Δy.

The results presented here could be extended in a number of ways. One interesting idea would be to push the hydrodynamic expansion to arbitrary high order and study numerically the evolution of the constraint set by the two-point functions. In particular, it is known that the hydrodynamic gradient expansion has a zero radius of convergence(!) [120] so one might wonder about the evolution of the bound (3.82). We could also generalize our findings to finite coupling by studying string theory α' corrections in the dual description of an expanding SYM plasma. Even though the universal behavior of the relaxation rates is expected to break down when considering finite λ, it would be of interest to investigate — at least for the SYM theory — the effects of the 't Hooft coupling on the range of validity of the hydrodynamic approximation.

Chapter 4

Dynamics in global AdS: quantum revivals

4.1 Introduction

Relaxation processes of quantum systems with *finite* number of degrees of freedom have been studied for many years, both from a theoretical and a experimental perspective, but we are still far from reaching a general consensus on the physical mechanism that governs their evolution and possible outcomes. On one hand, ergodic theory stipulates that many body systems perturbed away from equilibrium quickly approach to a final state where equipartition is expected. However, there are known cases where this conclusion does not hold — see [121] for a review on this topic. This surprising behavior has been found in spin chain systems [122, 123], conformal field theories [124, 125], and has been realized experimentally in cold atom experiments [126, 127]. In all these systems, the lack of ergodicity has been associated with integrability and/or additional conservation laws [128].

At the classical level, a similar phenomenon was found for the first time by Fermi, Pasta and Ulam (FPU) in their seminal work [129, 130]. FPU studied numerically a collection of nonlinear harmonic oscillators and expected to see thermalization. However, they observed that for a set of initial conditions

the presence of nonlinearities was not enough to trigger an ergodic behavior at late times. What they found in such cases was remarkable: the system evolved towards a state of coherent oscillations that repeated over time and never thermalized. They suspected that this apparent paradox was was something deep. In fact, their study lead to a set of ideas that rapidly evolved into two new areas of dynamical systems: integrability and chaos.

Very recently, there has been a particular interest in the possibility of realizing such states in the context of the AdS/CFT correspondence [131, 132]. Since thermalization in the holographic context corresponds to the study of black hole formation in AdS, the question of whether small perturbations can evolve towards a completely oscillatory state or must necessarily collapse into a black hole is equivalent to the question of whether AdS is stable at the nonlinear level. This is a subject of great interest over which there have been an incessant debate in the past few years [133, 134, 135, 136, 137, 138, 139, 140, 141, 142, 143].

The purpose of this Chapter is to argue that such oscillatory states can in fact be constructed as a small perturbation over *global* AdS. Indeed, as shown in [124], any CFT on a sphere supports states of completely undamped collective oscillations so it is natural to expect that such states also exist for theories with a gravity dual. From the field theory perspective, the existence of such permanently oscillating states is due to the existence of infinitely many conserved charges in CFT generated by conformal Killing vectors, and is guaranteed by $SL(2,\mathbb{R})$ subalgebras of the conformal algebra; these subalgebras

are formed from the Hamiltonian and combinations of operators which act as ladder operators for energy eigenstates. Thus, from this point of view it is not surprising that any CFT, regardless of its interactions, admits states that undergo undamped oscillations.

From the gravity perspective, the first detailed study on the dynamical evolution of small perturbations over global AdS was performed by Bizon and Rostworowski in [133]. They used tools of weakly nonlinear perturbation theory and showed that for arbitrarily small departures from AdS, the evolution of a massless, spherically symmetric scalar field *always* leads into black hole formation. At the linear level, the system is characterized by a set of undamped normal modes with frequencies $\omega_j = 2j + 3$. Due to the presence of a high number of resonances, they concluded that the nonlinear effects always lead to a turbulent cascade of energy to high mode numbers, thus, making gravitational collapse inevitable.

The same problem was studied from a numerical point of view by Garfinkle and Pando Zayas in [134, 136]. They found that for small values of the initial amplitude of the scalar field there is no black hole formation, rather, the scalar field performs undergoes a periodic oscillatory motion. However, their numerical scheme was questioned in [135]. At the same time Buchel, Lehner and Liebling showed in [137] that the argument of [133] actually breaks down if the mode amplitudes fall off sufficiently rapidly for high mode numbers. This conclusion was later elaborated on in [138], implementing a modified perturbation theory to properly take into account energy transfer

between modes.

In this Chapter we will implement the tools developed in [138] to sharpen their results and to extend them to a wider variety of scenarios. In Section 4.2 we start with a brief review of [124], showing that CFTs on a sphere support a set of states undergoing undamped collective oscillations. In addition, we discuss the holographic perspective and point out some properties of global AdS that allow such oscillatory solutions. In Section 4.3 we explain the perturbative formalism introduced in [138] and we obtain several families of undamped solutions for massive scalar fields. This provides further evidence in support of a recent numerical study on the collapse of massive scalar fields [144]. In Section 4.4 we compute the entanglement entropy of spherical caps and characterize its behavior as we change the mass of the scalar field.[1] We propose that these entanglement entropies can be thought of as conserved charges of the system since they split the Hilbert space into sectors that do not mix under time evolution. We close in Section 4.5 with some final remarks and conclusions.

4.2 Exact collective oscillations in CFTs on a sphere

To motivate the problem let us review the oscillating states constructed in [124]. We assume that the CFT lives on $(d-1)$-sphere and we measure energies in units of its inverse radius R^{-1}, which is set to unity. The conformal

[1] In the dual field theory, different masses of the scalar field correspond to perturbing the underlying CFT with operators of different conformal dimension.

algebra acting on the Hilbert space of the CFT contains d non-independent copies of the $SL(2,\mathbb{R})$ algebra,

$$[H, L^i_+] = L^i_+ \,, \qquad [H, L^i_-] = -L^i_- \,, \qquad [L^i_+, L^i_-] = 2H \,, \tag{4.1}$$

where $L_\pm$ are ladder operators and H is the Hamiltonian operator. Here $i = 1...d$ is an index labeling directions in the $\mathbb{R}^d$ in which S^{d-1} is embedded as the unit sphere. Also, notice that there is no implicit sum in the last equation of (4.1).

The construction of the oscillating states make use of the $SL(2,\mathbb{R})$ algebras as follows. Let $|\varepsilon\rangle$ be an eigenstate of H, $H|\varepsilon\rangle = \varepsilon|\varepsilon\rangle$. Now, consider a state vector $|\psi\rangle$ build up on $|\varepsilon\rangle$ in analogy with coherent or squeezed states in a harmonic oscillator,

$$|\psi(t=0)\rangle = N e^{\alpha L_+ + \beta L_-}|\varepsilon\rangle \,, \tag{4.2}$$

where $L_+ = L^i_+$ and $L_- = L^j_-$ for some $i, j \in \{1, ..., d\}$, N is a normalization constant, and α and β are complex numbers.[2] Using the Baker-Campbell-Hausdorff formula and the commutation relations (4.1), it can be checked that the above state evolves in time as follows

$$|\psi(t)\rangle = N e^{-iHt} e^{\alpha L_+ + \beta L_-}|\varepsilon\rangle = N e^{-i\varepsilon t} e^{\alpha(t) L_+ + \beta(t) L_-}|\varepsilon\rangle \,, \tag{4.3}$$

where $\alpha(t) = \alpha e^{-it}$ and $\beta(t) = \beta e^{it}$. We should keep in mind that we are working in units of the radius of the sphere R. Thus, the state $|\psi\rangle$ above is found to oscillate with frequency $1/R$.

[2]The possible values of α and β are constrained from normalizability [124].

More in general, the time evolution of a state

$$|\psi(t=0)\rangle = f(L_+^1, ..., L_+^d, L_-^1, ..., L_-^d)|\varepsilon\rangle \tag{4.4}$$

where f is any regular function of the $2d$ variables L_+^i, L_-^j, $1 \leq i, j \leq d$, is given by replacing $L_\pm^i$ with $L_\pm^i e^{\pm it}$ $\forall$ i. Bearing this in mind, then, it is easy to come up with states with different frequencies. These can be constructed by choosing the function f with the correct combination of ladder operators. For instance, one function that produces an oscillating state with frequency $2/R$ is given by[3]

$$f = \sum_{m=0}^{\infty} \frac{1}{(m!)^2} \left(\alpha L_+^2 + \beta L_-^2\right)^m , \tag{4.5}$$

where L_+ can be any of L_+^i, $1 \leq i \leq d$, and similarly for L_-. Finally, notice that not every function f produces an oscillating state. One simple example is $f = L_+$, which merely produces another energy eigenstate.

The states constructed above are said to be built up on $|\varepsilon\rangle$. In particular, we can assume that $|\varepsilon\rangle = |0\rangle$ in which case the oscillatory states are built up on top of the CFT vacuum. One can imagine more general situations in which $|\varepsilon\rangle$ is replaced by a nonstationary state $\sum_i c_i|\varepsilon_i\rangle$. However, since the different components evolve in time with distinct phases, the periodic behavior is not guaranteed. Another option is to replace $|\varepsilon\rangle$ with a stationary density matrix ρ, which evolves in time with a phase A

$$[H, \rho] = A\rho\,. \tag{4.6}$$

[3] The coefficient $(m!)^2$ in (4.5) is designed to give the state a finite norm.

We can consider, for instance, energy eigenstates for which $\rho = |\varepsilon\rangle\langle\varepsilon|$, or thermal density matrices $\rho = e^{-\beta H}$. Regardless of the choice, one finds that for an initial ensemble of the form

$$\tilde{\rho}(t=0) = N e^{\alpha L_+ + \beta L_-} \rho e^{\beta^* L_+ + \alpha^* L_-} \,, \tag{4.7}$$

its time evolution leads also to periodic oscillations

$$\tilde{\rho}(t) = N e^{-iAt} e^{\alpha(t) L_+ + \beta(t) L_-} \rho e^{\beta(t)^* L_+ + \alpha(t)^* L_-} \,, \tag{4.8}$$

where, again, $\alpha(t) = \alpha e^{-it}$ and $\beta(t) = \beta e^{it}$. These states are said to be built up on ρ, in the same way $|\psi\rangle$ was built up on $|\varepsilon\rangle$.

The authors of [124] gave a specific example for the holographic dual of an oscillatory state built up on a thermal density matrix. The bulk geometry that corresponds to such a state was constructed by applying a "conformal boost" to a regular AdS black hole, producing a "bouncing black hole" background. The conformal boost they considered is the equivalent to a conformal transformation in the boundary, $e^{\alpha L_+ + \beta L_-}$, and corresponds to a bulk diffeomorphism that falls off with the appropriate power to change the state of the dual CFT. Several observables such as the one point function of the stress energy tensor and the entanglement entropy of spherical regions were shown to display oscillations around the corresponding mixed state.

We will show that it is also possible to obtain gravitational backgrounds that are arbitrarily close to AdS and display stable periodic oscillations. Since pure AdS is dual to the vacuum of the CFT, we argue that such geometries should be identified as the holographic dual of states that are built up on $|0\rangle$.

Before proceeding further let us review some basic properties of AdS space that are crucial for the construction of such oscillatory states. Usually, the AdS/CFT correspondence is discussed in terms of a CFT living on a $R^{1,d-1}$ space, in which case the bulk geometry is naturally given by the Poincaré patch of AdS (1.7). However, using a different foliation of the bulk metric it is possible to discuss the same duality for CFTs living on a different background. To illustrate this point let us consider the global AdS metric,

$$ds^2 = -f(r)dt^2 + \frac{dr^2}{f(r)} + r^2 d\Omega_{d-1}^2\,, \qquad f(r) \equiv 1 + \frac{r^2}{L^2}\,. \tag{4.9}$$

The metric of the dual CFT is given by the coefficient of the non-normalizable mode as $r \to \infty$. From (4.9) one finds that

$$ds^2_{\rm CFT} = -dt^2 + L^2 d\Omega_{d-1}^2\,, \tag{4.10}$$

which is just the direct product $R \times S^{d-1}$. The key observation here is that there is a conformal embedding of $R^{1,d-1}$ to $R \times S^{d-1}$. Under the map a combination of the original generator of time translations and a generator of special conformal transformations is mapped to the the new Hamiltonian (*i.e.* the generator of time translations along the R factor) in $R \times S^{d-1}$.

The duality in global AdS is qualitatively different for several reasons. One crucial difference is the radius of the S^{d-1} provides a scale against which the energy and other physical quantities in the CFT can be measured. For example, if we study field theory at finite temperature T the system can undergo a phase transition (de-confinement transition) which can be associated

with the transition between an AdS black hole and a thermal AdS geometry (Hawking-Page transition). In the Poincaré patch, such phase transition does not appear and the field theory is always in the high temperature phase. In this case, the temperature can simply be scaled out since there is no other scale to compare with.

One might expect that the physics in out-of-equilibrium scenarios to be different as well. For instance, it has been shown that in the Poincaré patch the evolution of small perturbations over AdS always leads to black hole collapse [67]. We can understand this as follows: let us imagine an observer sending a signal from the boundary of AdS into the bulk. If we let the system to evolve, the signal will necessarily scape from the Poincaré patch at a later time — see Figure 4.1. From the observer's point of view, the signal is absorbed by the Poincaré horizon, and the system thermalizes. Since there is no energy gap in the spectrum of planar AdS black holes, then, the only possible outcome will necessarily be black hole formation. As discussed before, there are several indications that suggest that this may not be true in global AdS. Indeed, if we repeat the same experiment without restricting to the Poincaré patch, the signal could actually reach the opposite side of the boundary, bounce back and be collected again by the observer. However, if the energy of the signal emitted is large enough, black hole collapse might occur even before this process is completed. At any rate, we can already see that there is a clear distinction between the physics in the Poincaré patch and in global AdS. We will now proceed to the setup of the problem.

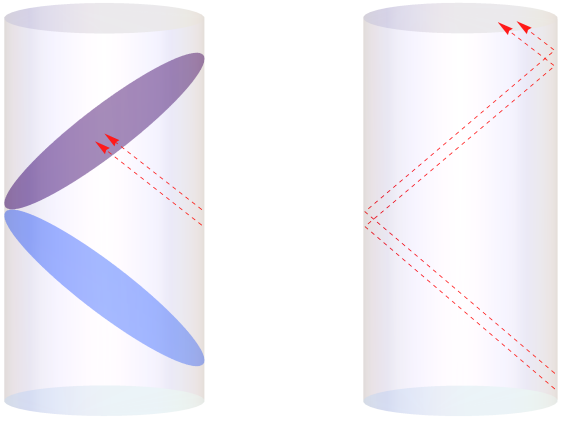

(a) (b)

Figure 4.1: (a) Pictorial representation of the Poincaré patch of AdS. Any signal sent from the boundary eventually escapes from the Poincaré patch and never comes back. When the signal is absorbed by the Poincaré horizon the system thermalizes. (b) Conformal diagram of global AdS. In this case, signals that are sent from the boundary can reach the opposite side and bounce back into the bulk. If the energy of the signals is small enough, this process can be repeated periodically over time and thermalization might be avoided.

4.3 The AdS story: setup of the problem

We will study the dynamics of a massive scalar coupled to gravity in an asymptotically AdS space. For concreteness we will focus on AdS_4 (so the dual CFT is $(2+1)$-dimensional), but we expect our results apply more generally, at least at the qualitative level.

The starting point is the following action:

$$S = \frac{1}{16\pi G_N}\int_{\mathcal{M}_4} d^4x\sqrt{-g}\left(R - 6 - 2(\partial\phi)^2 - 2m^2\phi^2\right)\,, \tag{4.11}$$

where ϕ is a real scalar and

$$\mathcal{M}_4 = \partial\mathcal{M}_3 \times \mathcal{I}\,, \quad \partial\mathcal{M}_3 = R\times S^2\,, \quad \mathcal{I} = \left\{x\in\left[0,\tfrac{\pi}{2}\right]\right\}\,. \tag{4.12}$$

Notice that in the action (4.11) we have directly set the AdS radius L to unity.

It is important to respect the topology of the bulk since we want to focus on situations where the boundary theory lives on a two-sphere. In order to do so, we propose the following ansatz for the metric,

$$ds^2 = \frac{1}{\cos^2 x}\left(-Ae^{-2\delta}dt^2 + A^{-1}dx^2 + \sin^2 x\, d\Omega_2^2\right)\,, \tag{4.13}$$

where x is related to the usual radial coordinate r through $r \equiv \tan x$. Therefore, in order to respect global AdS boundary conditions we must require that $A \to 1$ and $\delta \to 0$ as $x \to \pi/2$. We will also assume spherical symmetry. This implies that the metric functions A and δ, and the scalar field ϕ, depend only on the radial coordinate $x \in [0, \frac{\pi}{2}]$ and time $x \in (\infty, \infty)$.

The equation of motion for ϕ is given by

$$\ddot{\phi} = \left(\frac{\dot{A}}{A} - \dot{\delta}\right)\dot{\phi} + A^2 e^{-2\delta}\left(\frac{2}{\sin x \cos x} + \frac{A'}{A} - \delta'\right)\phi' + A^2 e^{-2\delta}\phi'' - m^2\frac{Ae^{-2\delta}}{\cos^2 x}\phi\,, \tag{4.14}$$

while the Einstein equations reduce to the constraints

$$A' = \frac{1+2\sin^2 x}{\sin x\cos x}(1-A) - \sin x\cos x A\left(\Phi^2 + \Pi^2\right) - m^2\tan x\,\phi^2, \tag{4.15}$$

$$\delta' = -\sin x\cos x\left(\Phi^2 + \Pi^2\right). \tag{4.16}$$

Here we have defined $\Pi \equiv e^{\delta}\dot{\phi}/A$ and $\Phi \equiv \phi'$.

At this point it is worth recalling that in $(3+1)$-dimensions the mass of the scalar field is related to the conformal dimension of the dual operator through

$$m^2 = \Delta(\Delta - 3) \qquad \text{or} \qquad \Delta = \frac{3}{2} \pm \sqrt{\frac{9}{4} + m^2}\,. \tag{4.17}$$

In particular, the minus sign in (4.17) is allowed for $m^2 < 0$ as long as the mass is above the Breitenlohner-Freedman bound [145]

$$m^2 \geq m^2_{\rm BF} = -\frac{9}{4}\,. \tag{4.18}$$

In these cases there is an ambiguity in the identification of the source of the dual operator and an "alternative quantization" is allowed. For concreteness, we will focus in the following four cases:

- Marginal operator with $(m^2, \Delta) = (0, 3)$.
- Relevant operator with $(m^2, \Delta) = (-2, 1)$, "alternative quantization".
- Relevant operator with $(m^2, \Delta) = (-2, 2)$, "standard quantization".
- Irrelevant operator with $(m^2, \Delta) = (4, 4)$.

We expect all other cases to be qualitatively equivalent to one of the above, depending on the conformal dimension of the dual operator.

4.3.1 Two time formalism

Following the work of [138], we now define the slow time $\tau = \epsilon^2 t$, where $\epsilon \ll 1$ is a dimensionless parameter, and expand the fields as follows:

$$\phi = \epsilon\phi_{(1)}(t, \tau, x) + \epsilon^3\phi_{(3)}(t, \tau, x) + \mathcal{O}(\epsilon^5)\,, \tag{4.19}$$

$$A = 1 + \epsilon^2 A_{(2)}(t, \tau, x) + \mathcal{O}(\epsilon^4)\,, \tag{4.20}$$

$$\delta = \epsilon^2\delta_{(2)}(t, \tau, x) + \mathcal{O}(\epsilon^4)\,. \tag{4.21}$$

We keep both, the rapid time t and the slow time τ, and treat them as independent variables. The reason is that by doing so we can extend the regime of validity of the naive perturbation theory, which usually breaks down at $t \propto 1/\epsilon^2$, to timescales of order $t \propto \tau/\epsilon^2 \propto 1/\epsilon^4$.

To obtain the perturbative equations we substitute the expansions (4.19)–(4.21) into (4.14)–(4.16) and replace $\partial_t \to \partial_t + \epsilon^2 \partial_\tau$. Then, we expand the equations at different orders in ϵ.

At order $\mathcal{O}(\epsilon)$, we obtain the wave equation for a massive scalar in pure AdS, namely

$$\ddot{\phi}_{(1)} = \phi''_{(1)} + \frac{2}{\sin x \cos x}\phi'_{(1)} - \frac{m^2}{\cos^2 x}\phi_{(1)} \equiv -L_m \phi_{(1)} \,, \tag{4.22}$$

where $\dot{} \equiv \partial_t$. In order to solve this equation we perform a Fourier decomposition and obtain the eigenvalues and eigenvectors ("oscillons") of the operator L_m. The general solution can be cast in terms of hypergeometric functions, and is given elsewhere — see *e.g.* [146]. Here we will focus on the particular cases mentioned in the previous section. Explicitly, we expand $\phi_{(1)}$ as

$$\phi_{(1)}(t,\tau,x) = \sum_{j=0}^{\infty} \left(A_j(\tau) e^{-i\omega_j t} + \bar{A}_j(\tau) e^{i\omega_j t} \right) e_j(x) \,, \tag{4.23}$$

where the ω_j and the functions $e_j(x)$ are given in Table 4.1. The constants d_j are normally chosen such that the oscillons form an orthonormal basis, *i.e.*

$$(e_i, e_j) = \int_0^{\pi/2} e_i(x) e_j(x) \tan^2 x \, dx = \delta_{ij} \,, \tag{4.24}$$

but they can be reabsorbed in the $A_j(\tau)$, if desired.

(m^2, Δ)	ω_j^2	$e_j(x)$
$(0,3)$	$(2j+3)^2$	$d_j \cos^3 x \ {}_2F_1\left(-j, 3+j; \frac{3}{2}; \sin^2 x\right)$
$(-2,1)$	$(2j+1)^2$	$d_j \frac{\sin((2j+1)x)}{\tan x}$
$(-2,2)$	$(2j+2)^2$	$d_j \frac{\sin((2j+2)x)}{\tan x}$
$(4,4)$	$(2j+4)^2$	$d_j \cos^4 x \ {}_2F_1\left(-j, 4+j; \frac{3}{2}; \sin^2 x\right)$

Table 4.1: Eigenvalues and eigenvectors of the massive wave equation (4.22).

At order $\mathcal{O}(\epsilon^2)$ the constraints (4.15)-(4.16) can be integrated to obtain

$$A_{(2)}(x) = -\frac{\cos^3 x}{\sin x} \int_0^x dy \left(\phi'^2_{(1)}(y) + \dot{\phi}^2_{(1)}(y) + \frac{m^2}{\cos^2 y} \phi^2_{(1)}(y) \right) \tan^2 y \,, \quad (4.25)$$

$$\delta_{(2)}(x) = -\int_0^x dy \left(\phi'^2_{(1)}(y) + \dot{\phi}^2_{(1)}(y)^2 \right) \sin y \cos y \,. \quad (4.26)$$

Finally, at order $\mathcal{O}(\epsilon^3)$, we obtain the following equation for $\phi_{(3)}$:

$$\ddot{\phi}_{(3)} + L_m \phi_{(3)} + 2\partial_\tau \dot{\phi}_{(1)} = S_m(t, \tau, x) \,, \quad (4.27)$$

where the source term is given by

$$S_m = (\dot{A}_{(2)} - \dot{\delta}_{(2)})\dot{\phi}_{(1)} - 2(A_{(2)} - \delta_{(2)}) L_m \phi_{(1)} + (A'_{(2)} - \delta'_{(2)})\phi'_{(1)} + \frac{m^2}{\cos^2 x} A_{(2)} \phi_{(1)} \,. \quad (4.28)$$

The source S_m contains resonant terms that might lead to secular growths in $\phi_{(3)}$. We can deal with these resonances as follows [138]. First, we project onto an individual oscillon mode:

$$\left(e_j, \ddot{\phi}_{(3)} + L_m \phi_{(3)} \right) - 2i\omega_j \left(\partial_\tau A_j e^{-i\omega_j t} - \partial_\tau \bar{A}_j e^{i\omega_j t} \right) = (e_j, S_m) \,. \quad (4.29)$$

For all triads (j_1, j_2, j_3) resonances in the right-hand side occur at $\omega_j = \omega_{j_1} + \omega_{j_2} - \omega_{j_3}$. These resonances may be avoided by taking advantage of the second term in the left-hand side of (4.29). Denoting by $f[\omega_j]$ the part of f proportional to $e^{i\omega_j t}$, we set

$$-2i\omega_j \partial_\tau A_j = (e_j, S_m)[-\omega_j] \equiv \sum_{kln} \mathcal{S}^{(j)}_{kln} \bar{A}_k A_l A_n \,, \tag{4.30}$$

where $\mathcal{S}^{(j)}_{kln}$ are real constants representing different resonance contributions. The right hand side of (4.30) is a cubic polynomial in A_j and $\bar{A}_j$. Thus, we have obtained a set of coupled first order differential equations in τ for A_j, which we shall refer to as the TTF equations.

4.3.2 Solutions to the TTF equations

4.3.2.1 Single-mode solutions

In practice, it is necessary to truncate the TTF equations at some finite $j = j_{\max}$. Here we will illustrate the method by obtaining the explicit solutions for a single-mode truncation, $j_{\max} = 0$.

Consider first the massless case $(m^2, \Delta) = (0, 3)$. For $j_{\max} = 0$ we have:

$$\phi_{(1)} = 4\sqrt{\frac{2}{\pi}} \left(A_0 e^{-3it} + \bar{A}_0 e^{3it}\right) \cos^3(x) \,. \tag{4.31}$$

We can easily perform the integrals in (4.25)-(4.26) to obtain

$$A_{(2)} = \frac{6\cos^3 x}{\pi \sin x} \left[2\left(A_0^2 e^{-6it} + \bar{A}_0^2 e^{6it}\right) \sin^3(2x) + 3|A_0|^2 \left(\sin(4x) - 4x\right) \right], \tag{4.32}$$

and

$$\delta_{(2)} = \frac{3\sin^2 x}{4\pi}\Big[\left(A_0^2 e^{-6it} + \bar{A}_0^2 e^{6it}\right)\left(90 + 77\cos(2x) + 22\cos(4x) + 3\cos(6x)\right) \\ -16|A_0|^2\left(15 + 8\cos(2x) + \cos(4x)\right)\Big], \qquad (4.33)$$

respectively. Finally, from (4.30) we obtain the differential equation

$$i\pi\partial_\tau A_0 - 153 A_0|A_0|^2 = 0\,, \qquad (4.34)$$

which has solution

$$A_0(\tau) = A_0(0)e^{-\frac{153}{\pi}i|A_0(0)|^2\tau}\,. \qquad (4.35)$$

We can repeat the exercise for the other three cases following the steps outlined above. The general observation is that, by solving (4.30), the resonances are absorbed into frequency shifts. In Table 4.2 we summarize our findings for all cases in consideration.

(m^2, Δ)	$\phi_{(1)}(t,x)$	$\tilde{\omega}_0$
$(0,3)$	$8\sqrt{\frac{2}{\pi}}\cos(\tilde{\omega}_0 t)\cos^3 x$	$3 + \frac{153\epsilon^2}{\pi}$
$(-2,1)$	$\frac{4}{\sqrt{\pi}}\cos(\tilde{\omega}_0 t)\cos x$	$1 + \frac{10\epsilon^2}{\pi}$
$(-2,2)$	$\frac{8}{\sqrt{\pi}}\cos(\tilde{\omega}_0 t)\cos^2 x$	$2 + \frac{48\epsilon^2}{\pi}$
$(4,4)$	$\frac{32}{\sqrt{5\pi}}\cos(\tilde{\omega}_0 t)\cos^4 x$	$4 + \frac{9216\epsilon^2}{25\pi}$

Table 4.2: Single-mode solutions for $\phi_{(1)}$, normalized such that $A_0(0) = 1$.

Finally, we can also consider single-mode solutions where the relevant mode is not necessarily the $j = 0$. In all these cases the conclusion we obtain is

the same: the resonances in the the scalar field that would potentially lead to secular growths at order $\mathcal{O}(\epsilon^3)$ are reabsorbed into frequency shifts.

4.3.2.2 Two-mode solutions

Going beyond single-mode solutions has some interesting physical implications [138]: (quasi-)periodic solutions, non-linear mixing for metric back-reaction and energy cascades among modes. Some of these effects are already visible by studying two-mode solutions which, at the same time, are the simplest generalization. Therefore, we will devote the present section to study these solutions. In the next section, we will attempt to draw more general lessons for multiple-mode solutions with arbitrary $j_{\max} > 1$.

Let us start with the massless case $(m^2, \Delta) = (0, 3)$. For $j_{\max} = 1$ the TTF equations lead to the following system of partial differential equations:

$$\begin{aligned} i\pi\partial_\tau A_0 - 153 A_0|A_0|^2 - 585 A_0|A_1|^2 = 0\,, \\ i\pi\partial_\tau A_1 - 159 A_1|A_0|^2 - 1175 A_1|A_1|^2 = 0\,. \end{aligned} \tag{4.36}$$

We take the following ansatz:

$$A_j = \alpha_j \exp(-i\beta_j \tau)\,, \tag{4.37}$$

where $\alpha_j, \beta_j \in \mathbb{R}$ are independent of τ. Plugging (4.37) into (4.36) the system reduces to a set of linear equations in β_j and quadratic in α_j:

$$\begin{aligned} \pi\beta_0 - 153\alpha_0^2 - 585\alpha_1^2 = 0\,, \\ \pi\beta_1 - 159\alpha_0^2 - 1175\alpha_1^2 = 0\,. \end{aligned} \tag{4.38}$$

The shifts in frequency, β_j, can be easily solved in terms of the amplitudes α_j:

$$\begin{aligned}\beta_0 &= \frac{153\alpha_0^2 + 585\alpha_1^2}{\pi}\,,\\ \beta_1 &= \frac{159\alpha_0^2 + 1175\alpha_1^2}{\pi}\,.\end{aligned} \tag{4.39}$$

We will define the quantity β_{01} as the ratio between the frequency shifts,

$$\beta_{01} = \frac{\beta_0}{\beta_1} = \frac{153\alpha_0^2 + 585\alpha_1^2}{159\alpha_0^2 + 1175\alpha_1^2}\,. \tag{4.40}$$

If $\beta_{01} \in \mathbb{Q}$, *i.e.* if the ratio between the two shifts is a rational number, then the full solution will be periodic in τ. If β_{01} is irrational, then the solution will be quasi-periodic. We will also normalize the solutions by imposing that[4]

$$\sum_i \alpha_i^2 = \alpha_0^2 + \alpha_1^2 = 1\,. \tag{4.41}$$

Solving (4.40)-(4.41) we obtain:

$$\alpha_0 = \pm\sqrt{\frac{5(235\beta_{01} - 117)}{8(127\beta_{01} - 54)}}\,, \qquad \alpha_1 = \pm\sqrt{\frac{3(51 - 53\beta_{01})}{8(127\beta_{01} - 54)}}\,. \tag{4.42}$$

In Figure 4.2 we show the behavior of α_0 and α_1 as a function of β_{01}. Finally, we can repeat the same exercise for the massive cases. The solutions for such cases are summarized in Table 4.3.

The general solution for a two-mode truncation (4.23) can be easily reconstructed from the oscillon functions (see Table 4.1) and the coefficients (4.37), taking into account the solutions (4.39) and (4.42). Here, it is worth

[4]Given the scaling symmetry $A_j(\tau) \to \epsilon A_j(\tau/\epsilon^2)$, changing this normalization is equivalent to a rescaling of ϵ.

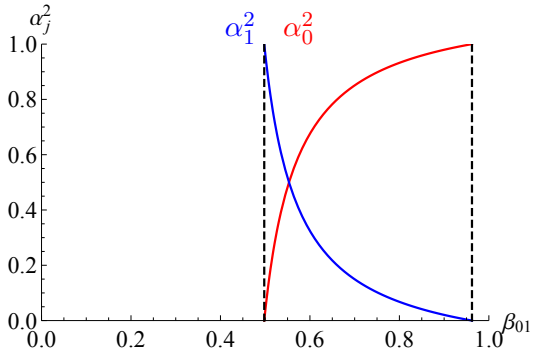

Figure 4.2: Solutions for α_0 and α_1 as a function of β_{01}, for the case $(m^2, \Delta) = (0, 3)$. Here we have chosen values of β_{01} in the range $\frac{117}{235} < \beta_{01} < \frac{51}{53}$ so that $\alpha_i^2 > 0 \; \forall \, i$. In the extremal values either $\alpha_0 = 0$ or $\alpha_1 = 0$, which means that we go back to a single-mode solution.

emphasizing that, although the solution for the scalar field is a linear superposition of oscillons (for any $j_{\max} > 0$), it is clear from (4.25) and (4.26) that the first order backreaction in the metric will generally contain mixed terms between any pair of modes. The metric solution is then a nonlinear superposition of eigenmodes. This will play a crucial role in the computation of entanglement entropy, later in Section 4.4

4.3.2.3 Periodic and quasi-periodic solutions for $j_{\max} > 1$

In general, both the amplitude and phase of the coefficients A_j can depend of τ in a nontrivial way. However, since we are interested in finding periodic solutions to the equations of motion we will focus on the ansatz (4.37) for which the energy of each mode is constant, $E_j = \omega_j^2 |A_j|^2$.

For more than two modes, however, the resulting TTF equations are more subtle given that for general α_j, β_j there are τ-dependent terms which

(m^2, Δ)	β_j	α_j^2
$(0,3)$	$\beta_0 = \dfrac{153\alpha_0^2 + 585\alpha_1^2}{\pi}$ $\beta_1 = \dfrac{159\alpha_0^2 + 1175\alpha_1^2}{\pi}$	$\alpha_0^2 = \dfrac{5(235\beta_{01} - 117)}{8(127\beta_{01} - 54)}$ $\alpha_1^2 = \dfrac{3(51 - 53\beta_{01})}{8(127\beta_{01} - 54)}$
$(-2,1)$	$\beta_0 = \dfrac{10\alpha_0^2 + 90\alpha_1^2}{\pi}$ $\beta_1 = \dfrac{26\alpha_0^2 + 582\alpha_1^2}{3\pi}$	$\alpha_0^2 = \dfrac{3(97\beta_{01} - 45)}{2(139\beta_{01} - 60)}$ $\alpha_1^2 = \dfrac{15 - 13\beta_{01}}{2(139\beta_{01} - 60)}$
$(-2,2)$	$\beta_0 = \dfrac{48\alpha_0^2 + 272\alpha_1^2}{\pi}$ $\beta_1 = \dfrac{152\alpha_0^2 + 1656\alpha_1^2}{3\pi}$	$\alpha_0^2 = \dfrac{3(69\beta_{01} - 34)}{4(47\beta_{01} - 21)}$ $\alpha_1^2 = \dfrac{18 - 19\beta_{01}}{4(47\beta_{01} - 21)}$
$(4,4)$	$\beta_0 = \dfrac{64512\alpha_0^2 + 187216\alpha_1^2}{175\pi}$ $\beta_1 = \dfrac{467488\alpha_0^2 + 2627636\alpha_1^2}{1225\pi}$	$\alpha_0^2 = \dfrac{656909\beta_{01} - 327628}{540037\beta_{01} - 214732}$ $\alpha_1^2 = \dfrac{56(2016 - 2087\beta_{01})}{540037\beta_{01} - 214732}$

Table 4.3: Coefficients α_j, β_j for two-mode solutions normalized according to (4.41).

imply that the system might not be self-consistent. To cancel these terms we impose the constraint

$$\beta_j = \beta_0 + j(\beta_1 - \beta_0)\,, \qquad \forall\ j > 1\,, \tag{4.43}$$

which leave us with $j_{\max} + 1$ algebraic equations:

$$-2\omega_j\alpha_j[\beta_0 + j(\beta_1 - \beta_0)] = \sum_{kln} \mathbb{S}^{(j)}_{kln}\alpha_k\alpha_l\alpha_n\,, \tag{4.44}$$

and $j_{\max} + 3$ unknowns $(\beta_0, \beta_1, \{\alpha_j\})$. We will normalize the solutions as in (4.41) and parametrize the solutions with respect to the ratio $\beta_{01} = \beta_0/\beta_1$. A few comments are in order. First notice that, because of (4.43), other ratios

are constrained to be

$$\beta_{0j} = \frac{\beta_0}{\beta_j} = \frac{\beta_{01}}{\beta_{01} + j(1-\beta_{01})}\,, \qquad \forall\ j > 1\,. \tag{4.45}$$

This implies that, if β_{01} is a rational number, then $\beta_{0j} \in \mathbb{Q}\ \forall\ \ j > 1$! In other words, the solution is periodic if and only if $\beta_{01} \in \mathbb{Q}$, otherwise it is quasi-periodic. Finally, it is worth pointing out that for general $j_{\max} > 1$ there might be multiple solutions for the coefficients α_j, leading to many physical branches.

Point aside, then, the conclusion here that it is indeed possible to construct oscillatory solutions with arbitrary number of modes! Moreover, since we can take ϵ arbitrarily close to zero, it is natural to identify the corresponding geometries as the holographic dual of states in the CFT that display periodic oscillations over the CFT vacuum.

4.4 Evolution of entanglement entropy

We will now proceed to compute the entanglement entropy and use it as a tool to characterize the evolution of the system. We will consider circular caps in the boundary theory,

$$A = \{(t_b, \theta, \varphi),\ \ |\theta| \leq \theta_b\}\ , \tag{4.46}$$

where θ and φ denote the polar and azimuthal angles on the sphere, respectively, and t_b stands for the boundary time. As explained in Section 1.2.4, in order to compute the entanglement entropy of such a region, we have to

find the bulk surface γ_A with minimal area and boundary condition given by (4.46). Exploiting the axial symmetry of the problem, γ_A can be chosen as a surface of revolution which only depends on the polar angle of the S^2,

$$X^\mu = \{t(\theta), x(\theta), \theta, \varphi\} \ , \tag{4.47}$$

satisfying

$$t(\theta_b) = t_b \, , \qquad x(\theta_b) = \frac{\pi}{2} \, , \qquad t'(0) = x'(0) = 0 \, . \tag{4.48}$$

For a bulk metric of the form (4.13), the area of γ_A is given by

$$\mathcal{A}(t_b, \theta_b) \equiv \text{Area}\,(\gamma_A) = 2\pi \int_0^{\theta_b} d\theta \, \sin\theta \sqrt{\frac{\tan^2 x}{A \cos^2 x} \, (x'^2 - A^2 e^{-2\delta} t'^2) + \tan^4 x} \, . \tag{4.49}$$

Our goal is to solve the equations of motion that follow from (4.49) subject to the boundary conditions (4.48) and then evaluate the area "on-shell". In general, the equations of motion for $t(\theta)$ and $x(\theta)$ are highly non-lineal and the problem has to be solved numerically. However, in the TTF formalism, the ϵ-expansion implies that the background remains very close to AdS_4 and therefore a perturbative approach is reliable. In the following I will briefly explain the general idea.

4.4.1 Perturbative calculation

Let us write the bulk metric in the following form:

$$g_{\mu\nu} = g^{(0)}_{\mu\nu} + g^{(2)}_{\mu\nu} + \mathcal{O}(\epsilon^4), \tag{4.50}$$

where $g^{(0)}_{\mu\nu}$ represents the metric of pure AdS_4 and $g^{(2)}_{\mu\nu}$ is the leading perturbation due to the backreaction, which is of order $\mathcal{O}(\epsilon^2)$. Using the above

expansion, we compute the minimal area perturbatively (see *e.g.* [81]):

$$\mathcal{A}(t_b,\theta_b) = 2\pi \int_0^{\theta_b} d\theta \sqrt{\det \gamma^{(0)}_{ab}} \left(1 + \frac{1}{2}\mathrm{Tr}\left[\gamma^{(2)}(\gamma^{(0)})^{-1}\right] + \mathcal{O}(\epsilon^4)\right) , \quad (4.51)$$

where

$$\gamma^{(0)}_{ab} = \partial_a X^\mu \partial_b X^\nu g^{(0)}_{\mu\nu} , \qquad \gamma^{(2)}_{ab} = \partial_a X^\mu \partial_b X^\nu g^{(2)}_{\mu\nu} , \qquad (a,b) = (\theta,\varphi) . \quad (4.52)$$

In particular, the embedding functions X^μ at this order are given by the solutions pure AdS_4. Notice the useful fact that we do not need to know the corrections to γ_A due to the perturbed metric to calculate (4.51)!

The leading order term in (4.51) is independent of t_b, so we will focus on the difference:

$$\Delta\mathcal{A}(t_b,\theta_b) \equiv \mathcal{A}^{(2)}(t_b,\theta_b) - \mathcal{A}^{(0)}(\theta_b) = \pi \int_0^{\theta_b} d\theta \sqrt{\det \gamma^{(0)}_{ab}}\, \mathrm{Tr}\left[\gamma^{(2)}(\gamma^{(0)})^{-1}\right] . \quad (4.53)$$

Notice that this subtraction automatically get rids of the UV divergences, so we do not need to regularize (4.53). A brief calculation yields

$$\Delta\mathcal{A}(t_b,\theta_b) = -\pi\epsilon^2 \int_0^{\theta_b} d\theta \, \frac{\sin\theta \tan x \left(A_{(2)} x'^2 + \left(A_{(2)} - 2\delta_{(2)}\right) t'^2\right)}{\cos(x)\sqrt{x'^2 - t'^2 + \sin^2 x}} . \quad (4.54)$$

Finally, we employ the embedding solutions for global AdS_4 (see *e.g.* [147]):

$$t(\theta) = t_b , \qquad x(\theta) = \arctan\left[\frac{\sqrt{2}\cos\theta_b}{\sqrt{\cos(2\theta) - \cos(2\theta_b)}}\right] . \quad (4.55)$$

Substituting back in (4.54) we obtain

$$\Delta\mathcal{A}(t_b,\theta_b) = -\frac{2\sqrt{2}\pi\epsilon^2 \cos^2\theta_b}{\sin\theta_b} \int_0^{\theta_b} d\theta \, \frac{A_{(2)} \sin^3\theta}{\left(\cos(2\theta) - \cos(2\theta_b)\right)^{3/2}} , \quad (4.56)$$

where it is understood that $A_{(2)}$ must be evaluated at t_b and $x(\theta)$.

4.4.2 Results for single-mode solutions

We can get relatively simple expressions for the single-mode solutions presented in section (4.3.2.2). Let us first consider the $(m^2, \Delta) = (0, 3)$ case. We only need $A_2(x,t)$, which is given by

$$A_{(2)}(t,x) = \frac{6\cos^3 x}{\pi \sin x}\left[4\cos(2\tilde{\omega}_0 t)\sin^3(2x) + 3\left(\sin(4x) - 4x\right)\right], \tag{4.57}$$

where

$$\tilde{\omega}_0 \equiv 3 + \frac{153\epsilon^2}{\pi}\,. \tag{4.58}$$

We can distinguish two terms in the entanglement entropy, one being time-dependent and the other one time-independent:

$$\Delta\mathcal{A}(t_b, \theta_b) = \Delta\mathcal{A}^{(\mathrm{A})}(t_b, \theta_b) + \Delta\mathcal{A}^{(\mathrm{B})}(\theta_b)\,. \tag{4.59}$$

Evaluating (4.57) at (4.55) and plugging it back into (4.56) we explicitly obtain

$$\Delta\mathcal{A}^{(\mathrm{A})}(t_b, \theta_b) = -\frac{384\epsilon^2}{35}\sin^6\theta_b \cos(2\tilde{\omega}_0 t_b)\,, \tag{4.60}$$

and

$$\Delta\mathcal{A}^{(\mathrm{B})}(\theta_b) = \frac{6\epsilon^2}{5\sin\theta_b}\Big(45\pi - 80\sin\theta_b - 15\sin(3\theta_b) + \sin(5\theta_b) \\ - 120\arctan(\cot\theta_b)\cos\theta_b + 15\pi\cos(2\theta_b)\Big)\,, \tag{4.61}$$

respectively. A few remarks are in order. First notice that in spite of the $\sin\theta_b$ term in the denominator of (4.61), the limit $\theta_b \to 0$ gives $\Delta\mathcal{A}(t_b, \theta_b \to 0) = 0$, as expected. Second, both $\Delta\mathcal{A}^{(\mathrm{A})}(t_b, \theta_b)$ and $\Delta\mathcal{A}^{(\mathrm{B})}(\theta_b)$ increase monotonically in θ_b, in the range $\theta_b \in (0, \pi/2)$. Outside of this range and given the symmetry

of the problem, we have that $\Delta\mathcal{A}(t_b, \frac{\pi}{2} + \vartheta) = \Delta\mathcal{A}(t_b, \frac{\pi}{2} - \vartheta)$ for $\vartheta \in (0, \pi/2)$. In particular, this implies that $S_A = S_{A^c}$. Therefore, at least at order $\mathcal{O}(\epsilon^2)$, we can safely say that these states are indistinguishable from pure states, supporting the interpretation as a state built on an energy eigenstate, rather than a mixed density matrix. Third, the frequency of the entanglement oscillations is twice the frequency of the scalar field mode.

We can repeat the same exercise for the massive cases. In general, the final form for the entanglement entropies have a similar structure as in (4.59) but with longer expressions that we will not transcribe here. In Figure 4.3 we plot the behavior of the oscillations in all four cases. We observe some crucial differences. For the case $(m^2, \Delta) = (4, 4)$ (irrelevant operator), the evolution of the entropy is qualitatively similar to the marginal case $(m^2, \Delta) = (0, 3)$. On the other hand, the case of relevant operators have some curious features. First, we observe that the at some point in the evolution, the entanglement entropy becomes negative. This applies for any θ_b in the case $(m^2, \Delta) = (-2, 1)$ (alternative quantization) of for sufficiently large θ_b in the case $(m^2, \Delta) = (-2, 2)$ (alternative quantization). This means that, at some point in the evolution, these states are less entangled than the pure AdS case (vacuum state). This is possible, because we are perturbing the theory with a relevant operator, which in principle can affect the IR degrees of freedom. Another curious feature is that, for the alternative quantization case, $\Delta\mathcal{A}^{(\mathrm{B})}(\theta_b)$ actually decreases in the range $\theta_b \in (0, \pi/2)$. However, the sum $\mathcal{A}^{(0)}(\theta_b) + \Delta\mathcal{A}^{(\mathrm{B})}(\theta_b)$ is monotonically increasing for "sufficiently small" ϵ. This guarantees that

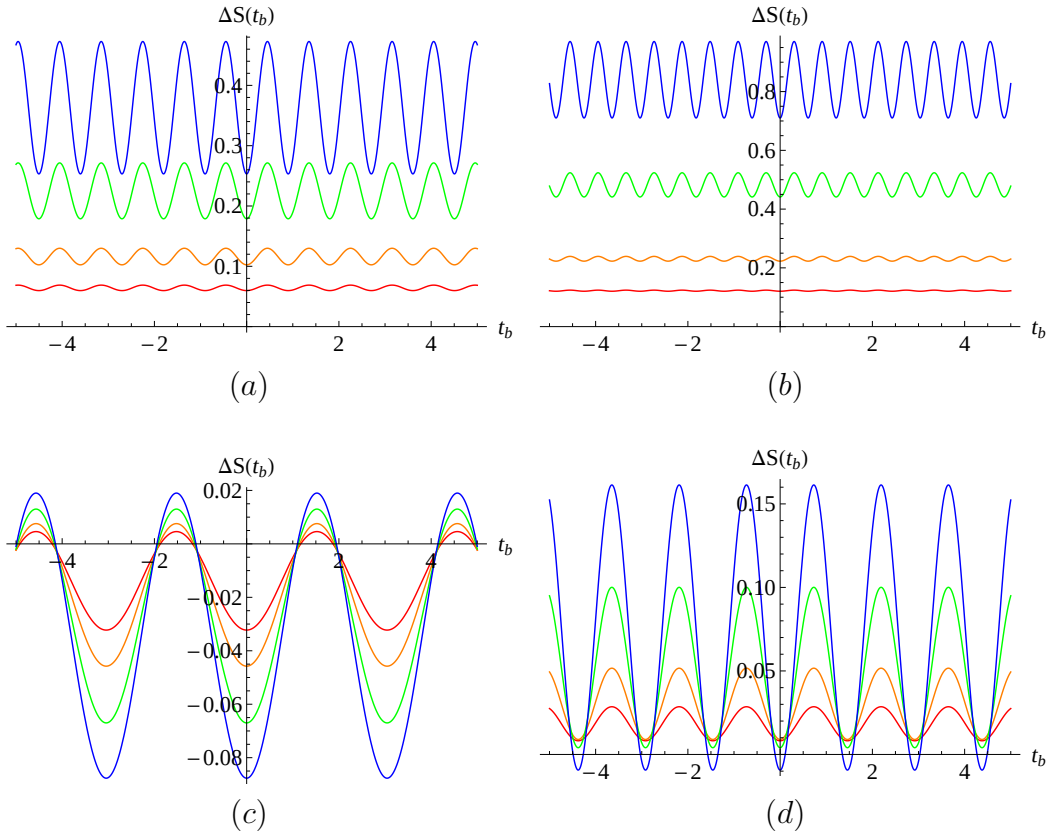

Figure 4.3: Entanglement oscillations for single-mode solutions of (a) $(m^2, \Delta) = (0, 3)$ marginal operator, (b) $(m^2, \Delta) = (4, 4)$ irrelevant operator, (c) $(m^2, \Delta) = (-2, 1)$ relevant operator (alternative quantization) and (d) $(m^2, \Delta) = (-2, 2)$ relevant operator (standard quantization). The different colors stand for $\theta_b = \pi/5$ (red), $\theta_b = \pi/4$ (orange), $\theta_b = \pi/3$ (green) and $\theta_b = \pi/2$ (blue). We also have set $\epsilon = 1/10$ and $4G_N = 1$.

the strong subadditivity inequality is satisfied [11, 148] but, at the same time, imposes a non-trivial constraint on the perturbative solution! Finally, the behavior for other single mode solutions, with $j \neq 0$, is qualitatively similar to those presented in Figure 4.3 and hence we will not present them here.

4.4.3 Results for two-mode solutions

The computation for multiple-mode solutions can be easily done by following the same steps as for the single-mode solutions. Therefore, we are only going to present the final results. Consider the massless case, $(m^2, \Delta) = (0, 3)$. For two modes, we can express the entanglement entropy as the sum of three contributions:

$$\Delta\mathcal{A}(t_b, \theta_b) = \alpha_0^2 \Delta\mathcal{A}_{00}(t_b, \theta_b) + \alpha_1^2 \Delta\mathcal{A}_{11}(t_b, \theta_b) + \alpha_0\alpha_1 \Delta\mathcal{A}_{01}(t_b, \theta_b)\,. \tag{4.62}$$

Evidently, if we set $\alpha_1 = 0$, $\alpha_0 = 1$, we should recover the single-mode solution presented in the previous section. Hence, we can identify

$$\Delta\mathcal{A}_{00}(t_b, \theta_b) = \Delta\mathcal{A}_{00}^{(\mathrm{A})}(t_b, \theta_b) + \Delta\mathcal{A}_{00}^{(\mathrm{B})}(\theta_b)\,, \tag{4.63}$$

where $\Delta\mathcal{A}_{00}^{(\mathrm{A})}$ and $\Delta\mathcal{A}_{00}^{(\mathrm{B})}$ are given in (4.60) and (4.61), respectively. Similarly, the $\Delta\mathcal{A}_{11}(t_b, \theta_b)$ term can be obtained by turning off the zero mode. In this case, we obtain

$$\Delta\mathcal{A}_{11}(t_b, \theta_b) = \Delta\mathcal{A}_{11}^{(\mathrm{A})}(t_b, \theta_b) + \Delta\mathcal{A}_{11}^{(\mathrm{B})}(\theta_b)\,, \tag{4.64}$$

where

$$\Delta\mathcal{A}_{11}^{(\mathrm{A})}(t_b, \theta_b) = -\frac{640\epsilon^2}{2079}\sin^6\theta_b \Big(113 + 128\cos(2\theta_b) + 56\cos(4\theta_b)\Big)\cos(2\tilde{\omega}_1 t_b)\,, \tag{4.65}$$

and

$$\begin{aligned}\Delta\mathcal{A}_{11}^{(\mathrm{B})}(\theta_b) = \frac{10\epsilon^2}{189\sin\theta_b}\Big(&2835\pi - 5040\sin\theta_b - 987\sin(3\theta_b) \\ &+ 117\sin(5\theta_b) - 27\sin(7\theta_b) + 5\sin(9\theta_b) \\ &- 7560\arctan(\cot\theta_b)\cos\theta_b + 945\pi\cos(2\theta_b)\Big).\end{aligned} \tag{4.66}$$

In (4.65) we have defined $\tilde{\omega}_1 = 5 + \beta_1\epsilon^2$. Finally, the cross term that mixes the two modes is given by

$$\Delta\mathcal{A}_{01}(t_b,\theta_b) = \frac{256\epsilon^2}{21\sqrt{3}}\sin^6\theta_b\Big(9\cos\left((\tilde{\omega}_1-\tilde{\omega}_0)t_b\right) + (4+5\cos(2\theta_b))\cos\left((\tilde{\omega}_1+\tilde{\omega}_0)t_b\right)\Big). \quad (4.67)$$

To study this solution we should plug in the values for α_j, β_j given in (4.39) and (4.42). The solution is then specified by one single parameter, the the ratio $\beta_0/\beta_1 = \beta_{01}$, which can be arbitrary. In Figure 4.4 we show the behavior of the entanglement entropy in two cases, one periodic (for $\beta_{01} = 3/5$) and the other one quasi-periodic (for $\beta_{01} = \pi/6$). Since the mixed term (4.67) does not contain a constant term, we oberve that the entanglement entropy in this case behaves similarly as for the single mode solutions, but in this case with some extra fourier modes: $\tilde{\omega}_0 + \tilde{\omega}_1$ and $\tilde{\omega}_0 - \tilde{\omega}_1$. The same is true for the massive cases, so the observations we made in the previous section for operators with different conformal dimensions seem to hold more generally (at the very least this is true for arbitrary two-mode solutions). Let us now see what happen for general $j_{\max} > 1$.

4.4.4 General expressions for entanglement entropy

Let us now focus on solutions for arbitrary number of modes and attempt to obtain general expressions. First, recall that

$$\Delta S(t_b,\tau_b,\theta_b) = -\frac{\sqrt{2}\pi\epsilon^2\cos^2\theta_b}{2G_N\sin\theta_b}\int_0^{\theta_b} d\theta\,\frac{A_{(2)}(t_b,\tau_b,x(\theta,\theta_b))\sin^3\theta}{(\cos(2\theta)-\cos(2\theta_b))^{3/2}}\,, \quad (4.68)$$

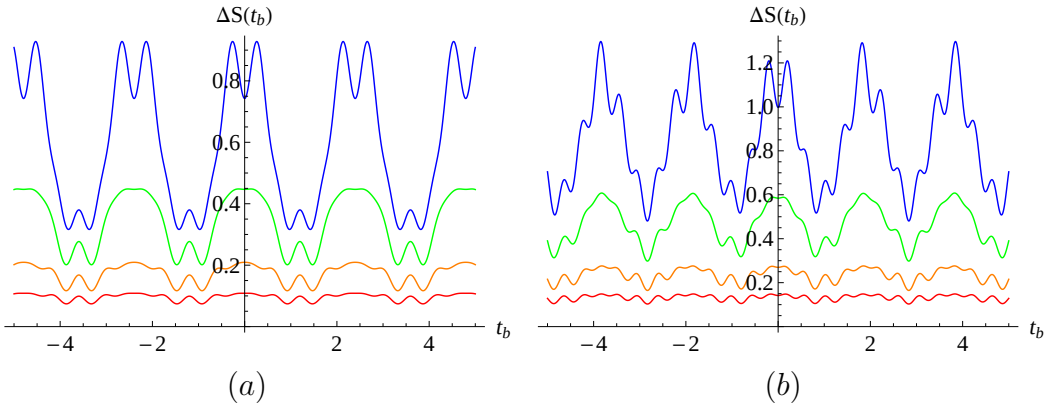

Figure 4.4: Entanglement oscillations for two-mode solutions of the $(m^2, \Delta) = (0, 3)$ case (marginal operator) for (a) $\beta_{01} = 3/5$ (periodic solution) and (b) $\beta_{01} = \pi/6$ (quasi-periodic solution). The different colors correspond to $\theta_b = \pi/5$ (red), $\theta_b = \pi/4$ (orange), $\theta_b = \pi/3$ (green) and $\theta_b = \pi/2$ (blue). We have also set $\epsilon = 1/10$ and $4G_N = 1$.

where $x(\theta, \theta_b)$ is given in (4.55). The metric function $A_{(2)}(t, \tau, x)$ can be determined from (4.25) upon substituting the coefficients $A_j(\tau) = r_j(\tau) \exp(-i\theta_j(\tau))$ obtained from the TTF equations. Notice that we are not assuming an ansatz of the form (4.37), so the solution might not even be (quasi-)periodic. From (4.25) it is clear that if $\phi_1(t, \tau, x)$ is a linear combination of oscillons, the integrand of $A_{(2)}(t, \tau, x)$ is in general a sum of bilinears in $e_j(x)$ (or its derivatives). Therefore, without loss of generality we can write:

$$A_{(2)}(t, \tau, x) = \sum_{jk} A^{jk}_{(2)}(t, \tau, x)\,, \tag{4.69}$$

where the term $A^{jk}_{(2)}(t, \tau, x)$ is proportional to the product $r_j(\tau) r_k(\tau)$. Hence, the entanglement entropy can also be expressed as a bilinear sum:

$$\Delta S(t_b, \tau_b, \theta_b) = \sum_{jk} \Delta S^{jk}(t_b, \tau_b, \theta_b)\,, \tag{4.70}$$

where

$$\Delta S^{jk}(t_b,\tau_b,\theta_b) = -\frac{\sqrt{2}\pi\epsilon^2\cos^2\theta_b}{2G_N\sin\theta_b}\int_0^{\theta_b} d\theta\,\frac{A^{jk}_{(2)}(t_b,\tau_b,x(\theta,\theta_b))\sin^3\theta}{(\cos(2\theta)-\cos(2\theta_b))^{3/2}}\,. \tag{4.71}$$

To determine the coefficients ΔS^{jk} more explicitly it is enough to consider a state of two arbitrary modes j and k:

$$\begin{aligned}\phi_{(1)}(t,\tau,x) = &\left(r_j(\tau)e^{-i(\omega_j t+\theta_j(\tau))} + r_j(\tau)e^{i(\omega_j t+\theta_j(\tau))}\right)e_j(x)\\ &+\left(r_k(\tau)e^{-i(\omega_k t+\theta_k(\tau))} + r_k(\tau)e^{i(\omega_k t+\theta_k(\tau))}\right)e_k(x)\,,\end{aligned} \tag{4.72}$$

A brief computation leads to

$$\begin{aligned}A^{jk}_{(2)}(t,\tau,x) = -4r_j(\tau)r_k(\tau)&\frac{\cos^3 x}{\sin x}\times\\ &\int_0^x dy\Big[\sin(\omega_j t+\theta_j(\tau))\sin(\omega_k t+\theta_k(\tau))\omega_j\omega_k e_j(y)e_k(y)\\ &\quad+\cos(\omega_j t+\theta_j(\tau))\cos(\omega_k t+\theta_k(\tau))\times\\ &\quad+\left(e_j'(y)e_k'(y)+\frac{m^2}{\cos^2 y}e_j(y)e_k(y)\right)\Big]\tan^2 y\,.\end{aligned} \tag{4.73}$$

Notice that by symmetry we have that $A^{jk}_{(2)}(t,\tau,x) = A^{kj}_{(2)}(t,\tau,x)$. There are also terms $A^{jj}_{(2)}$ and $A^{kk}_{(2)}$, but they are equivalent to (4.73) for $j=k$. Finally, the entanglement entropy contributions $\Delta S^{jk}(t_b,\tau_b,\theta_b)$ can be easily obtained by plugging (4.73) into (4.71) and performing the remaining integrals. It is worth pointing out that for quasi-periodic solutions, entanglement entropy is also quasi-periodic, even for arbitrary number of modes. This follows easily from (4.73) and (4.71): if we set $r_j(\tau)=\alpha_j$ and $\theta_j(\tau)=\beta_j\tau$, then, it can be seen that the entanglement entropy is a sum of harmonics with frequencies $|\tilde{\omega}_j+\tilde{\omega}_k|$ and $|\tilde{\omega}_j-\tilde{\omega}_k|$, where $\tilde{\omega}_j=\omega_j+\epsilon^2\beta_j$. The general case, however, is

more complicated given the explicit dependence on τ of the amplitudes $r_j(\tau)$ and the general dependence of the phases $\theta_j(\tau)$.

Let us now focus on the slow time evolution. If $\epsilon \to 0$, the rapid time oscillations are so fast that in practice they cannot be detected. The physical quantities of interest in this case are the averages over the fast time. If we analize the entanglement entropy formulas given above, we notice that it contains frequency modes that correspond to either $|\omega_j + \omega_k|$ or $|\omega_j - \omega_k|$. This means that, if we take the average over t, only the contributions with frequencies $|\omega_j - \omega_k|$, for $j = k$, survive. More specifically, we find that

$$\left\langle A^{jk}_{(2)} \right\rangle = 0\,, \qquad \text{for } j \neq k\,, \tag{4.74}$$

and

$$\left\langle A^{jj}_{(2)} \right\rangle = -2r_j(\tau)^2 \frac{\cos^3 x}{\sin x} \int_0^x dy \left(\omega_j^2 e_j(y)^2 + e_j'(y)^2 + \frac{m^2}{\cos^2 y} e_j(y)^2 \right) \tan^2 y\,. \tag{4.75}$$

The slow time dependence is completely given in terms of the amplitudes $r_j(\tau)$. This means that, for periodic or quasi-periodic solutions, taking the average over the rapid time t effectively kills all τ-dependence. Finally, the time averaged entanglement entropy is given by

$$\langle \Delta S(\tau_b, \theta_b) \rangle = \sum_j \left\langle \Delta S^{jj}(\tau_b, \theta_b) \right\rangle\,, \tag{4.76}$$

where

$$\left\langle \Delta S^{jj}(\tau_b, \theta_b) \right\rangle = -\frac{\sqrt{2}\pi\epsilon^2 \cos^2\theta_b}{2G_N \sin\theta_b} \int_0^{\theta_b} d\theta\, \frac{\left\langle A^{jj}_{(2)}(\tau_b, x(\theta, \theta_b)) \right\rangle \sin^3\theta}{\left(\cos(2\theta) - \cos(2\theta_b)\right)^{3/2}}\,. \tag{4.77}$$

We have seen here that for (quasi-)periodic solution with arbitrary number of modes the constant part of entanglement entropy is always given by the addition of single mode solutions. This proves that the conclusion we reach in the previous section is true, namely, that the behavior crucially depends on the nature of the operator and its conformal dimension.

4.5 Conclusions

In this Chapter we have studied a particular family of time-dependent solutions of the Einstein field equations with a negative cosmological constant and a massive scalar field. These solutions are characterized by periodic or quasi-periodic undamped oscillations and are of particular interest in the context of AdS/CFT correspondence due to the potential relevance for condensed matter applications. In particular, they may be useful to describe systems of cold atoms, quantum spin chains and quantum critical systems, among others.

The solutions presented here were obtained in the framework of the two time formalism, introduced in [138] and provide analytical evidence supporting the numerical results of [144] for the fate of the massive collapse in global AdS. In the holographic context, massive fields in the bulk are dual to operators of different conformal dimensions. Therefore, we can interprete these solutions as excited states over the CFT vacuum in which a relevant, irrelevant or marginal operator picks up a non-zero expectation value that is (quasi-)periodic in time. Indeed, such oscillatory states are expected to exist for any CFT on a sphere [124], which includes CFTs with a gravity dual as the ones cosidered here.

We studied the evolution of entanglement entropy for spherical caps in order to characterize the states in the field theory dual to these backgrounds and we found some crucial differences depending on the conformal dimension Δ of the dual operator. In general, the entanglement contains a time independent part and a time dependent part with harmonics of the modes we consider. For irrelenvant and marginal operators, we found that the time independent part is always possitive which implies that the system is more entangled than in the vacuum of the theory. However, for relevant operators this is no longer true. In this case we found that for large enough regions, at some point in the evolution these states are less entangled than the pure AdS case. This is possible because relevant operators can in principle modify the IR bahavior of the theory and the biggest contribution of the entanglement comes precisely from regions that are deep inside the bulk (IR region).

Another important lesson that we did not pointed out concerns to the nature of the periodic and quasi-periodic solutions: since the entanglement entropies split the Hilbert space into two sectors that do not mix under slow time evolution, these can be can be thought of as conserved charges of the system. Moreover, since there are infinitely many ways to split the system into two geometrical regions, we can conclude that there are infinitely many conserved charges. Hence, we can say that the system is integrable, in complete analogy to the FPU problem in dynamical systems.

Finally, it is worth pointing out possible future directions in the context of this work. One simple extension would be to relax the ansatz (4.37) for

the Fourier coefficients in terms of the slow time. It is know that general solutions to the TTF equations are not necesarily periodic or quasi-periodic [138]. In these cases the system is characterized by direct and inverse cascades, where the energy flows from low frequency modes to high frequency modes and viceversa. It would be interesting to study the behavior of entanglement entropy in such solutions. Another interesting idea is to come up with a simpler toy model for quantum revivals. This may be achieved by studying the dynamics of a shell of matter in global AdS and considering different equations of state. If the pressure is large enough, it might be possible to cancel out the gravitational attraction and avoid black hole formation. We hope to come back to these issues in the future.

Bibliography

[1] F. D. Lora-Clavijo, P. A. Ospina-Henao and J. F. Pedraza, "Charged Annular Disks and Reissner-Nordstrom Type Black Holes from Extremal Dust," Phys. Rev. D **82**, 084005 (2010) [arXiv:1009.1005 [gr-qc]].

[2] A. Guijosa and J. F. Pedraza, "Early-Time Energy Loss in a Strongly-Coupled SYM Plasma," JHEP **1105**, 108 (2011) [arXiv:1102.4893 [hep-th]].

[3] J. Ramos-Caro, J. F. Pedraza and P. S. Letelier, "Motion around a Monopole + Ring system: I. Stability of Equatorial Circular Orbits vs Regularity of Three-dimensional Motion," Mon. Not. Roy. Astron. Soc. **414**, 3105 (2011) [arXiv:1103.4616 [astro-ph.EP]].

[4] C. A. Agon, J. F. Pedraza and J. Ramos-Caro, "Kinetic Theory of Collisionless Self-Gravitating Gases: Post-Newtonian Polytropes," Phys. Rev. D **83**, 123007 (2011) [arXiv:1104.5262 [gr-qc]].

[5] M. Chernicoff, A. Guijosa and J. F. Pedraza, "The Gluonic Field of a Heavy Quark in Conformal Field Theories at Strong Coupling," JHEP **1110**, 041 (2011) [arXiv:1106.4059 [hep-th]].

[6] M. Chernicoff, J. A. Garcia, A. Guijosa and J. F. Pedraza, "Holographic Lessons for Quark Dynamics," J. Phys. G **39**, 054002 (2012) [arXiv:1111.0872

[hep-th]].

[7] M. Edalati, W. Fischler, J. F. Pedraza and W. Tangarife Garcia, "Fast Scramblers and Non-commutative Gauge Theories," JHEP **1207**, 043 (2012) [arXiv:1204.5748 [hep-th]].

[8] J. Ramos-Caro, C. A. Agon and J. F. Pedraza, "Kinetic Theory of Collisionless Self-Gravitating Gases: II. Relativistic Corrections in Galactic Dynamics," Phys. Rev. D **86**, 043008 (2012) [arXiv:1206.5804 [gr-qc]].

[9] W. Fischler, J. F. Pedraza and W. Tangarife Garcia, "Holographic Brownian Motion in Magnetic Environments," JHEP **1212**, 002 (2012) [arXiv:1209.1044 [hep-th]].

[10] M. Edalati, J. F. Pedraza and W. Tangarife Garcia, "Quantum Fluctuations in Holographic Theories with Hyperscaling Violation," Phys. Rev. D **87**, no. 4, 046001 (2013) [arXiv:1210.6993 [hep-th]].

[11] E. Caceres, A. Kundu, J. F. Pedraza and W. Tangarife, "Strong Subadditivity, Null Energy Condition and Charged Black Holes," JHEP **1401**, 084 (2014) [arXiv:1304.3398 [hep-th]].

[12] P. H. Nguyen and J. F. Pedraza, "Anisotropic Models for Globular Clusters, Galactic Bulges and Dark Halos," Phys. Rev. D **88**, 064020 (2013) [arXiv:1305.7220 [gr-qc]].

[13] M. Edalati and J. F. Pedraza, "Aspects of Current Correlators in Holographic Theories with Hyperscaling Violation," Phys. Rev. D **88**, 086004 (2013) [arXiv:1307.0808 [hep-th]].

[14] M. Chernicoff, A. Gijosa and J. F. Pedraza, "Holographic EPR Pairs, Wormholes and Radiation," JHEP **1310**, 211 (2013) [arXiv:1308.3695 [hep-th]].

[15] W. Fischler, S. Kundu and J. F. Pedraza, "Entanglement and out-of-equilibrium dynamics in holographic models of de Sitter QFTs," JHEP **1407**, 021 (2014) [arXiv:1311.5519 [hep-th]].

[16] T. Banks, W. Fischler, S. Kundu and J. F. Pedraza, "Holographic Spacetime and Black Holes: Mirages As Alternate Reality," arXiv:1401.3341 [hep-th].

[17] C. A. Agon, A. Guijosa and J. F. Pedraza, "Radiation and a dynamical UV/IR connection in AdS/CFT," JHEP **1406**, 043 (2014) [arXiv:1402.5961 [hep-th]].

[18] B. S. DiNunno, M. Ihl, N. Jokela and J. F. Pedraza, "Holographic zero sound at finite temperature in the Sakai-Sugimoto model," JHEP **1404**, 149 (2014) [arXiv:1403.1827 [hep-th]].

[19] W. Fischler, P. H. Nguyen, J. F. Pedraza and W. Tangarife, "Fluctuation and dissipation in de Sitter space," JHEP **1408**, 028 (2014) [arXiv:1404.0347 [hep-th]].

[20] J. F. Pedraza, "Evolution of nonlocal observables in an expanding boost-invariant plasma," Phys. Rev. D **90**, no. 4, 046010 (2014) [arXiv:1405.1724 [hep-th]].

[21] B. Fiol, A. Gijosa and J. F. Pedraza, "Branes from Light: Embeddings and Energetics for Symmetric k-Quarks in $\mathcal{N} = 4$ SYM," JHEP **1501**, 149 (2015) [arXiv:1410.0692 [hep-th]].

[22] E. Caceres, A. Kundu, J. F. Pedraza and D. L. Yang, "Weak Field Collapse in AdS: Introducing a Charge Density," JHEP **1506**, 111 (2015) [arXiv:1411.1744 [hep-th]].

[23] W. Fischler, P. H. Nguyen, J. F. Pedraza and W. Tangarife, "Holographic Schwinger effect in de Sitter space," Phys. Rev. D **91**, no. 8, 086015 (2015) [arXiv:1411.1787 [hep-th]].

[24] E. Caceres, P. H. Nguyen and J. F. Pedraza, "Holographic entanglement entropy and the extended phase structure of STU black holes," arXiv:1507.06069 [hep-th].

[25] J. M. Maldacena, "The Large N limit of superconformal field theories and supergravity," Int. J. Theor. Phys. **38**, 1113 (1999) [Adv. Theor. Math. Phys. **2**, 231 (1998)] [hep-th/9711200].

[26] S. S. Gubser, I. R. Klebanov and A. M. Polyakov, "Gauge theory correlators from noncritical string theory," Phys. Lett. B **428**, 105 (1998) [hep-th/9802109].

[27] E. Witten, "Anti-de Sitter space and holography," Adv. Theor. Math. Phys. **2**, 253 (1998) [hep-th/9802150].

[28] J. Casalderrey-Solana, H. Liu, D. Mateos, K. Rajagopal and U. A. Wiedemann, "Gauge/String Duality, Hot QCD and Heavy Ion Collisions," arXiv:1101.0618 [hep-th].

[29] S. A. Hartnoll, "Lectures on holographic methods for condensed matter physics," Class. Quant. Grav. **26**, 224002 (2009) [arXiv:0903.3246 [hep-th]].

[30] S. Mondal, D. Sen and K. Sengupta, "Non-equilibrium dynamics of quantum systems: order parameter evolution, defect generation, and qubit transfer," arXiv:0908.2922;

J. Dziarmaga, "Dynamics of a quantum phase transition and relaxation to a steady state," Adv. Phys. **59**, 1063 (2010) [arXiv:0912.4034 [cond-mat.quant-gas]];

A. Polkovnikov, K. Sengupta, A. Silva and M. Vengalattore, "Nonequilibrium dynamics of closed interacting quantum systems," Rev. Mod. Phys. **83**, 863 (2011) [arXiv:1007.5331 [cond-mat.stat-mech]];

[31] S. R. Das, "Holographic Quantum Quench," J. Phys. Conf. Ser. **343**, 012027 (2012) [arXiv:1111.7275 [hep-th]].

[32] P. Basu and S. R. Das, "Quantum Quench across a Holographic Critical Point," JHEP **1201**, 103 (2012) [arXiv:1109.3909 [hep-th]].

[33] S. R. Das, T. Nishioka and T. Takayanagi, "Probe Branes, Time-dependent Couplings and Thermalization in AdS/CFT," JHEP **1007**, 071 (2010) [arXiv:1005.3348 [hep-th]].

[34] U. H. Danielsson, E. Keski-Vakkuri and M. Kruczenski, "Spherically collapsing matter in AdS, holography, and shellons," Nucl. Phys. B **563**, 279 (1999) [hep-th/9905227].

[35] U. H. Danielsson, E. Keski-Vakkuri and M. Kruczenski, "Black hole formation in AdS and thermalization on the boundary," JHEP **0002**, 039 (2000) [hep-th/9912209].

[36] S. B. Giddings and A. Nudelman, "Gravitational collapse and its boundary description in AdS," JHEP **0202**, 003 (2002) [hep-th/0112099].

[37] P. M. Chesler and L. G. Yaffe, "Horizon formation and far-from-equilibrium isotropization in supersymmetric Yang-Mills plasma," Phys. Rev. Lett. **102**, 211601 (2009) [arXiv:0812.2053 [hep-th]].

[38] P. M. Chesler and L. G. Yaffe, "Boost invariant flow, black hole formation, and far-from-equilibrium dynamics in N = 4 supersymmetric Yang-Mills theory," Phys. Rev. D **82**, 026006 (2010) [arXiv:0906.4426 [hep-th]].

[39] M. P. Heller, R. A. Janik and P. Witaszczyk, "The characteristics of thermalization of boost-invariant plasma from holography," Phys. Rev. Lett. **108**, 201602 (2012) [arXiv:1103.3452 [hep-th]].

[40] M. P. Heller, R. A. Janik and P. Witaszczyk, "A numerical relativity approach to the initial value problem in asymptotically Anti-de Sitter spacetime for plasma thermalization - an ADM formulation," Phys. Rev. D **85**, 126002 (2012) [arXiv:1203.0755 [hep-th]].

[41] M. P. Heller, D. Mateos, W. van der Schee and D. Trancanelli, "Strong Coupling Isotropization of Non-Abelian Plasmas Simplified," Phys. Rev. Lett. **108**, 191601 (2012) [arXiv:1202.0981 [hep-th]].

[42] V. Balasubramanian, A. Bernamonti, J. de Boer, B. Craps, L. Franti, F. Galli, E. Keski-Vakkuri and B. Mller *et al.*, "Inhomogeneous Thermalization in Strongly Coupled Field Theories," Phys. Rev. Lett. **111**, 231602 (2013) [arXiv:1307.1487 [hep-th]].

[43] V. Balasubramanian, A. Bernamonti, J. de Boer, B. Craps, L. Franti, F. Galli, E. Keski-Vakkuri and B. Mller *et al.*, "Inhomogeneous holographic thermalization," JHEP **1310**, 082 (2013) [arXiv:1307.7086].

[44] G. T. Horowitz and A. Strominger, "Black strings and P-branes," Nucl. Phys. B **360**, 197 (1991).

[45] O. Aharony, S. S. Gubser, J. M. Maldacena, H. Ooguri and Y. Oz, "Large N field theories, string theory and gravity," Phys. Rept. **323**, 183 (2000) [hep-th/9905111].

[46] S. de Haro, S. N. Solodukhin and K. Skenderis, "Holographic reconstruction of space-time and renormalization in the AdS / CFT correspon-

dence," Commun. Math. Phys. **217**, 595 (2001) [hep-th/0002230].

[47] K. Skenderis, "Lecture notes on holographic renormalization," Class. Quant. Grav. **19**, 5849 (2002) [hep-th/0209067].

[48] S. S. Gubser, I. R. Klebanov and A. W. Peet, "Entropy and temperature of black 3-branes," Phys. Rev. D **54**, 3915 (1996) [hep-th/9602135].

[49] J. D. Bekenstein, "Black holes and entropy," Phys. Rev. D **7**, 2333 (1973).

[50] S. W. Hawking, "Black hole explosions," Nature **248**, 30 (1974).

[51] A. Fotopoulos and T. R. Taylor, "Comment on two loop free energy in N=4 supersymmetric Yang-Mills theory at finite temperature," Phys. Rev. D **59**, 061701 (1999) [hep-th/9811224].

[52] M. A. Vazquez-Mozo, "A Note on supersymmetric Yang-Mills thermodynamics," Phys. Rev. D **60**, 106010 (1999) [hep-th/9905030].

[53] S. S. Gubser, I. R. Klebanov and A. A. Tseytlin, "Coupling constant dependence in the thermodynamics of N=4 supersymmetric Yang-Mills theory," Nucl. Phys. B **534**, 202 (1998) [hep-th/9805156].

[54] C. Fefferman and C. R. Graham, "Conformal invariants," in *Élie Cartan et les Mathématiques d'Aujourd'hui*, (Astérisque, 1985), 95.

[55] P. Figueras, V. E. Hubeny, M. Rangamani and S. F. Ross, "Dynamical black holes and expanding plasmas," JHEP **0904**, 137 (2009) [arXiv:0902.4696 [hep-th]].

[56] D. T. Son and A. O. Starinets, "Minkowski space correlators in AdS/CFT correspondence: Recipe and applications," JHEP **0209**, 042 (2002) [hep-th/0205051].

[57] C. P. Herzog and D. T. Son, "Schwinger-Keldysh propagators from AdS/CFT correspondence," JHEP **0303**, 046 (2003) [hep-th/0212072].

[58] V. Balasubramanian and S. F. Ross, "Holographic particle detection," Phys. Rev. D **61**, 044007 (2000), [arXiv:hep-th/9906226].

[59] J. Louko, D. Marolf and S. F. Ross, "On geodesic propagators and black hole holography," Phys. Rev. D **62**, 044041 (2000) [hep-th/0002111].

[60] A. Karch and E. Katz, "Adding flavor to AdS / CFT," JHEP **0206**, 043 (2002) [hep-th/0205236].

[61] J. M. Maldacena, "Wilson loops in large N field theories," Phys. Rev. Lett. **80**, 4859 (1998) [hep-th/9803002].

[62] S. Ryu and T. Takayanagi, "Holographic derivation of entanglement entropy from AdS/CFT," Phys. Rev. Lett. **96**, 181602 (2006) [hep-th/0603001].

[63] V. E. Hubeny, M. Rangamani and T. Takayanagi, "A Covariant holographic entanglement entropy proposal," JHEP **0707**, 062 (2007) [arXiv:0705.0016 [hep-th]].

[64] D. Galante and M. Schvellinger, "Thermalization with a chemical potential from AdS spaces," JHEP **1207**, 096 (2012) [arXiv:1205.1548 [hep-th]].

[65] E. Caceres and A. Kundu, "Holographic Thermalization with Chemical Potential," JHEP **1209**, 055 (2012) [arXiv:1205.2354 [hep-th]].

[66] J. F. Pedraza, "Periodic and quasi-periodic solutions in global AdS," in preparation.

[67] S. Bhattacharyya and S. Minwalla, "Weak Field Black Hole Formation in Asymptotically AdS Spacetimes," JHEP **0909**, 034 (2009) [arXiv:0904.0464 [hep-th]].

[68] J. Abajo-Arrastia, J. Aparicio and E. Lopez, "Holographic Evolution of Entanglement Entropy," JHEP **1011**, 149 (2010) [arXiv:1006.4090 [hep-th]].

[69] V. Balasubramanian, A. Bernamonti, J. de Boer, N. Copland, B. Craps, E. Keski-Vakkuri, B. Muller and A. Schafer *et al.*, "Thermalization of Strongly Coupled Field Theories," Phys. Rev. Lett. **106**, 191601 (2011) [arXiv:1012.4753 [hep-th]].

[70] V. Balasubramanian, A. Bernamonti, J. de Boer, N. Copland, B. Craps, E. Keski-Vakkuri, B. Muller and A. Schafer *et al.*, "Holographic Thermalization," Phys. Rev. D **84**, 026010 (2011) [arXiv:1103.2683 [hep-th]].

[71] T. Albash and C. V. Johnson, "Evolution of Holographic Entanglement Entropy after Thermal and Electromagnetic Quenches," New J. Phys. **13**, 045017 (2011) [arXiv:1008.3027 [hep-th]].

[72] A. Andronic, P. Braun-Munzinger and J. Stachel, "Hadron production in central nucleus-nucleus collisions at chemical freeze-out," Nucl. Phys. A **772**, 167 (2006) [nucl-th/0511071].

[73] J. Stachel, A. Andronic, P. Braun-Munzinger and K. Redlich, "Confronting LHC data with the statistical hadronization model," J. Phys. Conf. Ser. **509**, 012019 (2014) [arXiv:1311.4662 [nucl-th]].

[74] A. Buchel, L. Lehner and R. C. Myers, "Thermal quenches in N=2* plasmas," JHEP **1208**, 049 (2012) [arXiv:1206.6785 [hep-th]].

[75] A. Buchel, L. Lehner, R. C. Myers and A. van Niekerk, "Quantum quenches of holographic plasmas," JHEP **1305**, 067 (2013) [arXiv:1302.2924 [hep-th]].

[76] A. Buchel, R. C. Myers and A. van Niekerk, "Nonlocal probes of thermalization in holographic quenches with spectral methods," arXiv:1410.6201 [hep-th].

[77] A. Buchel, R. C. Myers and A. van Niekerk, "Universality of Abrupt Holographic Quenches," Phys. Rev. Lett. **111**, 201602 (2013) [arXiv:1307.4740 [hep-th]].

[78] S. R. Das, D. A. Galante and R. C. Myers, "Universal scaling in fast quantum quenches in conformal field theories," Phys. Rev. Lett. **112**, 171601 (2014) [arXiv:1401.0560 [hep-th]].

[79] S. R. Das, D. A. Galante and R. C. Myers, "Universality in fast quantum quenches," arXiv:1411.7710 [hep-th].

[80] M. Nozaki, T. Numasawa and T. Takayanagi, "Holographic Local Quenches and Entanglement Density," JHEP **1305**, 080 (2013) [arXiv:1302.5703 [hep-th]].

[81] H. Liu and S. J. Suh, "Entanglement Tsunami: Universal Scaling in Holographic Thermalization," Phys. Rev. Lett. **112**, 011601 (2014) [arXiv:1305.7244 [hep-th]].

[82] H. Liu and S. J. Suh, "Entanglement growth during thermalization in holographic systems," arXiv:1311.1200 [hep-th].

[83] M. Alishahiha, A. F. Astaneh and M. R. M. Mozaffar, "Thermalization in backgrounds with hyperscaling violating factor," Phys. Rev. D **90**, no. 4, 046004 (2014) [arXiv:1401.2807 [hep-th]].

[84] P. Fonda, L. Franti, V. Kernen, E. Keski-Vakkuri, L. Thorlacius and E. Tonni, "Holographic thermalization with Lifshitz scaling and hyperscaling violation," JHEP **1408**, 051 (2014) [arXiv:1401.6088 [hep-th]].

[85] M. Alishahiha, M. R. M. Mozaffar and M. R. Tanhayi, "Evolution of Holographic n-partite Information," arXiv:1406.7677 [hep-th].

[86] Y. Sekino and L. Susskind, "Fast Scramblers," JHEP **0810**, 065 (2008) [arXiv:0808.2096 [hep-th]].

[87] L. Susskind, "Addendum to Fast Scramblers," arXiv:1101.6048 [hep-th].

[88] N. Lashkari, D. Stanford, M. Hastings, T. Osborne and P. Hayden, "Towards the Fast Scrambling Conjecture," JHEP **1304**, 022 (2013) [arXiv:1111.6580 [hep-th]].

[89] S. H. Shenker and D. Stanford, "Black holes and the butterfly effect," JHEP **1403**, 067 (2014) [arXiv:1306.0622 [hep-th]].

[90] A. Chamblin, R. Emparan, C. V. Johnson and R. C. Myers, "Charged AdS black holes and catastrophic holography," Phys. Rev. D **60**, 064018 (1999) [hep-th/9902170].

[91] P. F. Kolb and U. W. Heinz, In *Hwa, R.C. (ed.) et al.: Quark gluon plasma* 634-714.

[92] J. D. Bjorken, Phys. Rev. D **27**, 140 (1983).

[93] R. A. Janik and R. Peschanski, Phys. Rev. D **73** (2006) 045013; S. Nakamura and S. J. Sin, JHEP **0609**, 020 (2006); R. A. Janik, Phys. Rev. Lett. **98**, 022302 (2007).

[94] P. M. Chesler and L. G. Yaffe, Phys. Rev. Lett. **102**, 211601 (2009); P. M. Chesler and L. G. Yaffe, Phys. Rev. D **82**, 026006 (2010); M. P. Heller *et al.*, Phys. Rev. Lett. **108**, 191601 (2012);

[95] W. van der Schee, Phys. Rev. D **87**, 061901 (2013); P. Romatschke and J. D. Hogg, JHEP **1304**, 048 (2013).

[96] P. M. Chesler and L. G. Yaffe, Phys. Rev. Lett. **106**, 021601 (2011); M. P. Heller, R. A. Janik and P. Witaszczyk, Phys. Rev. Lett. **108**, 201602 (2012); M. P. Heller, R. A. Janik and P. Witaszczyk, Phys. Rev. D **85**, 126002 (2012).

[97] J. Abajo-Arrastia, J. Aparicio and E. Lopez, JHEP **1011**, 149 (2010); V. Balasubramanian *et al.*, Phys. Rev. Lett. **106**, 191601 (2011); V. Balasubramanian *et al.*, Phys. Rev. D **84**, 026010 (2011); J. Aparicio and E. Lopez, JHEP **1112**, 082 (2011); D. Galante and M. Schvellinger, JHEP **1207**, 096 (2012); E. Caceres and A. Kundu, JHEP **1209**, 055 (2012); W. Baron, D. Galante and M. Schvellinger, JHEP **1303**, 070 (2013); E. Caceres *et al.*, JHEP **1401**, 084 (2014); H. Liu and S. J. Suh, Phys. Rev. Lett. **112**, 011601 (2014); H. Liu and S. J. Suh, Phys. Rev. D **89**, 066012 (2014); W. Fischler, S. Kundu and J. F. Pedraza, arXiv:1311.5519 [hep-th].

[98] S. Bhattacharyya *et al.*, "Nonlinear Fluid Dynamics from Gravity," JHEP **0802**, 045 (2008).

[99] P. Benincasa, A. Buchel, M. P. Heller and R. A. Janik, "On the supergravity description of boost invariant conformal plasma at strong coupling," Phys. Rev. D **77**, 046006 (2008) [arXiv:0712.2025 [hep-th]].

[100] A. Buchel, "Shear viscosity of boost invariant plasma at finite coupling," Nucl. Phys. B **802**, 281 (2008) [arXiv:0801.4421 [hep-th]].

[101] A. Buchel and M. Paulos, "Second order hydrodynamics of a CFT plasma from boost invariant expansion," Nucl. Phys. B **810**, 40 (2009) [arXiv:0808.1601 [hep-th]].

[102] S. de Haro, S. N. Solodukhin and K. Skenderis, Commun. Math. Phys. **217**, 595 (2001); K. Skenderis, Class. Quant. Grav. **19**, 5849 (2002).

[103] M. P. Heller and R. A. Janik, Phys. Rev. D **76**, 025027 (2007); M. P. Heller, R. A. Janik and P. Witaszczyk, Phys. Rev. Lett. **110**, no. 21, 211602 (2013).

[104] B. S. DiNunno, J. F. Pedraza and S. Young, in preparation.

[105] V. E. Hubeny, JHEP **1207**, 093 (2012).

[106] L. Susskind and E. Witten, arXiv:hep-th/9805114; A. W. Peet and J. Polchinski, Phys. Rev. D **59** (1999) 065011; C. A. Agon, A. Guijosa and J. F. Pedraza, arXiv:1402.5961 [hep-th].

[107] W. Fischler and S. Kundu, JHEP **1305**, 098 (2013).

[108] S. Ryu and T. Takayanagi, Phys. Rev. Lett. **96**, 181602 (2006); V. E. Hubeny, M. Rangamani and T. Takayanagi, JHEP **0707**, 062 (2007).

[109] R. Baier, P. Romatschke, D. T. Son, A. O. Starinets and M. A. Stephanov, "Relativistic viscous hydrodynamics, conformal invariance, and holography," JHEP **0804**, 100 (2008) [arXiv:0712.2451 [hep-th]].

[110] S. Bhattacharyya, V. E. Hubeny, S. Minwalla and M. Rangamani, "Nonlinear Fluid Dynamics from Gravity," JHEP **0802**, 045 (2008) [arXiv:0712.2456 [hep-th]].

[111] S. Hod, "Universal Bound on Dynamical Relaxation Times and Black-Hole Quasinormal Ringing," Phys. Rev. D **75**, 064013 (2007) [gr-qc/0611004].

[112] G. Policastro, D. T. Son and A. O. Starinets, "The Shear viscosity of strongly coupled N=4 supersymmetric Yang-Mills plasma," Phys. Rev. Lett. **87**, 081601 (2001) [hep-th/0104066].

[113] A. Buchel and J. T. Liu, "Universality of the shear viscosity in supergravity," Phys. Rev. Lett. **93**, 090602 (2004) [hep-th/0311175].

[114] A. Buchel, "On universality of stress-energy tensor correlation functions in supergravity," Phys. Lett. B **609**, 392 (2005) [hep-th/0408095].

[115] P. Kovtun, D. T. Son and A. O. Starinets, "Viscosity in strongly interacting quantum field theories from black hole physics," Phys. Rev. Lett. **94**, 111601 (2005) [hep-th/0405231].

[116] S. R. Das, G. W. Gibbons and S. D. Mathur, "Universality of low-energy absorption cross-sections for black holes," Phys. Rev. Lett. **78**, 417 (1997) [hep-th/9609052].

[117] R. Emparan, "Absorption of scalars by extended objects," Nucl. Phys. B **516**, 297 (1998) [hep-th/9706204].

[118] M. P. Heller, R. A. Janik and P. Witaszczyk, "Hydrodynamic Gradient Expansion in Gauge Theory Plasmas," Phys. Rev. Lett. **110**, no. 21, 211602 (2013) [arXiv:1302.0697 [hep-th]].

[119] A. Polkovnikov, K. Sengupta, A. Silva and M. Vengalattore, *Nonequilibrium dynamics of closed interacting quantum systems*, Rev. Mod. Phys. **83**, 863 (2011) [arXiv:1007.5331 [cond-mat.stat-mech]].

[120] H. Rieger and F. Iglói, "Quantum relaxation after a quench in systems with boundaries," Phys. Rev. Lett. **106** 035701 (2011).

[121] J. Häppölä, G.B. Halász, A. Hamma, "Revivals of a closed quantum system and Lieb-Robinson speed," Phys. Rev. A **85**, 032114 (2012).

[122] B. Freivogel, J. McGreevy and S. J. Suh, "Exactly Stable Collective Oscillations in Conformal Field Theory," Phys. Rev. D **85**, 105002 (2012) [arXiv:1109.6013 [hep-th]].

[123] John Cardy, "Thermalization and Revivals after a Quench in Conformal Field Theory," arXiv:1403.3040 [cond-mat].

[124] M. Greiner, O.Mandel, T.W. Hänsh and I. Bolch, "Collapse and revival of the matter wave field of a Bose-Einstein condensate," Nature **419**, 51 (2002).

[125] T. Kinoshita, T. Wenger and D.S. Weiss, "A quantum Newton's cradle," Nature **440** 900 (2006).

[126] M. Rigol, V. Dunjko, V. Yurovsky and Maxim Olshanii, "Relaxation in a Completely Integrable Many-Body Quantum System: An Ab Initio Study of the Dynamics of the Highly Excited States in 1D Lattice Hard-Core Bosons," Phys. Rev. Lett. **98**, 050405 (2007).

[127] E. Fermi, J. Pasta and S. M. Ulam, "Studies of nonlinear problems," Document LA-1940 (1955).

[128] G. P. Berman and F. M. Izrailev, "The Fermi-Pasta-Ulam problem: Fifty years of progress," Chaos **15** 015104 (2005) [arXiv:nlin/0411062].

[129] J. Abajo-Arrastia, E. da Silva, E. Lopez, J. Mas and A. Serantes, "Holographic Relaxation of Finite Size Isolated Quantum Systems," JHEP **1405**, 126 (2014) [arXiv:1403.2632 [hep-th]].

[130] E. da Silva, E. Lopez, J. Mas and A. Serantes, "Collapse and Revival in Holographic Quenches," JHEP **1504**, 038 (2015) [arXiv:1412.6002 [hep-th]].

[131] P. Bizon and A. Rostworowski, "On weakly turbulent instability of anti-de Sitter space," Phys. Rev. Lett. **107**, 031102 (2011) [arXiv:1104.3702 [gr-qc]].

[132] D. Garfinkle and L. A. Pando Zayas, "Rapid Thermalization in Field Theory from Gravitational Collapse," Phys. Rev. D **84**, 066006 (2011) [arXiv:1106.2339 [hep-th]].

[133] J. Jalmuzna, A. Rostworowski and P. Bizon, "A Comment on AdS collapse of a scalar field in higher dimensions," Phys. Rev. D **84**, 085021 (2011) [arXiv:1108.4539 [gr-qc]].

[134] D. Garfinkle, L. A. Pando Zayas and D. Reichmann, "On Field Theory Thermalization from Gravitational Collapse," JHEP **1202**, 119 (2012) [arXiv:1110.5823 [hep-th]].

[135] A. Buchel, L. Lehner and S. L. Liebling, "Scalar Collapse in AdS," Phys. Rev. D **86**, 123011 (2012) [arXiv:1210.0890 [gr-qc]].

[136] V. Balasubramanian, A. Buchel, S. R. Green, L. Lehner and S. L. Liebling, "Holographic Thermalization, stability of AdS, and the Fermi-Pasta-Ulam-Tsingou paradox," Phys. Rev. Lett. **113**, 071601 (2014) [arXiv:1403.6471 [hep-th]].

[137] P. Bizo and A. Rostworowski, "Comment on "Holographic Thermalization, stability of AdS, and the Fermi-Pasta-Ulam-Tsingou paradox" by V. Balasubramanian et al," arXiv:1410.2631 [gr-qc].

[138] N. Deppe, A. Kolly, A. Frey and G. Kunstatter, "Stability of AdS in Einstein Gauss Bonnet Gravity," Phys. Rev. Lett. **114**, 071102 (2015) [arXiv:1410.1869 [hep-th]].

[139] A. Buchel, S. R. Green, L. Lehner and S. L. Liebling, "Universality of non-equilibrium dynamics of CFTs from holography," arXiv:1410.5381 [hep-th].

[140] B. Craps, O. Evnin and J. Vanhoof, "Renormalization, averaging, conservation laws and AdS (in)stability," JHEP **1501**, 108 (2015) [arXiv:1412.3249 [gr-qc]].

[141] A. Buchel, S. R. Green, L. Lehner and S. L. Liebling, "Conserved quantities and dual turbulent cascades in antide Sitter spacetime," Phys. Rev. D **91**, no. 6, 064026 (2015) [arXiv:1412.4761 [gr-qc]].

[142] H. Okawa, J. C. Lopes and V. Cardoso, "Collapse of massive fields in anti-de Sitter spacetime," arXiv:1504.05203 [gr-qc].

[143] P. Breitenlohner and D. Z. Freedman, "Stability in Gauged Extended Supergravity," Annals Phys. **144**, 249 (1982).

[144] A. Ishibashi and R. M. Wald, "Dynamics in nonglobally hyperbolic static space-times. 3. Anti-de Sitter space-time," Class. Quant. Grav. **21**, 2981 (2004) [hep-th/0402184].

[145] V. E. Hubeny and M. Rangamani, "Causal Holographic Information," JHEP **1206**, 114 (2012) [arXiv:1204.1698 [hep-th]].

[146] R. Callan, J. Y. He and M. Headrick, "Strong subadditivity and the covariant holographic entanglement entropy formula," JHEP **1206**, 081 (2012) [arXiv:1204.2309 [hep-th]].